Nanochemistry through self-assembly:

Polymerisation of the organised phases of polyelectrolyte-surfactant complexes

by

Desislava Evgenieva Ganeva

Dissertation presented for the Degree of Doctor of Philosophy

(Polymer Science)

at the

University of Stellenbosch

Promoter:
Prof. Ronald D. Sanderson

Co-promoter:
Dr. Charl F. J. Faul

Stellenbosch
December 2003

Declaration

I, the undersigned, hereby declare that the work contained in this dissertation is my own original work and that I have not previously in its entirety or in part submitted it at any university for a degree.

"Imagination is more important than knowledge"

A. Einstein

ABSTRACT

The general objective of this research was to develop a new approach to direct templating, where the organised phases of polyelectrolyte-surfactant complexes are used as hosts for organic polymerisation reactions.

The lamellar polyelectrolyte-surfmer complex of the tail-functionalised di (undecenyl) phosphate (ωC11) and polydiallyldimethylammonium chloride (pDADMAC) was identified as a host for organic polymerisation reactions. The complex showed higher stability (than the one found in the case of ωC11 alone) when used as a template, owing to the presence of the polyelectrolyte backbone.

The mobility of the reactive groups (positioned in the tails of the surfmer) was not sufficient for homopolymerisation reactions to take place. Direct, 1:1 templating was only achieved on the incorporation of an unbound co-monomer (a dithiol) in the complex. Furthermore the thiol-ene polyaddition reaction used offered the advantage over conventional free radical polymerisation that volume shrinkage was largely avoided and possibilities for phase disruption minimised. The pDADMA / ωC11 complex was able to withstand swelling with ~35 wt % of thiol co-monomer (constituting a 1:1 ratio of thiol to vinyl groups) without signs of phase disruption. The obtained polymer symplexes were cured copies of the template proving that no phase disruption or disordering occurred during the polyaddition. These results were confirmed using X-ray scattering and microscopy.

This is the first case of successful polyaddition within the organised phases of polyelectrolyte-surfactant complexes to be reported.

The addition of a second co-monomer (a diene) to the reaction system provided a possibility by which to vary the composition of the novel composite materials obtained through the ternary thiol-ene polyaddition within the complex. it therefore allowed for the investigation of the effect of increasing the amount of guest polymer on the structure of the host polyelectrolyte-surfactant complex. The increased *d*-spacing of the host structure with the increase in guest polymer content gave the possibility to tune the material properties of those highly anisotropic networks. Onset of phase disruption was only observed with 72 wt% copolymer included within the host. This unusually high degree of swelling under preservation of nanoscale order could be attributed to the flexible, linear structure of the co-monomers used, since the addition of rigid co-monomers was reported to cause phase disruption at only ~ 17 wt% of swelling of the host polyelectrolyte-surfactant complex.[1] The high loading capability of the pDADMA / ωC11 allowed for a large amount of otherwise unstructured material to be organised within the template.

OPSOMMING

Die doel van hierdie navorsing was om 'n nuwe benadering tot direkte afdrukvorming (Eng: templating) te ontwikkel, waar die georganiseerde fases van polielektroliet-seepkomplekse as gashere vir organiese polimerisasiereaksies gebruik is.

Die lamellêre (Eng: lamellar) polielektroliet-seepkompleks van die eindfunksionele verbinding di(undekiel)fosfaat (ωC11) en polidiallieldimetielammoniumcloried (pDADMAC) is as gasheer vir die organiese polimerisasiereaksies geïdentifiseer. Tydens gebruik van laasgenoemde vir afdrukvorming was die stabiliteit van die gevormde kompleks hoër as wanneer ωC11 alleen gebruik is. Dit word toegeskryf aan die teenwoordigheid van die polielektrolietskelet.

Die mobiliteit van die reaktiewe groepe (aan die punte van die seep/surfmer) was nie voldoende om homopolimerisasiereaksies te laat plaasvind nie. Direkte 1:1 afdrukvorming is slegs bereik met die byvoeging van 'n ongebonde komonomeer ('n ditiol) tot die kompleks. Gebruik van die tiol-een addisiepolimerisasiereaksie was meer voordelig as konvensionele vryeradikaal-polimerisasie, aangesien volume-inkrimping grootendeels vermy is en die kanse vir fase-ontwrigting tot 'n mimimum beperk is. Die pDADMA / ωC11 kompleks het swelling met ~35 massa % tiol-komonomeer (bestaande uit 'n 1:1 verhouding van tiol tot viniel groepe) sonder enige tekens van faseversteuring weerstaan. Die polimeersimplekse wat verkry is, was gesette kopieë van die patroonvorm. Dit het bewys dat daar geen faseversteuring of ontordening

gedurende die polimeeraddisie plaasgevind het nie. Hierdie bevindinge is dmv X-straalverstrooiing en mikroskopie bevestig.

Hierdie was die eerste keer dat meervoudige aanhegting binne-in die georganiseerde fases van polielektroliet-seepkomplekse suksesvol uitgevoer is.

Die byvoeging van 'n tweede komonomeer ('n dieen) het die moontlikheid geskep om die samestelling van die nuwe saamgestelde materiale, wat dmv ternêre tiol-een poliaddissie binne-in die kompleks verkry is, te varieer. Dit was gevolglik moontlik om die invloed van 'n toename in die hoeveelheid gaspolimeer op die struktuur van die gasheerpolielektroliet-seepkompleks te bepaal. Die toename in die *d*-spasiëring van die gas-struktuur, met die toename in gaspolimeerinhoud, het tot gevolg gehad dat die materiaaleienskappe verander kon word. Die aanvang van faseversteuring is opgemerk by 72 massa % kopolimeer in die gasheer. Die ongewone hoë swelling met behoud van die nano-skaalorde, is toegeskryf aan die buigbare, liniêre struktuur van die komonomere wat gebruik is. Volgens die literatuur het die byvoeging van starre komonomere alreeds faseversteuring by slegs ~ 17 massa % swelling van die gasheer polielektroliet-seepkompleks veroorsaak.

Die hoë ladingskapasiteit van die pDADMA / ωC11 het daartoe aanleiding gegee dat 'n groot hoeveelheid andersins ongestruktureerde materiaal binne-in die templaat gestruktureer kon word.

ACKNOWLEDGEMENTS

I am indebted to a large number of colleagues and friends who have helped me by giving advice, criticism, support and encouragement during the past four years. It would be impossible to acknowledge everyone who has been of help individually, however, I would like to single out certain people without whose help I would have not been able to write this dissertation.

Professor Sanderson for giving me this opportunity, his enthusiastic guidance and for managing necessary project funds. The Division for Polymer Science is thanked for the financial contribution to the project.

Dr Charl Faul (MPI-Golm) for his friendship, mentorship and endless patience.

Professor Markus Antonietti (MPI-Golm) for generosity in giving me the opportunity to broaden my scientific perspective. Financial support given by the Max Planck Society during my visits to Germany is also gratefully acknowledged.

Dr. Martin Bredenkamp (Stellenbosch University) and Dr Hans-Peter Hentze (MPI-Golm) for invaluable discussions and ideas.

Mohamed Jaffer (University of Cape Town) for the many hours spent doing TEM analysis and especially for being able to help me at a very short notice.

I would like to thank the staff at Polymer Science, Erinda, Johan, Aneli, Margie, Calvin for their help and assistance. Thanks to my special friends at Polymer Science, Valerie, Lillian, Jaco, Andre, Malan, Ewan, Martina, Peter, James, Matthew, Swen and Patrice, who made the past four years really exciting.

Special thanks to my parents who have been very tolerant and provided me with tons of love and support over the long years of my studies and Tania and Vince without whom I would have never experienced South Africa.

TABLE OF CONTENTS

LIST OF FIGURES

CHAPTER 2

CHAPTER 3

CHAPTER 5

LIST OF TABLES

CHAPTER 2

CHAPTER 4

CHAPTER 5

APPENDIX 1

LIST OF SCHEMES

CHAPTER 3

CHAPTER 4

CHAPTER 5

LIST OF ABBREVIATIONS

nm	Nanometer
DNA	Deoxyribonucleic acid
DVB	Divinylbenzene
Cocogem	Counterion-coupled gemini
Surfmer	Surface-active monomer
(pDADMA/DS)	Polydiallyldimethylammonium/dodecyl sulfate
ADA	12-Acryloyloxydodecanoic acid
ωC11	Di(undecenyl)phosphate
NMR	Nuclear magnetic resonance
HLB	Hydrophilic-lipophilic balance
Cmc	Critical micelle concentration
H_I	Hexagonal phase
L_α	Lamellar phase
H_{II}	Inverted hexagonal phase
2-D	Two dimensional
SDS	Sodium dodecyl sulfate
PEO	polyethyleneoxide
Cac	Critical aggregation concentration
PSS	Poly(styrenesulfonate)
SAXS	Small-angle-X-ray scattering
TEM	Transmission electron microscopy
PPE	Poly(2-ethylhexyloxycarbonyl-1,4-phenyleneethynylene carboxylate)
LLC	Lyotropic liquid-crystalline

CTAT	Cetyltrimethylammonium tosylate
SDBS	Sodium dodecylbenzenesulfonate
AOT	bis(2-ethylhexyl) sulfosuccinate sodium salt
Q_{II}	Inverse cubic phase
PPV	Poly(p-phenylenevinylene)
$Zn(DBS)_2$	Zinc dodecylbenzenesulfonate
P4VP	Poly(4-vinylpyridine)
UV	Ultraviolet
PEI	Polyethyleneimine
pDADMAC	Polydiallyldimethylammonium chloride
FTIR	Fourier transform infrared spectroscopy
EA	Elemental analysis
WAXS	Wide-angle-X-ray scattering
DSC	Differential scanning calorimetry
TGA	Thermogravimetric analysis
ESMS	Electrospray mass spectrometry
THF	Tetrahydrofurane
q	Scattering factor
KPS	Potassium peroxosulfate
6SH	1,6-Hexaneditiol
9SH	1,9-Nonanedithiol
AIBN	Azobis(isobutyronitrile)
PLM	Polarized light microscopy
SEM	Scanning electron microscopy
1,9-D	1,9-Decadiene
DMAP	N,N-dimethylaminopyridine

CHAPTER 1

MOTIVATION AND OBJECTIVES

1.1. Introduction

Inspired by Richard Feynman's remark that "there is plenty of room at the bottom",[1] the synthesis of nanostructured materials has become of increasing interest and a goal of modern material science. The synthesis of such nanostructured materials provides an opportunity to tailor materials properties for a range of desired applications. This is achieved with the aid of self-organisation, which enables control over the composition and the structure of the materials on the nanoscale. The resulting materials exhibit enhanced or entirely unique properties, derived from this nanoscale ordering.[2]

For chemists, nanostructures (materials with at least one dimension less than 100 nm)[3] are large and require the assembly of molecules into supramolecular assemblies with well-defined architecture. The synthesis of these large assemblies requires novel methodologies since the alternative, of manipulating molecules one-by-one, would not only be extremely difficult, but also impractical. Thus, in the recent years chemists have begun to utilise a process already well-known and widely used in nature – the formation of large assemblies of small molecules based on weak and kinetically labile bonds. The rules governing these weak noncovalent interactions are not new. They direct the self-assembly of molecules into living organisms, including the organisation of the DNA strands into a double helix. Van der Waals forces, π-π stacking

interactions, metal coordination bonds and hydrogen bonding are only now becoming an inherent part of the molecular toolbox of scientists, aiding in the construction of materials with controlled nanoscale architecture.[2,3] One of the available synthetic approaches makes use of the inherent self-organisation properties of amphiphilic molecules to construct templates, which finally direct the structure of some target molecule. Thus, precursor molecules capable of self-assembly are synthesised using conventional synthesis, assembled into a template, following the rules of noncovalent interactions and further stabilised by a polymerisation reaction. This approach therefore combines both chemical synthesis and self-assembly in order to produce large, structurally well-defined molecular assemblies.

The use of this technique for the production of inorganic polymers has reached a level of sophistication allowing for the synthesis on a panoscopic scale (*pano* = of any size).[4] In the case of organic polymers, however, the situation is much more complex than the simple 1:1 casting of the surfactant assembly.[5] Successful templating depends on both thermodynamic and kinetic parameters. Organic polymerisation reactions within self-organised media often lead to a disruption of the primary ordered phase and separation into a polymer phase and the original structure-directing host phase.[6] Researchers have attempted to avoid template disruption by: (i) kinetic stabilisation, achieved with the use of surfactant phases with slow exchange dynamics, (such as the lyotropic mesophases of amphiphilic block copolymers)[7-10] (ii) polymerisation within templates with long rearrangement times (e.g. bicontinuous cubic phases, which have the highest viscosity of all surfactant mesophases),[11] (iii) cross-linking of the formed polymer matrix to 'compensate' for the entropy loss caused by producing a polymer in a confined nano-environment (e.g. use of monomers with a high number of reactive entities per molecule that can be fully cross-linked at low conversions, or use of multifunctional monomers such as divinylbenzene (DVB), which can intrinsically form cross-linked networks),[12] (iv)

the coupling of surfactants to polyfunctional, organic counterions (e.g. counterion-coupled gemini (cocogem) surfactants)[13] in order to decrease the rearrangements dynamics.

As researchers gain more understanding of the kinetic and thermodynamic factors controlling these self-assembling systems, we should see an increase in successful examples of the templating of organic polymerisation reactions.

1.2. Motivation

In the past few years, scientists have successfully developed a number of stable templates for organic polymerisation reactions.[14-17] This was achieved by increasing the complexity of the amphiphilic molecules used to construct the self-assembled structure. The complex amphiphile molecule served to ensure, for example, the slower dynamics or the cross-linking of the assembly. Thus, it increased the chances for successful polymerisation within the template.

A different approach to slowing the dynamics of organised surfactant phases, while retaining the simplicity of the synthesis, is to bind surfactants into polyelectrolyte-surfactant complexes.[2] This allows the surfactant molecules to retain their ability to organise into a variety of mesostructures yet within thermally and mechanically stable materials. Even though the structure and properties of stoichiometric polyelectrolyte-surfactant complexes are well studied,[18-20] their potential, as hosts for organic polymerisation reactions, has not been fully explored.

Dreja *et al.*[21] only recently attempted polymerisations of some headgroup-functionalised, cationic, methacrylate surfactant monomers (surfmers)

electrostatically bound to an anionic polyelectrolyte (polystyrene sulfonate). The reduced mobility of the monomer units within the complex assembly led to monomer degradation rather than polymerisation and templating was not achieved. Faul *et al.*[22] then polymerised selected vinyl monomers in an ordered polydiallyldimethylammonium/dodecyl sulfate (pDADMA/DS) complex. Polymer nanoparticles (a colloidal copy of the template) rather than a 1:1 copy of the template, were obtained. This was due to the low loading capability of the complex; it was able to withstand only up to 17 wt% of monomer uptake before phase disruption occurred.

1.3. Objective

The overall objective of this proof-of-principle study was to achieve direct, 1:1 templating of the organised phases of polyelectrolyte-surfactant complexes. The aim was therefore to develop a new approach to molecular templating that utilises the simplicity of synthesis, structural perfection, and the stability that is characteristic of stoichiometric polyelectrolyte-surfactant complexes.

1.4. Methodology

This investigation was approached in the following manner:

1. Two tail-functionalised surfmers, 12-acryloyloxydodecanoic acid (ADA) and di(undecenyl)phosphate (ωC11), were to be synthesised for complexing with different polyelectrolytes. The reactive group being in the tail position in the surfmer chains was expected to provide an increased mobility inside the solid complex and therefore to enhance the possibility for successful polymerisation within the polyelectrolyte-surfmer template.

2. The tail-functionalised surfmers ADA ωC11 were to be complexed with different polyelectrolytes. A suitable template for directed organic polymerisation reactions was to be identified by structure investigations using X-ray scattering and microscopy.

3. Radiation induced homopolymerisation reactions were to be employed to determine whether the mobility of the reactive groups within the polyelectrolyte-surfmer complex was sufficient for a reaction to take place. NMR analysis of the irradiated samples was to be used to monitor the characteristic reactive group resonances before and after the reaction.

4. An unbound flexible co-monomer was to be introduced in the complex in order to improve the chances of successful polymerisation. The flexible structure of the co-monomer should enable high degrees of loading of the complex before phase disruption occurs. Structure investigations before and after the reaction were to be done to ensure

that the phase structure remains intact. A comparison was to be made to analogous reactions carried out in solution.

5. The inclusion of a second co-monomer in the complex was to be investigated in order to determine the degree to which otherwise unstructured materials can be organised by the polyelectrolyte-surfmer template while retaining its original structure.

1.5. References

1. Feynman, R. P. *Eng. and Sci.* **1960**, *23*, 22.
2. Antonietti, M.; Goeltner, C. *Angew. Chem. Int. Ed. Engl.* **1997**, *36*, 910.
3. Whitesides, G. M.; Mathias, J. P.; Seto, C. T. *Science* **1991**, *254*, 1312.
4. Ozin, G. A. *Chem. Commun.* **2000**, *1*, 419.
5. Hentze, H.-P.; Kaler, E. W. *Curr. Op. Coll. Interf. Sci.* **2003**, *8*, 164.
6. Paul, E. J.; Prud'homme, R. K. *Reactions and synthesis in surfactant systems*; Marcel Dekker, Inc, NY, **2001**; Vol. 100.
7. Suvegh, K.; Domjan, A.; Vanko, G.; Ivan, B.; Vertes, A. *Macromolecules* **1998**, *31*, 7770.
8. Hentze, H.-P.; Krämer, E.; Berton, B.; Förster, S.; Antonietti, M. *Macromolecules* **1999**, *32*, 5803.
9. Förster, S.; Berton, B.; Hentze, H.-P.; Kramer, E.; Antionietti, M.; Lindner, P. *Macromolecules* **2001**, *34*, 4610.
10. Ivan, B.; Almdal, K.; Mortensen, K.; Johannsen, I.; Kops, J. *Macromolecules* **2001**, *34*, 1579.
11. Jung, M.; German, A. L.; Fischer, H. R. *Coll. Polym. Sci.* **2001**, *279*, 105.
12. Hentze, H.-P.; Kaler, E. W. *Chem. Mater.* **2002**.
13. Antonietti, M.; Göltner, C. G.; Hentze, H.-P. *Langmuir* **1998**, *14*, 2670.
14. Lopez, E.; O'Brien, D. F.; Whitesides, T. H. *J. Am. Chem. Soc.* **1982**, *104*, 305.
15. O'Brien, D. F.; Armitage, B.; Benedicto, A.; Bennett, D. E.; Lamparski, H. G.; Lee, Y.-S.; Srisiri, W.; Sisson, T. M. *Acc. Chem. Res.* **1998**, *31*, 861.
16. Gin, D. L.; Gu, W.; Pindzola, B. A.; Zhou, W. J. *Acc. Chem. Res.* **2001**, *34*, 973.
17. Smith, R. C.; Fischer, W. M.; Gin, D. L. *J. Am. Chem. Soc.* **1997**, *119*, 4092.

18. Antonietti, M.; Conrad, J.; Thünemann, A. F. *Macromolecules* **1994**, *27*, 6007.
19. Ober, C. K.; Wegner, G. *Adv. Mater.* **1997**, *9*, 17.
20. Thünemann, A. F. *Prog. Polym. Sci.* **2002**, *27*, 1473.
21. Dreja, M.; Lennartz, W. *Macromolecules* **1999**, *32*, 3528.
22. Faul, C. F. J.; Antonietti, M.; Hentze, H.-P.; Sanderson, R. D. *Langmuir* **2001**, *17*, 2031.

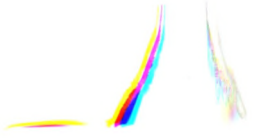

CHAPTER 2

THEORETICAL AND HISTORICAL BACKGROUND

2.1. Introduction

By definition, nanostructures are large supramolecular assemblies with well-defined architecture and at least one dimension in the range of 1 to 10^2 nanometers.[1] They are therefore inaccessible through synthesis based on the sequential formation of covalent bonds. Two different approaches can be used for the synthesis of these large assemblies, the "top-down" and the "bottom-up" approach.[2] The latter involves chemical synthesis and molecular self-assembly in order to produce large, structurally well-defined supramolecular assemblies. Thus, it places the synthesis of nanostructured materials beyond the field of molecular chemistry, into the field of supramolecular chemistry. This, so called chemistry beyond the molecule,[3] is based on the formation molecular assemblies through weak intermolecular bonds.

The use of self-assembled surfactant systems as reaction templates or media for the synthesis of nanostructured materials is one of the most promising "bottom-up" strategies. It combines a variety of synthetic techniques: i) the formation of molecules with intermediate complexity via covalent synthesis, ii) the assembly of the precursor molecules into large, stable aggregates/templates by means of weak noncovalent links such as hydrogen bonds and van der Waals interactions, iii) the stabilization of the fragile self-assembled template by polymerisation of and within the self-organised media.

This chapter describes some basic theory and definitions related to surfactant molecules and their self-assembly into ordered aggregates. Recent trends and achievements in materials synthesis by polymerisation of and within ordered surfactant and surfmer mesophases and those of polyelectrolyte-surfactant complexes will be discussed. The templating of organic polymers within other self-organised media, such as microemulsions[4] and block-polymer bulk phases[5] will, however, not be considered in detail here.

2.2. Surfactants and self-assembly

2.2.1. Surfactants – definition and classification

Surfactants are surface-active agents, characterized by their tendency to adsorb at surfaces and interfaces and lower the free energy of that phase boundary. This arises from their amphipilic character (the term is derived from the Greek words *amphi*, meaning both and *philic*, meaning loving), which relates to the two parts comprising the surfactant's molecule. The first part, referred to as a lyophobic group, consists of molecular components with little attraction for the solvent or bulk material. The second part, referred to as a lyophilic group, consists of chemical units with strong attraction for the solvent or bulk phase.[6] When the solvent is water the groups are referred to as hydrophilic (i.e. "water loving") and hydrophobic (i.e. "water hating") (Figure 2.1).

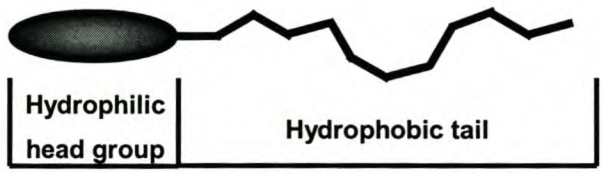

Figure 2.1. *The basic chemical structure of a surface-active molecule (redrawn from ref 6).*

Surfactants may be classified in many ways; the most common classification is based on the charge of the polar head group.[7] The four basic classes of surfactants that can be defined using the above classification are anionic, cationic, non-ionic and zwitterionic (Table 2.1). Depending on the presence of a characteristic chemical property other than surface activity, surfactants can be further divided into: polymerisable (polymerisable surfactants will be discussed in Chapter 3, Section 3.1), hydrolysable and polymeric.

Table 2.1. Structures of representative surfactants (adapted from ref 7).

Surfactant types - examples	Important facts
Anionic surfactants 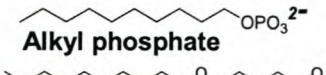 **Alkyl phosphate** 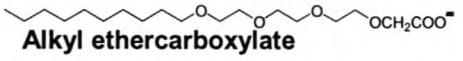 **Alkyl ethercarboxylate** 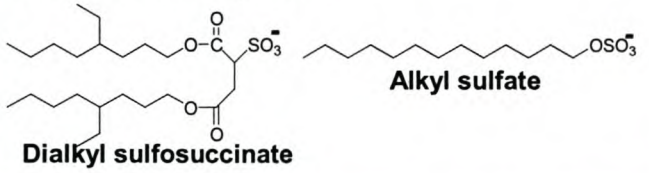 **Alkyl sulfate** **Dialkyl sulfosuccinate**	Not compatible with cationic surfactants; Sensitive to hard water; A short polyoxyethylene chain between the charged group and the tail improves salt tolerance and solubility in organic solvents.
Cationic surfactants 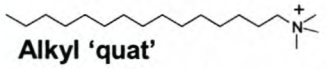 **Alkyl 'quat'** 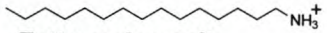 **Fatty amine salt** 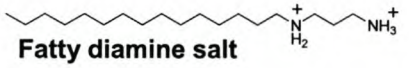 **Fatty diamine salt**	Not compatible with anionic surfactants; Hydrolytically stable cationic surfactants show the highest aquatic toxicity than most surfactants; Adsorb strongly to most surfaces
Non-ionic surfactants 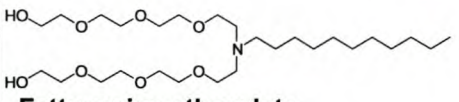 **Fatty amine ethoxylate** 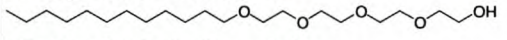 **Fatty alcohol ethoxylate** 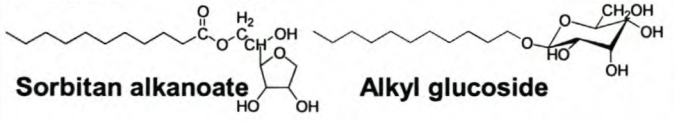 **Sorbitan alkanoate** **Alkyl glucoside**	Compatible with all other types of surfactants; Not sensitive to hard water; Their physicochemical properties are not markedly affected by electrolytes; Ethoxylated compounds become less water-soluble at higher temperatures
Zwitterionic surfactants 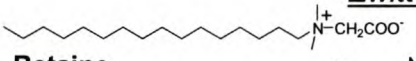 **Betaine** 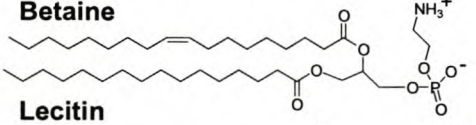 **Lecitin** 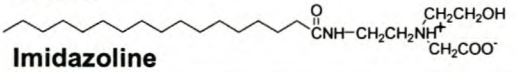 **Imidazoline**	Compatible with all other types of surfactants; Not sensitive to hard water; Stable to acid and bases; cause very low eye and skin irritation.

Surfactants can be further classified as emulsifiers, wetting agents, foaming agents and dispersants (Table 2.2), using the hydrophilic-lipophilic balance concept (HLB concept). Griffin introduced this concept in 1949 as a useful tool for the quantitative correlation of the chemical structure of non-ionic surfactants to their surface activity.[8,9] Griffin proposed to calculate the HLB of a surfactant from its chemical structure and to match that number with the HLB of the oil phase to be dispersed. Thus, the effectiveness of a given surfactant in a particular emulsion system would depend upon the balance between the HLBs of the surfactant and the oil phase involved.

Table 2.2. Griffin's HLB number concept (adapted from ref 7).

HLB number	Appearance of the aqueous solution	HLB number	Application
1 – 4	No dispersibility		
3 – 6	Poor dispersibility	3 – 6	W/O* emulsifier
6 – 8	Milky dispersion after agitation	7 – 9	Wetting agent
8 – 10	Stable milky dispersion	8 – 18	O/W* emulsifier
10 – 13	From translucent to clear	13 – 15	Detergent
13 – 20	Clear solution	15 – 18	Solubilizer

* - water in oil and oil in water emulsifier

2.2.2. Self-assembly principles and thermodynamics

Surfactant molecules spontaneously aggregate into a variety of super-structures in solution. This takes place in order to minimise unfavourable solvophobic interactions caused by their amphiphilic character.[10] Their self-organisation in dilute or concentrated solutions can be defined as the spontaneous association of molecules under equilibrium conditions into stable well-defined aggregates joined by many weak, reversible, noncovalent interactions.[1,3] Some of the typical types of noncovalent interactions that prevail in self-assembly are: hydrogen bonds,[11-13] van der Waals interactions, π-stacking,[14,15] donor-acceptor bonds, electrostatic interactions[16] (involving charges or dipoles) and hydrophobic interactions. Not all of these interactions are entirely different, for example, the hydrophobic interactions combine van der Waals interactions with the thermodynamic consequences of restricting the hydrogen bonding of water near a nonpolar interface.[17]

The strengths of some of the weak, noncovalent interactions used in self-assembly are in the range of 0.5 – 50 kJ/mol.[18] They differ significantly from the strengths of typical covalent bonds (~ 350 kJ/mol) but are comparable to thermal energies (RT ≅ 2.5 kJ/mol at 300 K). Therefore thermal energy can cause the weak bonds in 'soft' materials (soft because of the weakness of the interactions that hold them together) to break and reform, which enables the system to reach thermodynamic equilibrium. The following thermodynamic factors ensure the stability of self-assembled structures (Figure 2.2):

1. The unfavourable entropy ($T\Delta S$) resulting from the loss of translational entropy (on bringing two molecules together) and conformational entropy (on freezing of a freely rotating bond) can be significant on aggregation of a number of molecules.
2. Since the enthalpy contribution is small (due to the weakness of the interactions), large complementary areas of molecular surface must be in contact via van der Waals interactions or multiple hydrogen bonds to ensure the stability of the assembly. For instance, this is found in DNA double helix where hydrogen bonding and π-stacking interactions are important factors providing the stable molecular architecture.
3. The entropically favourable release of structured water on aggregation can compensate for the loss in translational entropy.

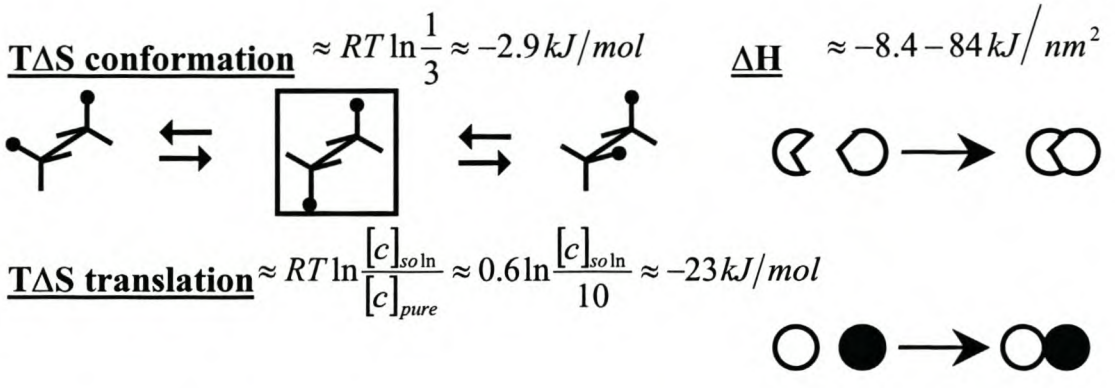

Figure 2.2. *Types of thermodynamic influences on self-assembly. ΔH depends on the types of molecular interactions, while $T\Delta S_{translational}$ depends on concentration and is given only as an approximation [redrawn from ref 1].*

2.2.2. Surfactant self-assembly at low and high surfactant concentrations

2.2.2.1. Micelles and interfacial curvature

When a surfactant molecule is introduced into water a distortion of the water structure to accommodate the solute molecules leads to an increase in the free energy of the system. This results in a tendency of the solute molecules to adsorb at solution interfaces, where their preferred molecular orientations reduce the surface free energy of the solution (an air-water interface has a higher surface tension than a air-hydrocarbon interface).[19] The surfactant molecules arrange at the air-water interface with their hydrocarbon tails directed away from the water.[10] An increase in surfactant concentration leads to a further decrease in the surface tension of the solution. At a specific surfactant concentration the surface tension of the solution remains constant over a wide composition range. This change in the solution properties is characterised by a large change in the rearrangement of the amphiphilic molecules. The "free monomeric" amphiphiles in solution aggregate into spherical-like aggregates termed micelles.

McBain and Martin first introduced the term micelle in 1914 when they tried to explain the considerable degree of aggregation present in surfactant solutions above a certain concentration.[20] McBain suggested the formation of two distinct types of micelles: i) spherical – composed of ionised salt molecules and ii) lamellar – from nonionic aggregates.[21] It was established that micelle formation occurs above a certain surfactant concentration, namely the critical micelle concentration (*cmc*) and a certain temperature – Kraft temperature (the temperature at which the solubility of the surfactant equals the *cmc*), when the interface is 'saturated' with surfactant molecules and a range of self-assembled surfactant structures originate in solution. The type and shape of the

aggregates formed in surfactant solutions (e.g. micelles, lamellae, hexagonal arrays of cylinders etc.) depend on the curvature of the surfactant-water interface. The latter has been explained on the basis of two models. The first model describes the curvature by a molecular packing parameter, *P*, while in the second one the curvature is analysed using differential geometry.

Introduced by Israelachvili *et al.*, the model based on the packing of molecules establishes geometric factors for the control of the packing of surfactants into association structures.[22,23] The effective area of the headgroup (a_0) with respect to the length of the hydrophobic tail for a given molecular volume (V/l_c) controls the interfacial curvature. The packing parameter is defined as the ratio between two areas: the effective headgroup area and the area occupied by the surfactant tails ($P = V/a_0 l_c$), where V is the volume of the molecule and l_c is the critical length of an extended hydrophobic chain, i.e. the maximum extent to which the chain can be stretched out before it can be no longer considered a fluid. Simple geometrical equations can be used to determine a_0 and the preferred aggregate shape. Tanford[24] provided equations for the determination of the critical length l_c of an extended saturated chain with n carbon atoms and the volume V of the hydrocarbon tail.

$$l_c[nm] \leq l_{\max} \approx (0.154 + 0.1265n) \qquad \textbf{(2.1)}$$

$$V[nm^3] \approx (27.4 + 26.9n) \times 10^{-3} \qquad \textbf{(2.2)}$$

where l_{max} is the maximum length of an extended saturated hydrocarbon tail.

The value of a_0 can be determined once the mean aggregation number (M) and the radius (R) of the aggregate are known. X-ray, neutron and light scattering, diffusion studies and sedimentation by ultracentrifugation are some of the

techniques used to determine aggregation numbers. For a micellar aggregate equation 2.3 can be used.

$$M = 4\pi R^2 / a_0 \qquad \textbf{(2.3)}$$

The effective area (a_0) is strongly influenced by the balance between the hydrophobic interactions between surfactant tails, which reduces a_0, and the tendency of headgroups to maximise their contact with water. Other parameters affecting a_0 are counterion concentration and pH.

Some of the typical aggregate structures characteristic for certain values of the packing parameter are summarised in Table 2.3.

Table 2.3. Preferred aggregate structure related to the critical packing parameter [adapted from ref 7].

Surfactant – critical packing shape and parameter	 $P < 1/3$	 $1/3 < P < 1/2$	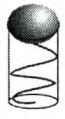 $P \approx 1$	 $P > 1$
Aggregate structure	Micelles	Hexagonally-packed cylinders	Bilayers and vesicles	Reversed micelles

The second model for the interfacial curvature is based on differential geometry of surfaces.[25] It uses the mean (H) and the Gaussian (K) curvatures to describe the curvature at each point of the surface of a continuous surfactant film (equation 2.4).

$$H = \frac{1}{2}\left(\frac{1}{R_1} + \frac{1}{R_2}\right) \qquad K = \left(\frac{1}{R_1 R_2}\right) \tag{2.4}$$

Where R_1 and R_2 are the radii for the so-called saddle surface in two perpendicular directions (Figure 2.3).

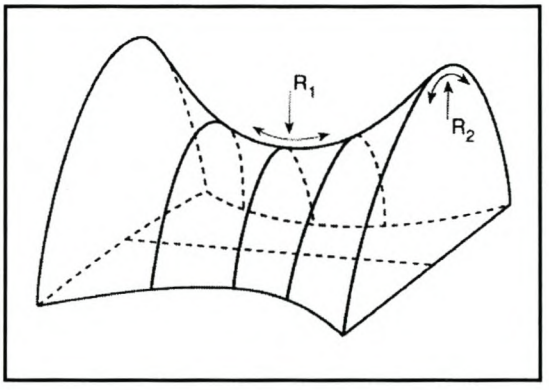

Figure 2.3. *Principle radii of the curvature of a saddle surface (portion of a surfactant film in a bicontinuous cubic structure). The surface is conventionally defined as positive if it points outwards at a point (e.g. $1/R_2$) [from ref 10].*

The interfacial curvature model is useful as it is associated with the elastic free-energy density, defined, for small deformations, as the sum of the mean and Gaussian curvatures. The interfacial curvature model is thus useful as it defines the elastic modules κ and $\bar{\kappa}$ for mean and Gaussian curvature, which characterise the flexibility of a surfactant film.[2]

2.2.2.2. Liquid-crystalline mesophases

Binary- or single-component surfactant systems exhibit a number of ordered phases (liquid-crystalline mesophases). These ordered phases possess orientational and/or weak positional order and thus reveal some of the physical properties of crystals but flow like liquids. The first liquid-crystalline phases were observed by the botanist F. Reinitzer,[26] however Lehmann[27] was the first to use the name liquid crystals. Liquid crystals or mesophases can be defined as condensed matter, which exhibit intermediate thermodynamic phases between the crystalline solid and the liquid states. Transitions between liquid-crystalline mesophases can arise from a change in temperature – thermotropic liquid crystals (Figure 2.4), concentration – lyotropic, or both temperature and concentration – amphotropic liquid crystals.

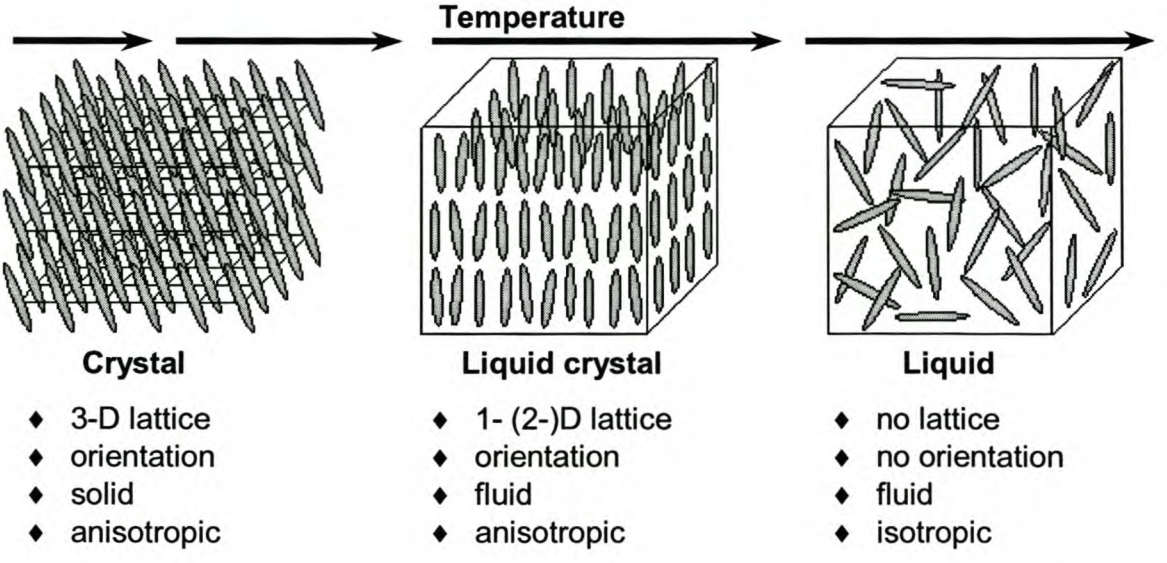

Figure 2.4. *Thermotropic liquid-crystalline mesophases between the solid and the isotropic liquid phase.*

In the simplest case of nematic liquid crystals the molecules possess only orientational, but no positional, long-range order. Smectic liquid crystals possess an additional positional order since the molecules are arranged in layers. Depending on whether the director is perpendicular to the layers or not, smectic A and C phases can be defined.

Binary surfactant/water systems have a more complex lyotropic liquid-crystalline behaviour than single-component systems. Phase transitions are observed to occur with an increase in surfactant concentration or temperature.[25] A typical phase diagram of a binary surfactant-water mixture of a single-tailed surfactant is illustrated in Figure 2.5.

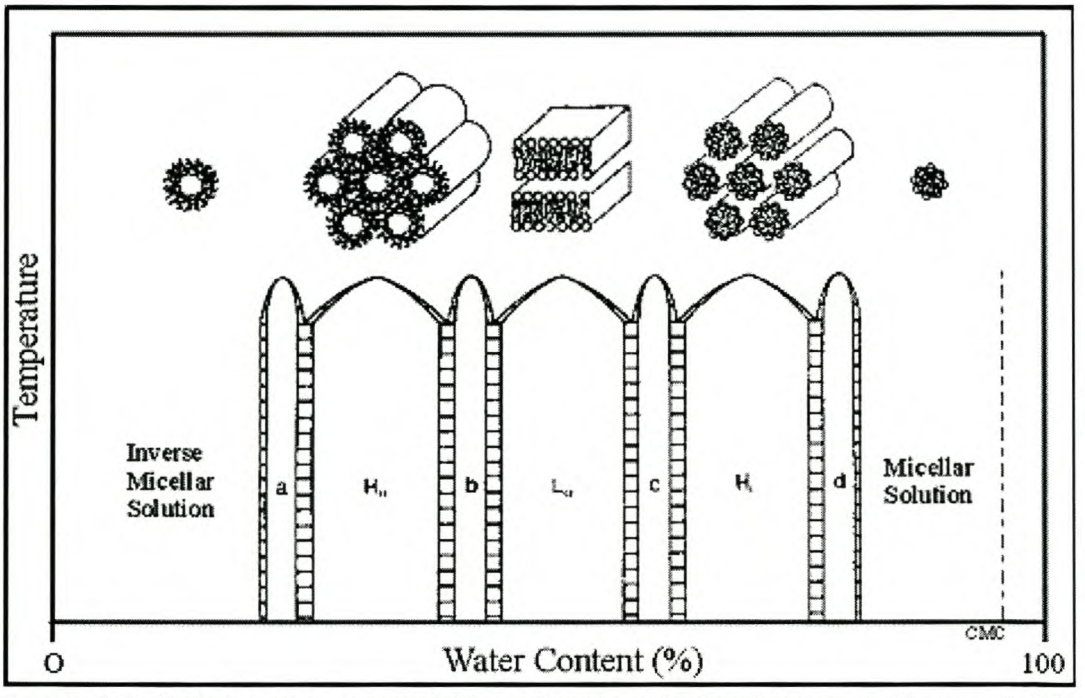

Figure 2.5. *Schematic representation of various lyotropic phases [from ref. 25].*

The almost vertical phase boundaries indicate that composition is the most important factor driving the transitions between the phases. However, for many binary systems the phase transitions are also temperature dependent and the boundaries deviate from vertical. For example, the boundaries of binary systems of double chain surfactants are often closer to horizontal, i.e. the change on temperature induces the transitions. Thus, with an increase in surfactant concentration/temperature the normal hexagonal (H_I), lamellar (L_α) and inverted hexagonal (H_{II}) phases are normally observed. Additionally, cubic phases (a,b,c,d) may occur between the isotropic and H_I, and also between the hexagonal and lamellar phases. Not all of the above mentioned phases are observed in the phase diagram of a given surfactant since the phase formation in individual systems is strongly dependent on the mean and the Gaussian curvatures of the interface. The presence of the intermediate phases between the hexagonal and lamellar mesophases is suggested to be necessary for the transition of the system from a system with a high curvature (cylinders) to a system with no curvature (bilayers).[28,29] Kekicheff *et al*. reported that the phase transitions (between high and zero curvature system) in the binary SDS/water system occur through the deformation of the hexagonally packed cylinders into the ribbons of the 2-D monoclinic phase, which merge to form a rhomboedral phase. Further deformation increases the change in the mean curvature of the interface and leads, trough a cubic, to a lamellar (zero curvature) phase.

The interfacial curvature is also influenced by the presence of other components (e.g. polyelectrolytes) in the mixture, which give rise to the variety of complex, self-organised structures existing in polyelectrolyte-surfactant complexes.

2.2.3. Aqueous solutions of ionic surfactants and oppositely charged polyelectrolytes

At low surfactant concentrations ($< T_1$) the aqueous solutions of surfactants and oppositely charged polyelectrolytes show a synergistic lowering of the surface tension. This is caused by the association of the two components and implies the formation of a highly surface-active complex. This observation was made originally by Jones who investigated the surface tension of mixtures of sodium dodecyl sulfate (SDS) and polyethyleneoxide (PEO).[30,31] It was also shown that the presence of a relatively low surface-active polymer in a surfactant solution leads to two new transitions in the surface tension/logarithm concentration of the surfactant plot (Figure 2.6).

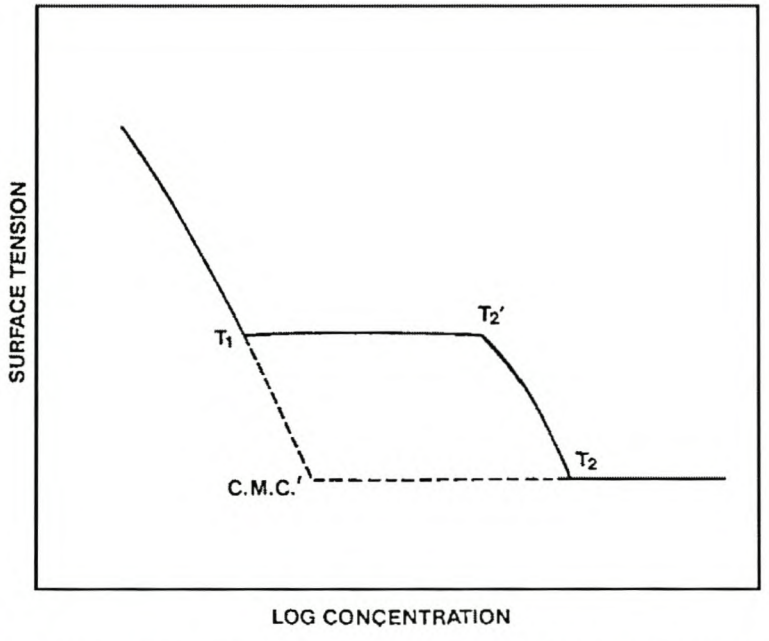

Figure 2.6. *Idealised surface tension/log concentration plot of a surfactant in the presence of a complexing polymer [from ref 33].*

The transition T_1 illustrates the commencement of interaction between the surfactant and the polymer, and T_2 the saturation point, beyond which increasing formation of regular micelles was observed. T_2^1 indicates the 'saturation' of the polymer sites with surfactant. Today T_1 is often referred to as the critical aggregation concentration (*cac*) and indicates the start of aggregate formation upon the interaction of surfactant molecules with the polymer chains. The values of T_1 are often two three orders of magnitude lower than the *cmc* of the surfactant. This is attributed to the fact that binding is a spontaneous de-charging process, while micelle formation and binding of charged surfactants to neutral polymers is a charging process.[32] Goddard illustrated the aggregation behaviour of mixtures of polyelectrolytes and surfactants in solution and at the interface as follows (see Figure 2.7).

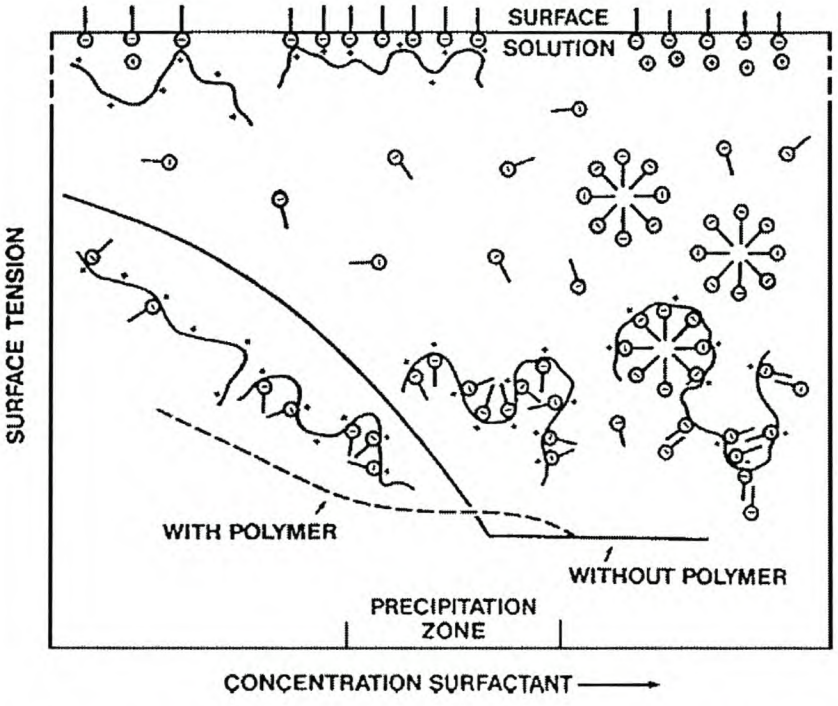

Figure 2.7. *Bulk and surface of a solution of a polycation with a fixed concentration and an anionic surfactant. [Based on a model proposed by Goddard[33]].*

The presence of the polyelectrolyte can be detected at very low surfactant concentrations (Figure 2.7, far left), where the formation of highly surface-active macromolecular complexes (with the alkyl groups pointing outwards, away from the solvent) are formed. The surface tension of the solution is already much lower than that of the surfactant-only system, indicating the much higher surface-activity of the formed species. With an increase in surfactant concentration more interaction with the polyelectrolyte is observed in solution and at the interface. The surface tension remains lower than that characteristic of the binary surfactant/water system. As the region of 1:1 stoichiometry between surfactant and polyelectrolyte is approached the complex starts to precipitate, which is first seen as turbidity in the solution. The surface tension is still lower in comparison with the system without the polyelectrolyte. Further increase in surfactant concentration leads to values for the surface tension similar to those of a surfactant-only system. This indicates that none of the polyelectrolyte molecules are at the air-water interface. Beyond the point of charge neutralisation the complex precipitate is redissolved according to a beads-on-a-string mechanism. In this model, introduced by Shirahama[34] in 1974, the excess surfactant interacts with the bound surfactant, forming micelle-like structures. These are in close association with the polyelectrolyte and resemble beads on a string. These 'beads' convert the complex into a polyelectrolyte of an opposite charge and are the reason for the re-solubilization of the complex.

The interactions between polyelectrolytes and surfactants of opposite charge are highly cooperative. They are driven not only by electrostatic interactions but mainly by the hydrophobic interactions between the alkyl tails of the bound surfactants.[35] This is suggested by the fact that monovalent surfactants add to polyelectrolytes even in the presence of divalent metal ions with higher concentration.[36] Cooperativity can be measured from the binding isotherms, which illustrate the interactions between polyelectrolytes and surfactants. The

binding isotherms are usually presented as the degree of binding β (defined as the amount of surfactant per ionic site on the polyelectrolyte) versus the overall surfactant concentration[37] (Figure 2.8).

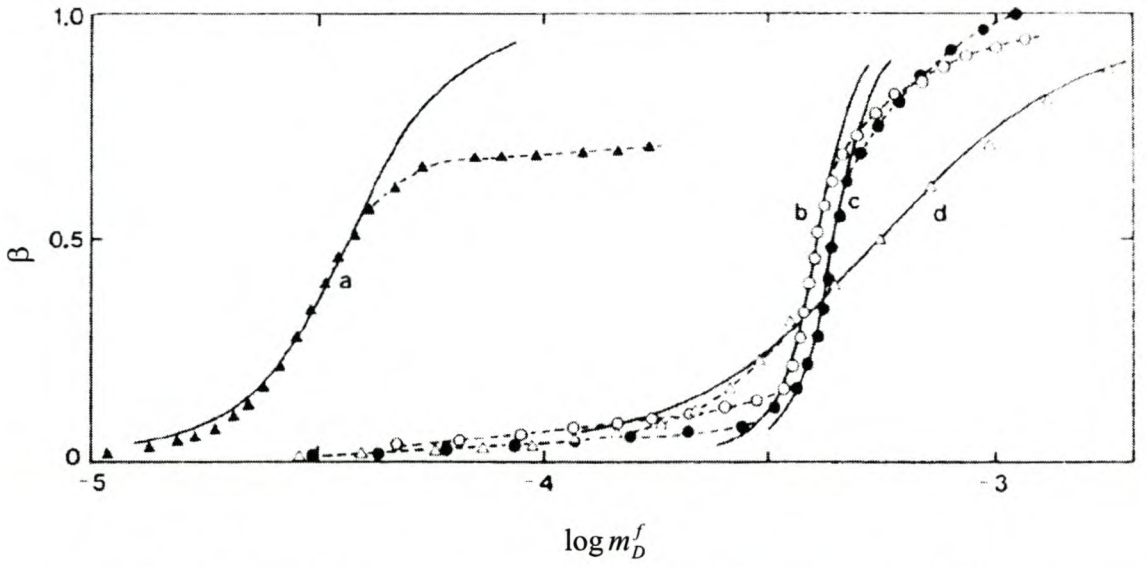

Figure 2.8. *Binding isotherms of dodecyltrimethylammonium (DTA^+) to different polyelectrolytes with an opposite charge [from ref. 37].*

The binding of the surfactant to the polyelectrolyte occurs at concentration (critical aggregation concentration, *cac*),[33] which is well below the *cmc* of the surfactant, i.e. the binding to the polyelectrolyte (involving both electrostatic and hydrophobic interactions) is much stronger than the binding between surfactants. The levelling of the binding isotherm at high surfactant concentrations represents saturation of the polymer with surfactant. However, in many systems levelling is not observed due to the resolubilisation of the complex following the beads-on-a-string model.

The Zimm-Bragg theory for helix coil transition, based on the nearest-neighbour interaction mode,[38] is a convenient way to describe the cooperativity of binding

of small ions by polyions. Schwarz[39] and Satake and Yang[40] derived the following relationships for the degree of binding, based on the assumption of nearest neighbour interactions only between the hydrophobic parts of bound surfactant ions (Eq. 2.5). The polyelectrolyte chains are also supposed to be sufficiently long so that the end effect is negligible.

$$2\beta - 1 = \frac{(y-1)}{\left[(1-y)^2 + 4yu^{-1}\right]^{1/2}} \qquad y = Kum_D^f \qquad \textbf{(2.5)}$$

Where

K: Binding constant between the surfactant and a binding site on the polyelectrolyte backbone

u: Cooperativity parameter, determined by the hydrophobic interaction between adjacent bound surfactants

Ku: Binding constant between a surfactant and a binding site adjacent to an already occupied binding site

m_D^f: Equilibrium concentration of free surfactant ions

Both K and u can be determined from the binding isotherm. The precise determination of u can however be difficult due to the strong cooperativity. For polyelectrolyte surfactant complexes u can easily have values as high as 1000. Ku can be determined from the isotherm as the reciprocal of the free surfactant concentration at $\beta = 0.5$.

The binding of surfactants to oppositely charged polyelectrolytes could be influenced by changes in both the surfactant and the polyelectrolyte structure (Table 2.4).

Table 2.4. A summary of some of the different parameters that affect the interactions between polyelectrolyes and surfactants.

Parameter	Effect
Polyelectrolyte	
1. Charge density	With decreasing charge density, phase transitions between structures are observed. In addition, the structures become less ordered[41] and the binding constant decreases.[42]
2.Chain hydrophobicity	The cooperativity of the interaction decreases with an increase in chain hydrophobicity.[43,44]
3. Molecular mass	The critical aggregation concentration increases and the cooperativity of binding decreases with a decreasing in polyelectrolyte molecular mass.[45]
Surfactant	
1. Chain length	Increase in the chain length leads to a decrease in *cac* and an increase in the interaction.[44,46]
2. Tail topology	Interactions of a polyelectrolyte with dimeric (gemini) surfactants is stronger than with the corresponding single-tailed ones.[43]
Salt concentration	The cooperativity parameter u is independent of salt concentration, while the binding constant K decreases strongly with increasing salt content.[35,36]
Temperature	Temperature may cause reversible volume and structure changes upon heating.[47]

2.2.4. Structure of polyelectrolyte-surfactant complexes in the solid state

Polyelectrolyte-surfactant systems in the solid state have only been extensively studied in recent years.[48-50] It is now well established that the 1:1 stoichiometric complexes can give rise to well-ordered mesoscopic structures.[51,52] The complexation, as described in 2.2.3, arises from ionic interactions or hydrogen bonding between the polyelectrolyte and the surfactant. A cooperative process involving the aggregation of the alkyl tails of the bound surfactant molecules further reinforces these ionic interactions. The resulting structures with high mechanical and thermal stability are essentially supramolecular comb copolymers, where every polymer unit has an electrostatically bound 'side-chain'.[53] The complexation is schematically shown in Figure 2.9.

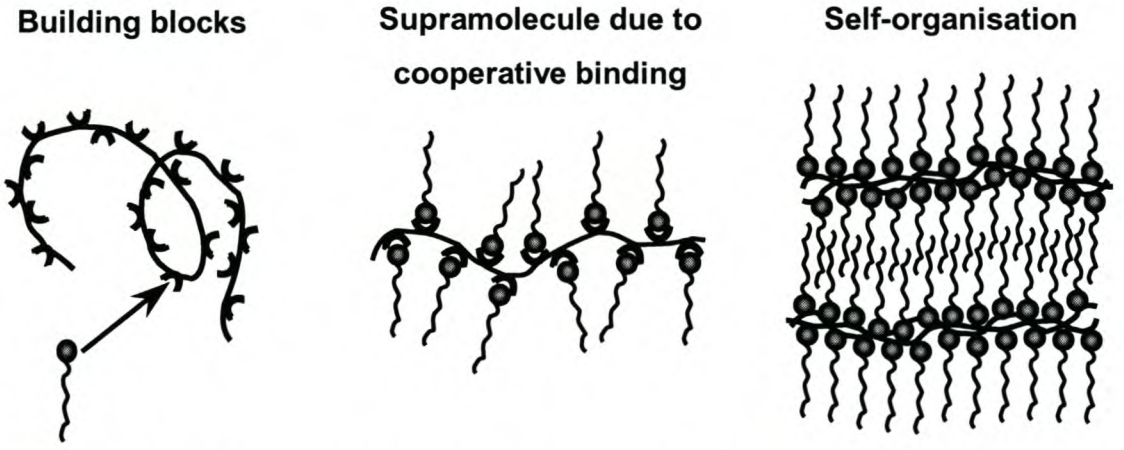

Figure 2.9. *The formation of comb-shaped supramolecules by the cooperative zipper mechanism between a polyelectrolyte and a surfactant, and their self-organisation into ordered structures [adapted from ref 53].*

The synthetic procedure is simple. It involves mixing of stoichiometric quantities of dilute aqueous solutions of the two building blocks (polyelectrolyte and surfactant).[16] The solid complex is then washed, until no more soluble

surfactant can be removed, and subsequently dried and cast into films. The properties of the dried complex may vary from elastomeric to brittle and from crystalline to non-crystalline depending on the type of building blocks used for the complexation. The simplicity of the synthesis and the wide variety of available polyelectrolytes and surfactants provides an opportunity for the design of ordered materials with adjustable macroscopic properties.

Lamellar structures, made of stacks of alternating hydrophilic and hydrophobic layers, are the most common architectures observed in the solid state of polyelectrolyte-surfactant complexes. This may be ascribed to the relative volume fractions of the two components and the fact that only a few common examples have been investigated. Only a few cases of hexagonal[54-56] and cubic[44] complexes have been described in the literature, while lamellar complexes have been formed when using linear[16,57], branched[58-61] and cross-linked[12,62] polyelectrolytes and oppositely charged single- or double-tail surfactants. Data suggests that polyelectrolyte chains impose some restrictions on surfactant chain packing that decrease the tendency of the surfactant to form ordered structures. The influence of the surfactant on the lamellar structures of polyelectrolyte-surfactant complexes has been illustrated in the work of Antonietti *et al.*[51] on complexes of poly(styrenesulfonate) (PSS) and alkyltrymethylammonium surfactants with different chain-lengths (C_n). An increase in the length of the alkyl tails of the surfactants destabilised the lamellar structure and leads to the appearance of undulations (ripples), with a body-centred cubic arrangement for the PSS-C_{18} complex. This was attributed to a change in the spontaneous interfacial curvature with increasing alkyl chain-length, leading to instability of the lamellar phase and finally to transitions to different phase structures. The increase in the spontaneous curvature, resulting in this case from the replacement of lecithin with inositol-enriched lecithin for complexation with poly(diallyldimethyammonium) chloride lead to a change from an undulating layered structure to an "egg-carton" structure for the latter

complex.[63] Thünemann *et al.*[64] reported a change from an ordinary lamellar phase for a poly(diallyldimethylammonium)-fluorinated sulfonate (Fluowet SB) complex to a perforated lamellar structure for a poly(diallyldimethylammonium)-fluorinated phosphate (Zonyl FSE) complex. The perforated lamellar phase was confirmed by both SAXS analysis and TEM. The positions of the reflections in the X-ray diagram of the phosphate complex (two broad reflections with relative positions $1:1^{1/3}$ and three equidistant reflections) were consistent with ordered lamellar stacks with hexagonally-ordered perforations with an in-plane centre-to-centre distance of 3.7 nm.

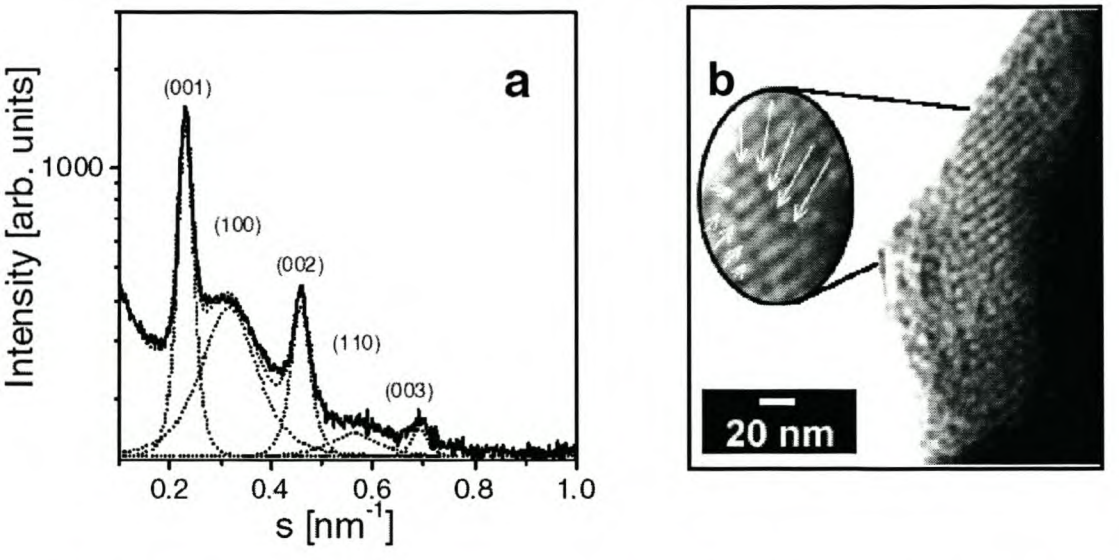

Figure 2.10. *The perforated lamellar structure of the poly(diallyldimethylammonium)/Zonyl FSE complex visualised by a) x-ray scattering and b) transmission electron microscopy [from ref 64].*

The structure of and glass transitions in polyelectrolyte-surfactant complexes are also sensitive towards changes in the charge density of the polyelectrolyte backbone. The systematic variation of the charge density in a series of ionene-lipid complexes lead to an increase in the glass transition and a decrease in the layer thickness with the increase in charge density of the polyelectrolyte.[65] The

decrease in layer thickness was attributed to an interdigitated morphology of the alkyl tails at low charge densities, which strengthens the hydrophobic interactions and aids the structure forming and the stability of the complexes. The increase in charge density of the polyelectrolyte has also been reported to increase molecular order on the atomic length scale.[64]

The supramolecular structuring of polyelectrolyte-surfactant complexes has a substantial influence on their properties and can be utilised as a powerful tool for the production of novel functional materials. Research in the field shows that the incorporation of functionalities into solid polyelectrolyte-surfactant complexes leads to polymeric nanostructured materials with a variety of tuneable properties. Thus, fluorescent,[66] electroluminescent,[67,68] conducting,[54] low surface energy[64,69] and polymerisable[70] complexes have been synthesized. The dependence of optical properties on polymer morphology has recently been illustrated by complexing a highly fluorescent alkylated polymer, poly(2-ethylhexyloxycarbonyl-1,4-phenyleneethynylene carboxylate) (PPE), with dialkylammonium bromides. The effect of the complexation is pronounced in the solid state where the emission properties of the PPE are structureless, while those of the PPE complex show detailed structuring.[66] Thin films of PPE complexes with a variety of counter ions have also been reported to exhibit electroluminescence tuneable with the type of counter ion – electroluminescence spectra shift to higher wavelengths when more polarizable counter ions are used. The turn-on points (calculated from the current-voltage diagrams) of thin films of the complexes were much lower than those of an analogue with covalently bound side chains.[68] Furthermore, dye-surfactant complexes (formed in a similar, highly cooperative manner, to polyelectrolyte-surfactant complexes) with almost perfect pleochroism, resulting from a supramolecular, fibrillar morphology of the complex, have been reported.[14]

Low-energy surfaces and coatings have been prepared by the self-assembly of complexes of polyelectrolytes and fluorinated surfactants.[64] The surface energy of these materials on different substrates can easily be tuned with the surfactant's chain length. The surface energy decreases with increasing chain length and is in the range 6-18 mJm^{-2}.

Surfactant chains containing an acidic group may act as plasticizers and as dopants for conjugated polymers such as polyaniline. This leads materials with enhanced thermoplastic processibility and an increased conductivity.[54]

The structural complexity of polyelectrolyte-surfactant complexes combined with the use of different functionalities within a single material offer exciting possibilities for the design of "smart" materials with tuneable macroscopic properties. The variety of structures available within these mechanically and thermally stable materials are still to be explored as templates for organic polymerisation reactions.

2.3. Templating of organic polymerisation reactions

Templating or creating a 1:1 copy of the inherently fluid lyotropic liquid-crystalline (LLC) phases is a promising approach to the design of new nanostructured materials, required for a variety of material applications. This synthetic strategy involves the formation of self-assembled aggregates and their subsequent stabilization by polymerisation of or within the self-organised medium.[71,72] The process is complex due to the fact that the reaction takes place in a highly dynamic, non-equilibrium medium, where, as the monomer is being consumed, a new polymer phase appears. Further complications arise from the tendency of the polymer chain to coil rather than stay constrained in the organised reaction medium or the chemical incompatibility of the polymer with the surfactant. Reactions have been performed in the LLC phases of ordinary or reactive surfactants with the success of the templating relying on adjusting thermodynamic as well as kinetic parameters. Surfactant phases with slow exchange dynamics and long rearrangement times were used in order to suppress phase separation and disruption. Cross-linking of or within the template during polymerisation is often used to 'compensate' for the entropy loss caused by confining the formed polymer network to the reaction geometry.

2.3.1. Templating of surfactant phases – "transcriptive" and "reconstructive" templating approaches

Self-organised surfactant solutions have received much attention as reaction templates for the synthesis of organic nanostructured materials.[73] The surfactant aggregates act as templates for the polymerisation of organic monomers, which polymerise around the self-assembled template and the final product, after template removal, is a copy of the original template structure – "transcriptive" synthesis (Figure 2.11).

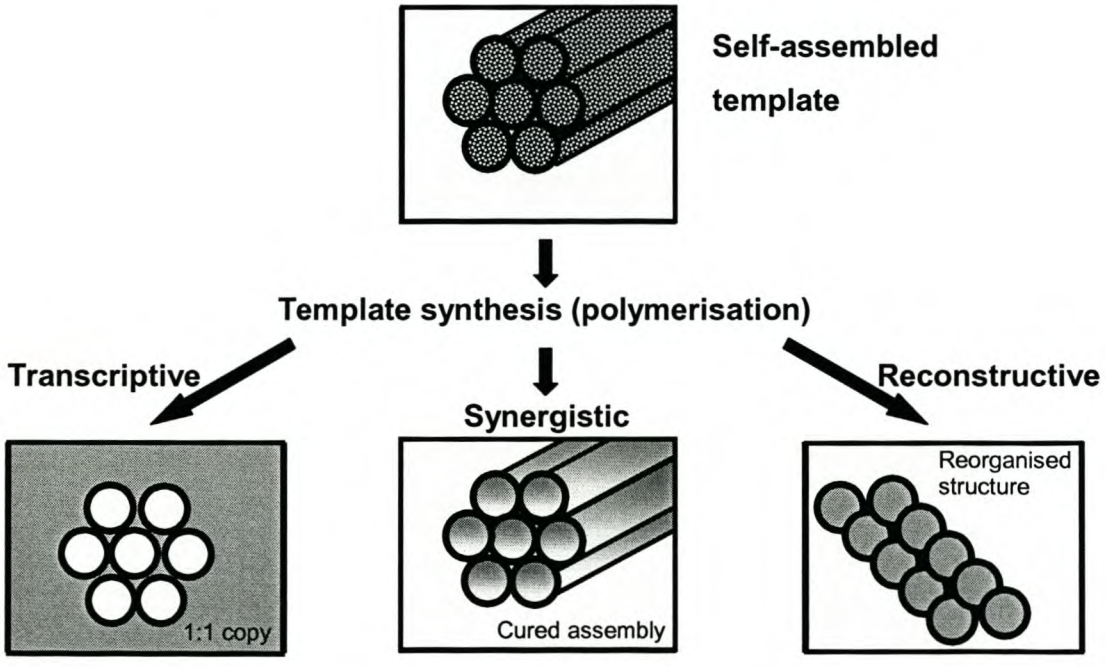

Figure 2.11. *Scheme of various templating approaches [redrawn from ref. 73].*

Transcriptive synthesis offers the advantage of working with common monomers and surfactants with well-known phase diagrams. Only a few cases with retention of template structure have however been reported in the literature.[74-76] This is due not only to the dynamic nature of the self-assembled

2.3.1. Templating of surfactant phases – "transcriptive" and "reconstructive" templating approaches

Self-organised surfactant solutions have received much attention as reaction templates for the synthesis of organic nanostructured materials.[73] The surfactant aggregates act as templates for the polymerisation of organic monomers, which polymerise around the self-assembled template and the final product, after template removal, is a copy of the original template structure – "transcriptive" synthesis (Figure 2.11).

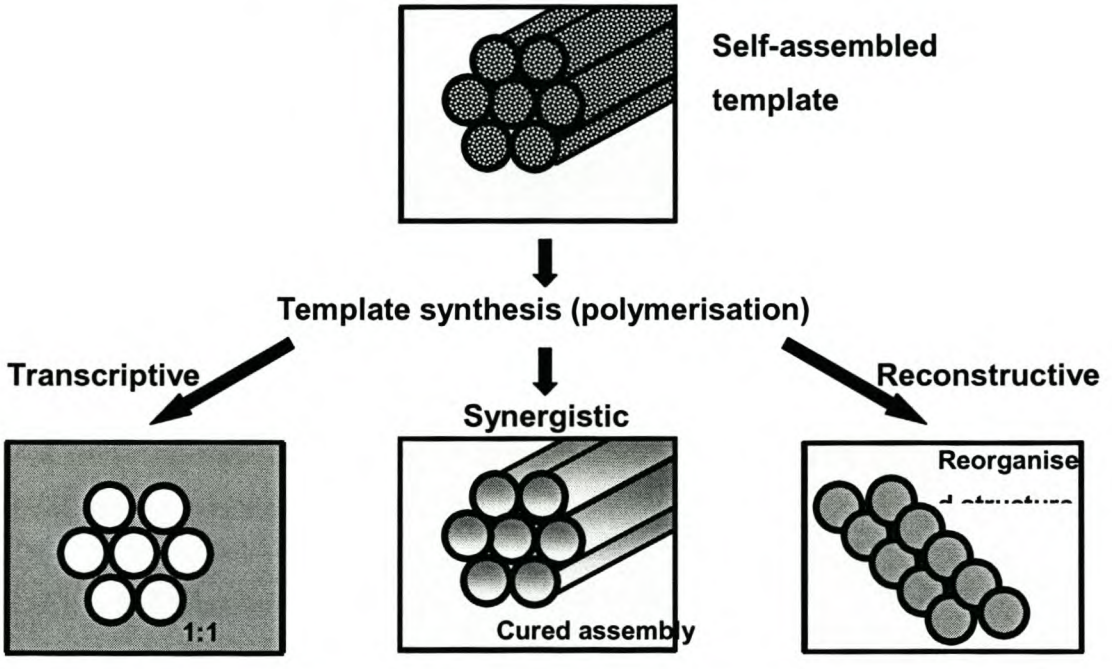

Figure 2.11. *Scheme of various templating approaches [redrawn from ref. 73].*

Transcriptive synthesis offers the advantage of working with common monomers and surfactants with well-known phase diagrams. Only a few cases with retention of template structure have however been reported in the literature.[74-76] This is due not only to the dynamic nature of the self-assembled

aggregates but also to the fact that the phase behaviour of the starting monomer/surfactant/water system is generally quite different from that of the polymerised polymer/surfactant/water system. In addition, non-equilibrium conditions can be expected, as the composition gradually changes during polymerisation. The loss of entropy due to the confinement of the polymer chains to the template geometry also plays a key role. Thus, phase separation into polymer-rich and surfactant-rich phases often occurs in these systems. Furthermore, the process of extraction of the template from the formed polymer matrix may itself cause morphological changes to occur. Despite the phase separation, which takes place during polymerisation, polymers with interesting hierarchical morphologies may arise as a result of the indirect templating of the parental template structure – "reconstructive" synthesis.[72,77,78] The template aggregates serve only as the locus of polymer nucleation, while polymer growth takes place on a larger length scale. The resulting polymers are indirect copies of the template. They have high porosities and surface areas and order on length scales from nano- to micrometer.

Templating of equilibrium cationic vesicles of cetyltrimethylammonium tosylate (CTAT) and sodium dodecylbenzenesulfonate (SDBS) is one of the few reported cases of direct templating in surfactant phases when using standard monomers such as styrene and DVB.[76] Hollow polymer spheres of 60 nm in diameter that are stable to dialysis, vacuum drying and resuspension were obtained. On the other hand, templating of kinetically stabilized vesicles (formed after shearing) lead to morphologies that do not resemble the vesicle structure. "Parachute", "necklace" and "matrioshka" morphologies of the vesicle-polymer hybrid have been reported.[79-81]

Templating of the lamellar[82] and hexagonal phases has been unsuccessful mainly due to the low viscosity and the flexibility of these phases, which allows for rearrangement and phase disruption to take place during polymerisation.

Mesoscopic demixing was observed on cross-linking within lamellar and hexagonal systems of bis(2-ethylhexyl) sulfosuccinate sodium salt (AOT)/styrene/DVB/water.[73] Strands of polymer beads 100 nm in diameter resulted from the polymerisation in the two-dimensional hexagonal phase, while only clusters of polymer particles were formed on the templating of the lamellar phase. Monomer content, initiator concentration and degree of cross-linking strongly affect structure formation.

Templating of the bicontinuous cubic phase was investigated as a synthetic tool for the production of monodisperse microporous materials. Anderson[83,84] believed that the slow rearrangement dynamics in the highly viscous cubic phases (the highest viscosity of all surfactant mesophases) would prevent template disruption during polymerisation. Templated cubic materials from a variety of monomers (styrene, methyl methacrylate and acrylamide) were reported. However, subsequent work in this field gave materials with pore size orders of magnitude larger than the original template. A mechanism for the change in pore size suggests that after polymerisation the surfactant template is embedded in the polymer gel and the SAXS patterns are those of the template-polymer composite and not necessarily those of the pure polymer matrix. Indirect adjustment of the pore size of the gels by varying the type and the amount of surfactant allows for an exciting possibility of creating materials with desired porosity and mechanical properties.

2.3.2. Templating of the organised phases of polymerisable surfactants – synergistic approach

In synergistic synthesis the monomer must possess surface activity and be the only, or at least one of the, entities forming the template aggregates, therefore the use of polymerisable surfactants is required. Cured template structures, instead of the 1:1 copies product of the transcriptive approach, result from this synthesis. Thus, template extraction is no longer required since after polymerisation the surfmers forming the template are covalently fixed into a mechanically and chemically stable supramolecular material.

Initially it was not possible to preserve the template structure when applying the synergistic synthesis to lyotropic phases and vesicular solutions. Phase transitions or low conversions were observed.[85-87] However, the pioneering work of O'Brien showed that the self-organisation of lipids can be sufficiently robust to allow polymerisation of the constituting components.[88,89] This was attributed to the fact that self-organised lipids do not optimise their assembled structures via exchange of lipids between the single layers and between the assemblies (due to very low molecular solubility). Only lateral diffusion within the bilayers occurs, which provides high probability for successful polymerisation. A variety of polymerisable groups have been polymerised in phospholipid vesicle bilayers using photo-, thermally-sensitive or redox initiators.[90] In some cases the reactive amphiphiles were converted to polymers with high yield (>90%).[91] Linear and cross-linked polymer networks were formed from monomeric lipid assemblies depending, on the number of polymerisable groups per monomeric lipid. The presence of two or more reactive groups in a lipid molecule led to cross-linked polymer networks. Cross-linking led to an increase in bilayer stability (expressed as resistance to dissolution by either surfactants or organic solvents) coupled with a decrease in permeability.[92]

O'Brien *et al.* further extended their research to nonlamellar lipid phases and successfully templated the inverse hexagonal (H_{II}) and the inverse cubic (Q_{II})[93] lipid phases. Polymerisation of the H_{II} phase, formed by phosphoethanolamine, a di-functional phospholipid with a polymerisable group in each chain, produced encapsulated aqueous lipid nanotubes with tuneable dimensions. The polymerisation, induced by a redox initiator, was used to "fix" the size of the temperature-dependent hexagonally arranged aqueous channels.[94] The Q_{II} phase was stabilized by the thermal polymerisation of the bicontinuous mixture (3:1 molar mixture) of mono-dienoyl-substituted phosphoethanolamine and bis-dienoyl-substituted phosphocholine. Transmission electron microscopy (TEM) of thin sections of the polymerised samples showed square lattices suggestive of a cubic phase, interpenetrated with water channels ~ 6 nm in diameter and a centre-to-centre distance between the channels of 12-17 nm.[95] The fact that this successful approach, i.e., sufficient robustness and low solubility is not restricted to the polymerisation of lipids was again proven by O'Brien, by the one-dimensional polymerisation of octa-substituted phtalocyanines with reactive sites placed at the side chains of the disk-like monomer.[96]

Further advances in the field were made by Gin *et al.*, who designed new surfmers permitting the stabilization of the H_{II} phase.[97] The surfmers, with a characteristic tapered shape (i.e., a small hydrophilic head group and a broad flattened hydrophobic tail), contained styrene,[98] acrylate and diene groups as polymerisable moieties. The three-tailed acrylate[99] and diene[100] derivatives of gallic acid salts were polymerised in the H_{II} phase using radical photoinitiators, to form robust organic networks of hexagonally packed channels. Tuning of the network dimensions was achieved by varying of the tail length[101] of the surfmers or the type of the head group counter ion.[102] The networks were mechanically and thermally stable and insoluble in common organic solvents. The networks were furthermore used as templates for the conversion of

different reagents trapped inside the aqueous nano-sized channels (Figure 2.12).

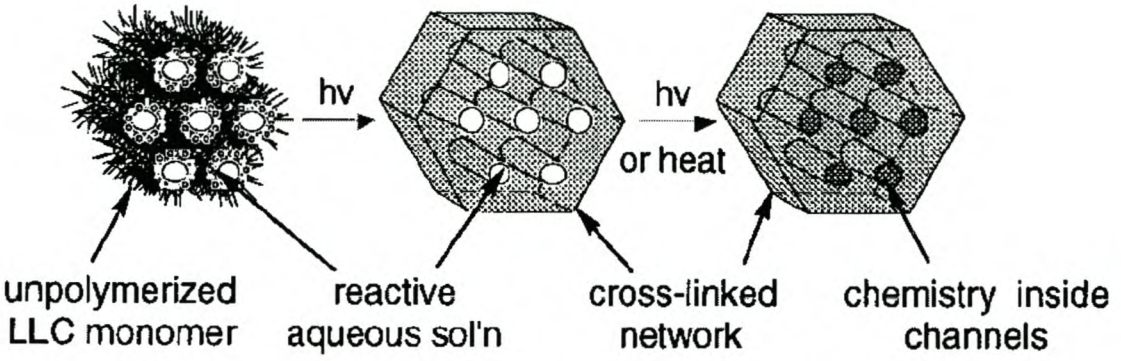

Figure 2.12. *Synthesis of nanocomposites using polymerisable H_{II} assemblies. [from ref 97].*

Nanocomposites of the luminescent poly(p-phenylenevinylene) (PPV) obtained in the hexagonally-packed aqueous channels exhibited significantly enhanced photoluminescence and long-term stability.[99] Gin *et al*. also developed the first phosphonium diene amphiphiles to be homopolymerised in the hexagonal (H_I) phase with phase retention and a high degree of polymerisation (>90%).[103]

2.3.3. Templating of the organised phases of comb-shaped polymer-amphiphile systems

Amphiphilic graft copolymers are only one of the examples of macromolecules with comb-shaped or 'hairy-rod' architectures. The side chains are attached to the polymer backbone by means of covalent bonding. Similarly to their low molecular surfactant analogues, both amphiphilic block and graft copolymers self-assemble into variety of structures, but on much larger length-scales (10 to 200 nm).[104-106] The high viscosity and the slow exchange dynamics characteristic of the assemblies of amphiphilic copolymers make them more robust templates than surfactants. This robustness has already been used for the synthesis of an array of organic[107,108] and inorganic mesoporous materials.[109]

Polyelectrolyte-surfactant complexes are also an example of macromolecules with comb-shaped architecture. They offer the advantage of utilizing both the order on the smaller length scales, characteristic of dynamic surfactant systems, and the robustness provided by the polymer molecules. The side chains of the comb-shaped macromolecules, composed of low molecular weight amphiphilic molecules, can be attached to the polymer chain by hydrogen or coordination bonds,[110] or as already discussed in Section 2.2.4, by ionic interactions. Ikkala and ten Brinke *et al.*[53] used this concept for the production of functional materials with controlled structure at several length scales. Instead of performing polymerisation reactions within the organised assemblies, selective cleaving of the hydrogen bonded amphiphilic side chains was performed, which yielded solid structures with empty cylindrical 'hairy' walls.[111] Furthermore, by cleaving the amphiphilic zinc dodecylbenzenesulfonate ($Zn(DBS)_2$) molecules coordinated to the poly(4-vinylpyridine) (P4VP) block of a polystyrene-P4VP block copolymer, dense polymer brushes can be formed.[112] Coordination offers an advantage over

hydrogen bonding as it allows the bonding of higher molecular weight amphiphiles.

As mentioned before, amphiphilic molecules can also be attached ionically polyelectrolyte backbone and form, through self-assembly, a variety of mechanically and thermally stable mesomorphous structures (see 2.2.4). Little is yet known about templating of organic polymer reactions within the polyelectrolyte-surfactant complexes. Recently a polydiallyldimethylammonium / dodecylsulfate (pDADMA/DS) hexagonal complex was swollen selectively with hydrophobic monomers.[55] After thermal polymerisation and template removal the polymer structures were investigated by small-angle X-ray scattering and transmission electron microscopy, revealing that needle-like polymer particles were formed instead of extended replicas of the template. This was due to the low loading capabilities of the template, which only allowed swelling with up to 17 wt% of monomer before phase disruption. Complexes of a polyelectrolyte containing photo-labile diazosulfonate chromophores were reported to lose the ionic interactions between the polyelectrolyte and the surfactant on irradiation with UV light.[113] Radiation-induced polymerisation in complexes of head-group functionalised methacrylate surfactants also did not yield a cured template structure.[70] Instead, monomer degradation was observed due to the reduced mobility of the surfmer tails within the complex assembly.

It is clear that the potential of polyelectrolyte-surfactant complexes as templates for polymerisation reactions has not been explored to the fullest. This creates a unique niche to be investigated, namely approaching templating from a different perspective. In this work the author describes an improved technique for successful templating within polyelectrolyte-surfactant complexes. Tail-functionalised surfmers with enhanced flexibility of their reactive groups are used in combination with flexible hydrophobic co-monomers. Allowing the complexes to withstand high degrees of swelling.

2.4. References

1. Whitesides, G. M.; Mathias, J. P.; Seto, C. T. *Science* **1991**, *254*, 1312.
2. Hamley, I. W. *Angew. Chem. Int. Ed.* **2003**, *42*, 1692.
3. Lehn, J.-M. *Supramolecular Chemistry*; VCH: Weinheim, **1995**.
4. Co, C. C.; Cotts, P.; Burauer, S.; de Vries, R.; Kaler, E. W. *Macromolecules* **2001**, *34*, 3245.
5. Lipic, P. M.; Bates, F. S.; Hillmyer, M. A. *J. Am. Chem. Soc.* **1998**, *120*, 8963.
6. Myers, D. *Surfactant Science and Technology second edition*; VCH Publishers, Inc.: New York, **1992**.
7. Jönsson, B.; Lindman, B.; Holmberg, K.; Kronberg, B. *Surfactants and polymers in aqueous solution*; John Wiley & Sons: Chilchester, **1999**.
8. Griffin, W. C. *J. Soc. Cosmet. Chem.* **1949**, *1*, 311.
9. Griffin, W. C. *J. Soc. Cosmet. Chem.* **1954**, *5*, 259.
10. Evans, D. F.; Wennerström, H. *The Colloidal Domain*; Wiley-VCH:, **1994**.
11. Rebek, J. *Angew. Chem. Int. Ed. Engl.* **1990**, *29*, 245.
12. Luyten, M. C.; Alberda van Ekenstein, G. O. R.; Wildeman, J.; ten Brinke, G.; Ruokolainen, J.; Ikkala, O.; Torkkeli, M.; Serimaa, R. *Macromolecules* **1998**, *31*, 9160.
13. Faul, C. F. J.; Camerel, F. *Chem. Commun.* **2003**, *15*, 1958.
14. Faul, C. F. J.; Antonietti, M. *Chem. Eur. J.* **2002**, *8*, 2764.
15. Hunter, C. A.; Sanders, J. K. M. *J. Am. Chem. Soc.* **1990**, *112*, 5525.
16. Antonietti, M.; Conrad, J. *Angew. Chem. Int. Ed. Engl.* **1994**, *33*, 1869.
17. Dill, K. A. *Science* **1990**, *250*, 297.
18. Faul, C. F. J.; Antonietti, M. *Adv. Mater.* **2003**, *15*, 673.
19. Hartley, G. S. *Progress in the Chemistry of Fats and Other Lipids*; Pergamon Press: London, **1955**.
20. McBain, J. W.; Martin, J. T. *J. Chem. Soc.* **1914**, *105*, 957.

21. McBain, J. W.; Salmon, C. S. *J. Am. Chem. Soc.* **1920**, *43*, 426.
22. Israelachvili, J. N.; Mitchell, D. J.; Ninham, B. W. *J. Chem. Soc. Faraday Trans.* **1976**, *72*, 1525.
23. Israelachvili, J. N. *Intermolecular and Surface Forces*; Academic press: new York, **1992**.
24. Tanford, C. *The Hydrophobic Effect: Formation of Micelles and Biological Membranes*; Wiley: New York, **1980**.
25. Seddon, J. M. *Biochim. Biophys. Acta* **1990**, *1031*, 1.
26. Reinitzer, F. *Liq. Cryst.* **1989**, *5*, 7.
27. Lehmann, O. *Ztschr. Phys. Chem.* **1889**, *4*, 462.
28. Kekicheff, P.; Grabielle-Madelmont, C.; Ollivon, M. *J. Colloid Interf. Sci.* **1989**, *131*, 112.
29. Kekicheff, P.; Orsay, F. *J. Colloid Interf. Sci.* **1989**, *131*, 133.
30. Jones, M. N. *J. Colloid Interf. Sci.* **1967**, *23*, 36.
31. Jones, M. N. *J. Colloid Interf. Sci.* **1968**, *26*, 532.
32. Shirahama, K.; Sato, S.; Niino, M.; Takisawa, N. *Coll. Surf. A: Psychochem. Eng. Asp.* **1996**, *112*, 233.
33. Goddard, E. D. *Coll. Surf.* **1986**, *19*, 301.
34. Shirahama, K.; Tsujii, K.; Takagi, T. *J. Biochem.* **1974**, *75*, 309.
35. Hayakawa, K.; Kwak, J. C. T. *J. Phys. Chem.* **1982**, *86*, 3866.
36. Hayakawa, K.; Kwak, J. C. T. *J. Phys. Chem.* **1983**, *87*, 506.
37. Hayakawa, K.; Santerre, J. P.; Kwak, J. C. T. *Macromolecules* **1983**, *16*, 1642.
38. Zimm, B. H.; Bragg, J. K. *J. Chem. Phys.* **1959**, *31*, 526.
39. Schwarz, G. *Eur. J. Biochem.* **1970**, *12*, 442.
40. Satake, I.; Yang, J. T. *Biopolymers* **1976**, *15*, 2263.
41. Zhou, S.; Burger, C.; Yeh, F.; Chu, B. *Macromolecules* **1998**, *31*, 8157.
42. Kosmella, S.; Koetz, J.; Shirahama, K.; Liu, J. *J. Phys. Chem. B* **1998**, *102*, 6459.
43. Zana, R.; Benrraou, M. *J. Colloid Interf. Sci.* **2000**, *226*, 286.

44. Zhou, S.; Yeh, F.; Burger, C.; Chu, B. *J. Phys. Chem. B* **1999**, *103*, 2107.
45. Liu, J.; Takisawa, N.; Shirahama, K.; Abe, H.; Sakamoto, K. *J. Phys. Chem. B* **1997**, *101*, 7520.
46. Kogej, K.; Skerianc, J. *Langmuir* **1999**, *15*, 4251.
47. Isogai, N.; Gong, J. P.; Osada, Y. *Macromolecules* **1996**, *29*, 6803.
48. Ober, C. K.; Wegner, G. *Adv. Mater.* **1997**, *9*, 17.
49. Macknight, W. J.; Ponomarenko, E. A.; Tirrel, D. A. *Acc. Chem. Res.* **1998**, *31*, 781.
50. Zhou, S.; Chu, B. *Adv. Mater.* **2000**, *12*, 545.
51. Antonietti, M.; Conrad, J.; Thünemann, A. F. *Macromolecules* **1994**, *27*, 6007.
52. Thünemann, A. F. *Prog. Polym. Sci.* **2002**, *27*, 1473.
53. Ikkala, O.; ten Brinke, G. *Science* **2002**, *295*, 2407.
54. Kosonen, H.; Ruokolainen, J.; Knaapila, M.; Torkkeli, M.; Jokela, K.; Serimaa, R.; ten Brinke, G.; Bras, W.; Monkman, A.; Ikkala, O. *Macromolecules* **2000**, *33*, 8671.
55. Faul, C. F. J.; Antonietti, M.; Hentze, H.-P.; Sanderson, R. D. *Langmuir* **2001**, *17*, 2031.
56. Thünemann, A.; Ruppelt, D.; Shunji, I.; Müllen, K. *J. Mater. Chem.* **1999**, *9*, 1055.
57. Ponomarenko, E. A.; Waddon, A. J.; Bakeev, K. N.; Tirrel, D. A.; MacKnight, W. J. *Macromolecules* **1996**, *29*, 4340.
58. Ujiie, S.; Takagi, S.; Sato, M. *High Perform. Polym.* **1998**, *10*, 139.
59. Chen, H.-L.; Hsiao, M.-S. *Macromolecules* **1999**, *32*, 2967.
60. Thünemann, A. F.; Kubowicz, S.; Pietsch, U. *Langmuir* **2000**, *16*, 8562.
61. Thünemann, A. F.; General, S. *Langmuir* **2000**, *16*, 9634.
62. Khandurina, Y. V.; Dembo, A. T.; Rogacheva, V. B.; Zezin, A. B.; Kabanov, V. A. *Polym. Sci.* **1994**, *36*, 189.
63. Antionietti, M.; Wenzel, A.; Thünemann, A. *Langmuir* **1996**, *12*, 2111.

64. Thünemann, A. F. *Polym. Int.* **2000**, *49*, 636.
65. Antionietti, M.; Wenzel, A. *Coll. Surf. A: Psychochem. Eng. Asp.* **1998**, *135*, 141.
66. Thünemann, A.; Ruppelt, D. *Langmuir* **2000**, *16*, 3221.
67. Cimrova, V.; Schmidt, W.; Rulkens, R.; Schulze, M.; Meyer, W.; Neher, D. *Adv. Mater.* **1996**, *8*, 585.
68. Thünemann, A. F.; Ruppelt, D. *Langmuir* **2001**, *17*, 5098.
69. Thünemann, A. F. *Langmuir* **2000**, *16*, 824.
70. Dreja, M.; Lennartz, W. *Macromolecules* **1999**, *32*, 3528.
71. Paul, E. J.; Prud'homme, R. K. *Reactions and synthesis in surfactant systems*; Marcel Dekker, Inc: NY, **2001**; Vol. 100.
72. Hentze, H.-P.; Kaler, E. W. *Curr. Op. Coll. Interf. Sci.* **2003**, *8*, 164.
73. Hentze, H.-P.; Kaler, E. W. *Chem. Mater.* **2002**.
74. Laversanne, R. *Macromolecules* **1992**, *25*, 489.
75. Hotz, J.; Meier, W. *Langmuir* **1998**, *14*, 1031.
76. McKelvey, C. A.; Kaler, E. W.; Zasadzinski, J. A.; Coldren, B.; Jung, H.-T. *Langmuir* **2000**, *16*, 8285.
77. Hentze, H.-P.; Göltner, C. G.; Antionietti, M. *Ber. Bunsenges. Phys. Chem.* **1997**, *101*, 1699.
78. Antonietti, M.; Göltner, C. G.; Hentze, H.-P. *Langmuir* **1998**, *14*, 2670.
79. Jung, M.; Hubert, D. H. W.; Bomans, P. H. H.; Frederik, P. M.; Meuldijk, J.; van Herk, A. M.; Fischer, H.; German, A. L. *Langmuir* **1997**, *13*, 6877.
80. Jung, M.; den Ouden, I.; Montoya-Goni, A.; Hubert, D. H. W.; Frederik, P. M.; van Herk, A. M.; German, A. L. *Langmuir* **2000**, *16*, 4185.
81. Krafft, M. P.; Schieldknecht, L.; Marie, P.; Giulieri, F.; Schmutz, M.; Poulain, N.; Nakache, E. *Langmuir* **2001**, *17*, 2872.
82. Pacios, I. E.; Renamayor, C. S.; Horta, A.; Lindman, B.; Thuresson, K. *Macromolecules* **2002**, *35*, 7553.
83. Anderson, D. M., *Microporous materials*, U.S. Patent 5238613 5238613, **1993**.

84. Anderson, D. M., *Preparation of a polymeric hydrogel containing micropores and macropores for use as a cell culture substrate*, U.S. Patent 5244799 5244799, **1993**.

85. Friberg, S. E.; Thundathil, R.; Stoffer, J. O. *Science* **1979**, *205*, 607.

86. McGrath, K. M. *Coll. Polym. Sci.* **1996**, *274*, 399.

87. McGrath, K. M. *Coll. Polym. Sci.* **1996**, *274*, 499.

88. O'Brien, D. F.; Whitesides, T. H.; Klingbiel, R. T. *J. Polym. Sci., Part C: Polym. Lett.* **1981**, *19*, 95.

89. Lopez, E.; O'Brien, D. F.; Whitesides, T. H. *J. Am. Chem. Soc.* **1982**, *104*, 305.

90. O'Brien, D. F.; Armitage, B.; Benedicto, A.; Bennett, D. E.; Lamparski, H. G.; Lee, Y.-S.; Srisiri, W.; Sisson, T. M. *Acc. Chem. Res.* **1998**, *31*, 861.

91. Okada, S.; Peng, S.; Spevak, W.; Charych, D. *Acc. Chem. Res.* **1998**, *31*, 229.

92. Sisson, T. M.; Lamparski, H. G.; Kölchens, S.; Elyadi, A.; O'Brien, D. F. *Macromolecules* **1996**, 8321.

93. Srisiri, W.; Benedicto, A.; O'Brien, D. F.; Trouard, T. P.; Orädd, G.; Persson, S.; Lindblom, G. *Langmuir* **1998**, *14*, 1921.

94. Srisiri, W.; Sisson, T. M.; O'Brien, D. F.; McGrath, K. M.; Han, Y.; Gruner, S. M. *J. Am. Chem. Soc.* **1997**, *119*, 4866.

95. Lee, Y.-S.; Yang, J.-Z.; Sisson, T. M.; Frankel, D. A.; Gleeson, J. T.; Aksay, E.; Keller, S. L.; Gruner, S. M.; O'Brien, D. F. *J. Am. Chem. Soc.* **1995**, *117*, 5573.

96. Drager, A. S.; Zangmeister, R. A. P.; Armstrong, N. R.; O'Brien, D. F. *J. Am. Chem. Soc.* **2001**, *123*, 3595.

97. Gin, D. L.; Gu, W.; Pindzola, B. A.; Zhou, W. J. *Acc. Chem. Res.* **2001**, *34*, 973.

98. Reppy, M. A.; Gray, D. H.; Pindzola, B. A.; Smithers, J. L.; Gin, D. L. *J. Am. Chem. Soc.* **2001**, *123*, 363.

99. Smith, R. C.; Fischer, W. M.; Gin, D. L. *J. Am. Chem. Soc.* **1997**, *119*, 4092.
100. Hoag, B. P.; Gin, D. L. *Macromolecules* **2000**, *33*, 8549.
101. Resel, R.; Leising, G.; Markart, P.; Kriechbaum, M.; Smith, R.; Gin, D. L. *Macromol. Chem. Phys.* **2000**, *201*, 1128.
102. Deng, H.; Gin, D. L.; Smith, R. C. *J. Am. Chem. Soc.* **1998**, *120*, 3522.
103. Pindzola, B. A.; Hoag, B. P.; Gin, D. L. *J. Am. Chem. Soc.* **2001**, *123*, 4617.
104. Bates, F. S.; Fredrickson, G. H. *Annu. Rev. Phys. Chem.* **1990**, *41*, 525.
105. Antonietti, M.; Goeltner, C. *Angew. Chem. Int. Ed. Engl.* **1997**, *36*, 910.
106. Muthukumar, M.; Ober, C. K.; Thomas, E. L. *Science* **1997**, *277*, 1225.
107. Förster, S.; Berton, B.; Hentze, H.-P.; Kramer, E.; Antionietti, M.; Lindner, P. *Macromolecules* **2001**, *34*, 4610.
108. Saito, R. *Macromolecules* **2001**, *34*, 4299.
109. Hentze, H.-P.; Krämer, E.; Berton, B.; Förster, S.; Antonietti, M. *Macromolecules* **1999**, *32*, 5803.
110. Ruokolainen, J.; Makinen, R.; Torkkeli, M.; Makela, T.; Serimaa, R.; ten Brinke, G.; Ikkala, O. *Science* **1998**, *280*, 557.
111. Maki-Ontto, R.; de Moel, K.; de Odorico, W.; Ruokolainen, J.; Stamm, M.; ten Brinke, G.; Ikkala, O. *Adv. Mater.* **2001**, *13*, 117.
112. Valkama, S.; Ruotsalainen, T.; Kosonen, H.; Ruokolainen, J.; Torkkeli, M.; Serimaa, R.; ten Brinke, G.; Ikkala, O. *Macromolecules* **2003**, *36*, 3986.
113. Antonietti, M.; Kublickas, R.; Nuyken, O.; Voit, B. *Macromol. Rapid Commun.* **1997**, *18*, 287.

CHAPTER 3

SYNTHESIS AND COMPLEXATION OF POLYMERISABLE SURFACTANTS

3.1. Introduction

Polymerisable surfactants (surfmers) have generated much interest due to their dual nature, i.e., of surfactants and monomers. Thus they have the ability to both decrease the surface tension of the medium they are dissolved in and to undergo polymerisation reactions. Since the synthesis of the first vinyl surfmers in 1958 by Freedman[1] a wide variety of surfmers have been synthesized worldwide. Anionic, cationic, zwitterionic and non-ionic surfmers have been synthesized, varying the surfmers' chain-length, the type of charged-group and polymerisable group, as well as the positions of the reactive group along the surfmer. As reactive monomers, these materials have been used for a range of applications. For example, surfmers replace conventional surfactants in heterogeneous polymerisations, e.g. emulsions where they improve the latex properties towards freeze and thaw cycles, or applied shear stress.[2,3] In template polymerisations surfmers are used to achieve polymerisation in structurally ordered media. Self-assembled phases of some lipid-like surfmers have already been successfully utilised as templates for organic polymerisation reactions.[4] The success of this synergistic templating approach relies mainly on the low molecular solubility of lipids in water, which prevents exchange of lipid molecules between assemblies. The high mobility existing in the organised

phases of other surfmers often make 1:1 templating not easy to achieve.[5] The rapid monomer exchange between the ordered assemblies (with a characteristic time constant of 10^{-5} – 10^{-9} s for micelles[6]) is generally faster than the characteristic time for chain propagation, thus preventing topochemical polymerisations from taking place.[7]

Polyelectrolyte-surfactant complexes (Section 2.2.4) on the other hand provide the possibility of using both the structural variety characteristic of ordered surfactant phases and the robustness of polymers.[8,9] Their potential as hosts for organic polymerisation reactions, however, has only been explored in few cases where 1:1 templating was not achieved due to the low loading capabilities of the complex used[10] or to the low mobility of the reactive groups of the head-functionalised surfmer.[11]

In this chapter we focus on the synthesis of two polymerisable, tail-functionalised surfmers, and their complexes with different polyelectrolytes. We expect that the position of the reactive groups along the alkyl tail of the surfmer should provide enhanced flexibility of the monomer units and enable polymerisation reactions within the ordered complexes to take place. The structure of the polyelectrolyte-surfmer complexes was investigated by means of X-ray scattering and microscopy.

3.2. Materials

The following chemicals were purchased from Aldrich Co. and used as received: 12-hydroxydodecanoic acid, acryloyl chloride, 10-undecene-1-ol, phosphorous oxychloride, sodium tetraborate decahydrate, sodium hydroxide, high molecular mass polydiallyldimethylammonium chloride (pDADMAC, M_w 375 000 – 500 000). Water-free, high molecular weight polyethyleneimine (PEI, M_w = 25 000 g/mol) was supplied by BASF (South Africa). Water used for the synthesis of the complexes was distilled and deionised in a "Milli-Q" water purification system (Millipore Corp.). Dry benzene (refluxed over calcium chloride, distilled and stored over molecular sieve, 4Å) was used as solvent for the preparation of di(undecenyl)phosphate. Other solvents used for the syntheses: chloroform, dichloromethane, methanol, acetone, hexane hydrochloric acid (37%), were purchased from Acros Organics.

3.3. Experimental procedures

3.3.1. Synthesis of surfactants

3.3.1.1. Synthesis and purification of 12-acryloyloxydodecanoic acid (ADA)

A solution of 1 g (4,62 mmol) 12-hydroxydodecanoic acid, 2.58 ml (18.49 mmol) triethylamine in 4 ml dichloromethane was added slowly, drop-wise, over a period of 3 h to a solution of 1.5 ml (18.49 mmol) acryloyl chloride in 2.2 ml dichloromethane at –5 °C. The mixture was stirred for four days at 0 °C. 1.0 ml of water was then added, followed by a solution of 1.13 g (28.25 mmol) NaOH in 2.5 ml water. The mixture was stirred for 1 h at this temperature. The cold

solution was then acidified with a solution of HCl acid to pH 1. The dichloromethane was removed by evaporation under reduced pressure. In the water residue a yellowish oily layer appeared, which was extracted with dichloromethane. After removing all the solvent by evaporation the product was purified by chromatography (Merck Kieselgel 60<43-60 μm>, acetone:methanol (4:1)). The first fraction contained the desired product ADA with some acrylic acid contamination, which was removed under reduced pressure in the dark.
Yield: 72%

^{1}H-NMR ($CDCl_3$, 600 MHz): δ/ppm = 1.23, *br. s*, [14H, –(CH_2)$_7$-], 1.60 *q* [4H, (-CH_2-C-O-) and (-CH_2-C-COOH)], 2.23 *t* [2H, (-CH_2-COOH)], 4.12 *t* [2H, (CH_2-O)], 5.80 [1H, (*trans* =CH)], 6.05 [1H, (-CH=CH_2)], 6.43 [1H,(*cis* =CH)].

FTIR: ν/cm^{-1} = 3300-2500 (OH), 1740 (C=O), 1630 (C=C).

Elemental Analysis $C_{15}H_{26}O_4$ (M_w= 270.37)
Calc.: C=66.64%, H=9.69%
Found: C=65.75%, H=9.52%

3.3.1.2. Synthesis of the sodium 12-acryloyloxydodecanoate

Sodium 12-acryloyloxydodecanoate was obtained by treating 12-acryloyloxydodecanoic acid with a stoichiometric amount of NaOH in dry methanol.[12] The salt was then recrystallised from dry acetone.
Yield: 76%

3.3.1.3. Synthesis of di(undecenyl)phosphate (ωC11)

The surfactant ωC11 was prepared according to a general procedure employed for the synthesis of di(n-alkyl) phosphates.[13,14] The reaction was carried out by refluxing 20.44 g (0.12 moles) undecenyl alcohol and 3.73 ml (0.04 moles) phosphorous oxychloride (3:1 molar ratio) in 30 ml dry benzene for 24 h. Benzene and unreacted alcohol were distilled off under vacuum and the product precipitated in water. After freeze-drying, white crystals of pure ωC11, T_m =37-38°C, were obtained.
Yield: 60%

^{1}H-NMR ($CDCl_3$, 600 MHz): δ/ppm = 1.25m [24H, 2 x –(CH_2)$_6$-], 1.64p [4H, 2 x (CH_2-C-O-)], 1.99q [4H, 2 x (CH_2-C=C)], 3.96q [4H, 2 x (CH_2-O)], 4.91 [2H, 2 x (*trans* =CH_2)], 4.98 [2H, 2 x (*cis* =CH)], 5.79 [2H, 2 x (-CH=CH_2)].
^{13}C-NMR ($CDCl_3$, 150 MHz): δ/ppm = 28.8, 28.9, 29.0, 29.2, 29.3, 30.0, 30.1 (-CH_2-), 33.6 (-C-C=C), 67.6 (-C-O-), 114.2 (=CH_2), 139.4 (-C=CH_2)
^{31}P-NMR ($CDCl_3$, 242 MHz): δ/ppm = 2.5

FTIR: ν/cm^{-1} = 3077 (=C-H), 2924, 2853 (CH_2), 1642 (CHR=CH_2), 1465 (CH_2), 1231 (P=O), 1091 (P-O-R), 995, 910 (CHR=CH_2)

Elemental Analysis $C_{22}H_{43}O_4P$ (M_w= 402.55)
Calc.: C=65.64%, H=10.76%
Found: C=65.80%, H=11.26%

3.3.2. Synthesis of polyelectrolyte-surfactant complexes

3.3.2.1. Synthesis of polydiallyldimethylammonium/12-acryloyloxydodecanoate complex (pDADMA/ADA)

A 2 wt% aqueous solution of pDADMAC was added drop-wise to a 2 wt% aqueous solution of the sodium salt of an acrylate surfactant (ADA) in a 1:1 molar ratio with respect to the charges. The mixture was stirred for an hour at room temperature. No complex formation was observed even after extending the reaction time to several hours, varying the reaction pH and trying to extract the organic phase with different organic solvents (2-butanol, chloroform).

3.3.2.2. Synthesis of polyethyleneimine/12-acryloyloxydodecanoic acid complex (PEI/ADA)

0.119 g (2.8 mmol) PEI were dissolved in 5 ml of a 4:1 ratio mixture of ethanol to water. The PEI solution was then added to a solution of 0.372 g (1.4 mmol) of the acrylic ester in ethanol at 65°C and the reaction mixture stirred for 30 min. The product precipitated immediately with the addition of the PEI and did not dissolve in any of the common organic solvents listed below: water, methanol, ethanol, 2-butanol, chloroform, dichloromethane, trichlorobenzene, THF, DMF, DMSO, acetone, propanol, benzene, toluene, acrilonitrile, triethylamine, ethylacetate, pyridine, styrene, methylmethacrylate.

3.3.2.3. Synthesis of polydiallyldimethylammonium/di(undecenyl)phosphate complex (pDADMA/ωC11)

In order to prepare the complex of pDADMA / ωC11, the surfactant ωC11 was first dispersed in a buffer solution of pH 9 (65 ml 0.1M borax mixed with 5 ml 0.4M hydrochloric acid) at 65 °C to form a 2 wt% solution of the sodium salt of

di(undecenyl)phosphate. A 2 wt% aqueous solution of high molecular mass pDADMAC was added drop-wise to the surfactant solution in a 1:1 molar ratio. After stirring the solution for 1 h at 65 °C the precipitated complex was filtered off and washed several times with water to remove salt and excess surfactant. The washing procedure was repeated until no more chloride could be detected with a silver nitrate solution. The complex was dried overnight at 60 °C followed by drying under vacuum at room temperature for 24 h, then redissolved in chloroform and the solution cast onto Teflon-coated foil. After overnight drying at room temperature the film was further dried at 50 °C and 20 mbar vacuum.
Yield: 87%

^{31}P-NMR ($CDCl_3$, 242 MHz): δ/ppm = 1.32

FTIR: ν/cm^{-1} = 3077 (=C-H), 2924, 2853 (CH_2), 1642 ($CHR=CH_2$), 1465 (CH_2), 1231 (P=O), 1091 (P-O-R), 995, 910 ($CHR=CH_2$)

Elemental analysis ($C_{30}H_{58}NO_4P$ M_w=527.76)
Calc.: C=65.5%, H=12.2%, N=2.02%
Found: C=63.9%, H=11.2%, N=2.03%

3.3.2.4. Synthesis of polyethyleneimine/di(undecenyl)phosphate complex (PEI/ωC11)

For complex preparation 10 mmol (0.431 g) PEI was dissolved in 10 ml aqueous ethanol (4:1 ethanol to water). The PEI solution was then slowly added to 5 mmol (2.013 g) ωC11 in 10 ml ethanol at 65 °C. The transparent solution was stirred for 30 min at 65 °C and then cast into films. The molar ratio of the surfactant in the complex was varied until the intense carboxylic acid band at a wavenumber of 1712 cm^{-1} disappeared from the IR spectra of the complex.[15] This served as an indication that a stoichiometric 1:1 complexation

had occurred. The desired stoichiometry was achieved at a 2:1 molar ratio of PEI to the acid with respect to the charges.
Yield: 85%

3.3.3. Instrumental techniques

Nuclear magnetic resonance (NMR) spectra were recorded on either a 300 MHz Varian VXR spectrometer equipped with a Varian magnet (7.0 T) and a 5 mm switchable probe, or a 600 MHz Varian Unity Inova spectrometer equipped with an Oxford magnet (14.09 T) and a 5 mm inverse detection PFG probe. Standard pulse sequences were used for obtaining ^{1}H, ^{13}C and ^{31}P spectra.

Elemental analysis (EA) was performed on a Fisons elemental analyzer, model 1108, using combustion analysis, at the University of Cape Town. Samples were tested for C, H, N, and, in some cases, for O content. The commercial pDADMAC used for complex preparation gave some deviations from the theoretical values. On the basis of these new values the mass percentages of the different elements in the complex were recalculated and new predictions for the theoretical values made.

Electrospray mass spectrometry (ESMS) was performed on a Micromass (Manchester, UK) Quattro triple quadropole mass spectrometer. Samples were diluted 1/100 in methanol and injected, as such, through a Rheodyne injector into a carrier stream of methanol at a flow rate of 20 µl/min. Ionization was in the negative mode, applying a capillary voltage of 3.5 kV with the cone voltage set at 70 V. The instrument was calibrated using NaI as a standard, under the same conditions used for the sample analysis. The data was acquired by scanning from m/z = 100 – 1000 at a scan rate of 5 sec.

Small-angle-X-ray scattering (SAXS) diffractograms were obtained with an Anton Paar compact Kratky camera using a Phillips PW1830 generator as the source of the Cu-Kα incident radiation (λ = 1.54 Å). Monochromatization was accomplished using a nickel filter and pulse height discrimination. The intensity profile was plotted as the scattering intensity (I) vs the scattering factor, $q = 4\pi / \lambda \sin\theta$, where 2θ is the angle between incident and scattered light. The measurements were performed in a q range of $1.0 \times 10^{-2} < q/2\pi < 9.0 \times 10^{-1}$ nm^{-1}.

Wide-angle-X-ray scattering (WAXS) diffractograms were obtained on a Nonius PFS120 powder diffractometer in transmission geometry. A FR590 generator was used as the source of Cu-Kα radiation. All X-ray measurements were done at the Max Planck Institute of Colloids and Interfaces, Golm, Germany.

Differential scanning calorimetry (DSC) was performed on a Netzsch DSC 200. The samples were examined at a scanning rate of 10 $K.min^{-1}$ by applying two heating and one cooling cycle.

Thermogravimetric analysis (TGA) was performed on a Netzsch TG 209. The samples were examined at a scanning rate of 20 $K.min^{-1}$.

Bright-field transmission electron microscopy (TEM) was performed on a JEM 200CX (Jeol Tokyo, Japan) TEM at an accelerating voltage of 120 kV. Samples of pDADMA / ωC11 complex were first stained with OsO_4. Pieces of complex were left overnight into a 1 wt% aqueous solution of OsO_4, then washed twice with distilled water followed by washing with acetone (up to four times) to ensure that they were dry. Acetone solution of an epoxy resin was added to the samples, which were then left to shake for 30 min. The solution was then discarded and the procedure repeated another four times. The samples were

then transferred into a plastic container, embedded in epoxy resin, and cured overnight at 60 °C. Ultra-thin sections (~100 nm) were cut from the embedded specimen using a Reichert Ultracut S ultramicrotome and a diamond knife, at room temperature. Sections were picked up on 300-mesh copper grids. The analyses were performed at the Electron Microscopy Unit at the University of Cape Town.

Fourier transform infrared spectroscopy (FTIR) spectra were recorded on a Perkin Elmer Paragon 1000 FTIR. A photo acoustic cell was used in some cases (samples were then placed in an MTEC 300 chamber and flushed with ultra high-purity helium prior to the measurements).

3.4. Results and discussion

3.4.1. Synthesis of 12-acryloyloxydodecanoic acid (ADA) and di(undecenyl)phosphate (ωC11)

Two tail-functionalised surfactant monomers (surfmers) were synthesized: a surfactant containing an acrylic ester group, 12-acryloyloxydodecanoic acid (ADA), and a phosphodi-ester with a terminal alkene group, di(undecenyl)phosphate (ωC11). They differ in the nature of their polymerisable group, the type of head group, and the number of hydrocarbon tails attached to the head group. The surfmers also differ greatly in terms of reactivity: while the acrylic ester group is an example of a very reactive polymerisable group under free radical conditions, the terminal olefin group has only limited reactivity under similar conditions. Using well-described methods, both surfactants were

synthesised in high yields and with high purity. The main factor considered in choosing the synthetic methods was the availability of starting materials.

3.4.1.1. 12-acryloyloxydodecanoic acid (ADA)

The modified Schotten-Baumann reaction (scheme 3.1), in which acryloyl chloride and a hydroxy acid are used as starting materials, was chosen for the synthesis of the acrylic ester ADA.[16]

Scheme 3.1. A synthetic route to acrylate ester formation.

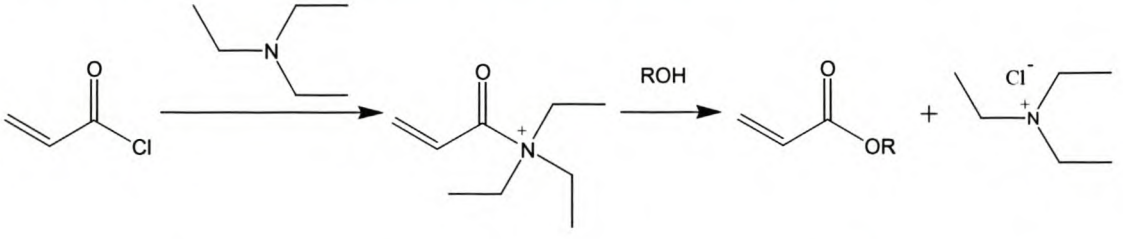

Dichloromethane was preferable to THF as reaction solvent. It has a lower boiling point; hence difficulties in handling the resulting surfactant were avoided. Care was required during removal of the reaction solvent in order to prevent facile oligomerisation and polymerisation of the acrylate surfmer taking place. Finding suitable recrystallising solvents was not a simple task because of the amphiphilic structure of the surfactant monomer.

Thus, following the dichloromethane procedure (Section 3.3.1.1), the pure ester ADA was obtained in 72% yield. The purity of the surfactant was confirmed by NMR analyses (Figure 3.1).

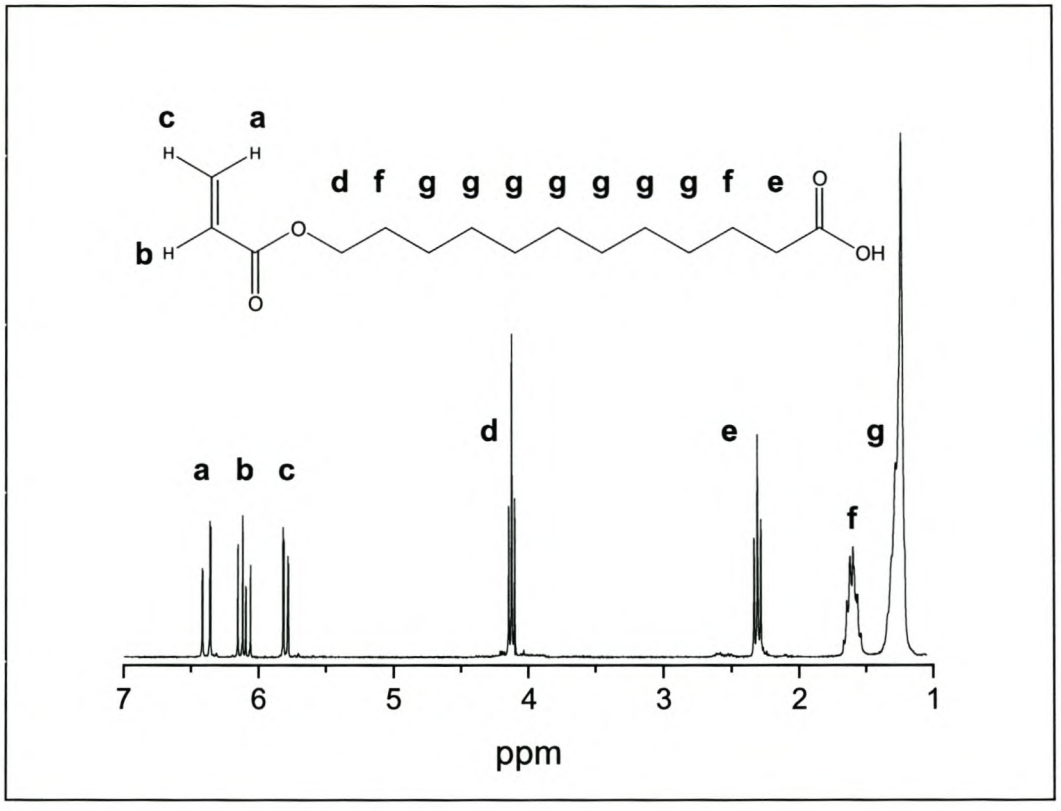

Figure 3.1. *^{1}H-NMR spectrum of the pure ADA surfactant. The signal at 4.12 ppm is characteristic of the presence of an ester bond.*

3.4.1.1. Di(undecenyl)phosphate (ωC11)

Di(undecenyl)phosphate (a phosphoric acid derivative) can be synthesized using undecenyl alcohol and either P_4O_{10} or $POCl_3$. The use of $POCl_3$, however, offers a few advantages over P_4O_{10}.[17] The polymeric structure of P_4O_{10} makes it difficult to achieve the correct stoichiometry between the starting materials. Esters of the polymeric phosphoric acid are found as side products of this reaction. The ratio of mono- to di-ester obtained is 1:1, which further complicates the purification of the di-ester.

When using $POCl_3$, the two reagents (alcohol and $POCl_3$) are used in a 3 : 1 molar ratio. Furthermore, side-product formation can be avoided by the removal of HCl formed during the reaction. The latter shifts the reaction equilibrium towards product formation. Mixtures of primary and secondary esters are obtained. Mono-ester formation is suppressed by the use of dry reagents,[18] and by using an excess of the starting alcohol.

The reaction between $POCl_3$ and 10-undecene-1-ol was carried out in two different solvents and at different reaction temperatures as described previously in the literature[13,19,20] (Scheme 3.2).

Scheme 3.2. Possible routes to the synthesis of the ωC11 surfactant.

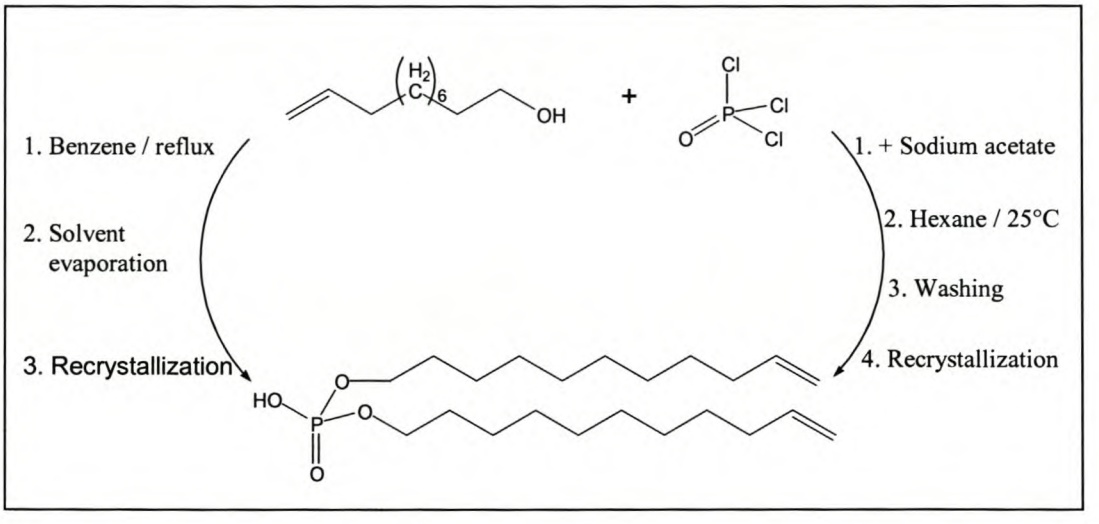

Both routes rendered mixtures of mono- and di(undecenyl)phosphate as reaction product. However, the amount of mono-ester, formed when performing the reaction in benzene, was significantly smaller (~ 10 %) than that obtained when following the hexane route (> 50 %), as shown by ESMS analyses (see Figure 3.2). The lack of byproducts in the crude product from the reaction in benzene (Figure 3.2b) was another advantage of this route.

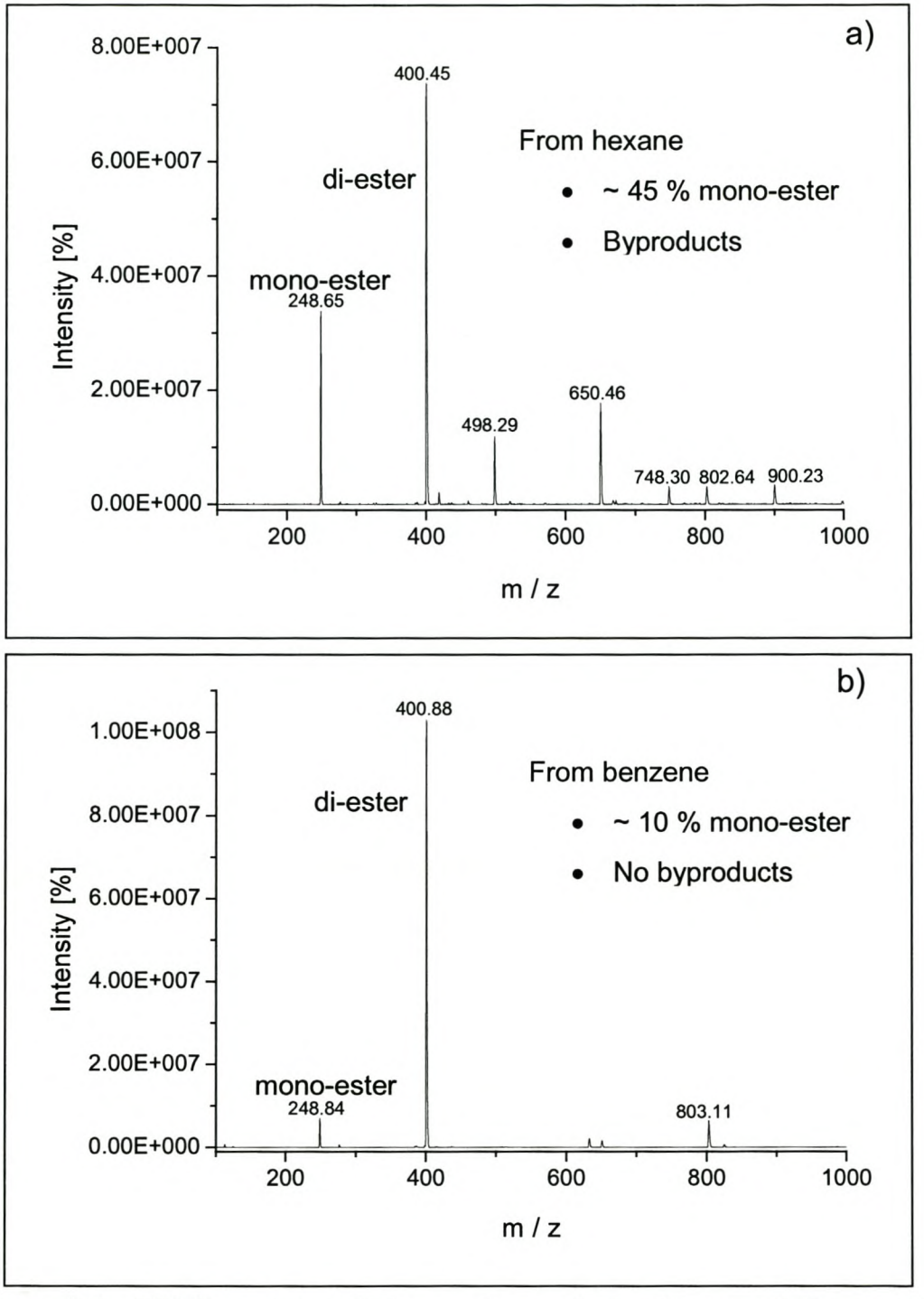

Figure 3.2. *ESMS spectra of the crude product mixtures of the reaction between $POCl_3$ and undecenyl alcohol, carried out in a) hexane and b) benzene.*

Thus, by refluxing undecenyl alcohol and phosphorous oxychloride in dry benzene overnight, pure di(undecenyl)phosphate was obtained in ~ 60 % yield. The purity of the product was determined by means of ^{1}H-NMR analysis (Figure 3.3).

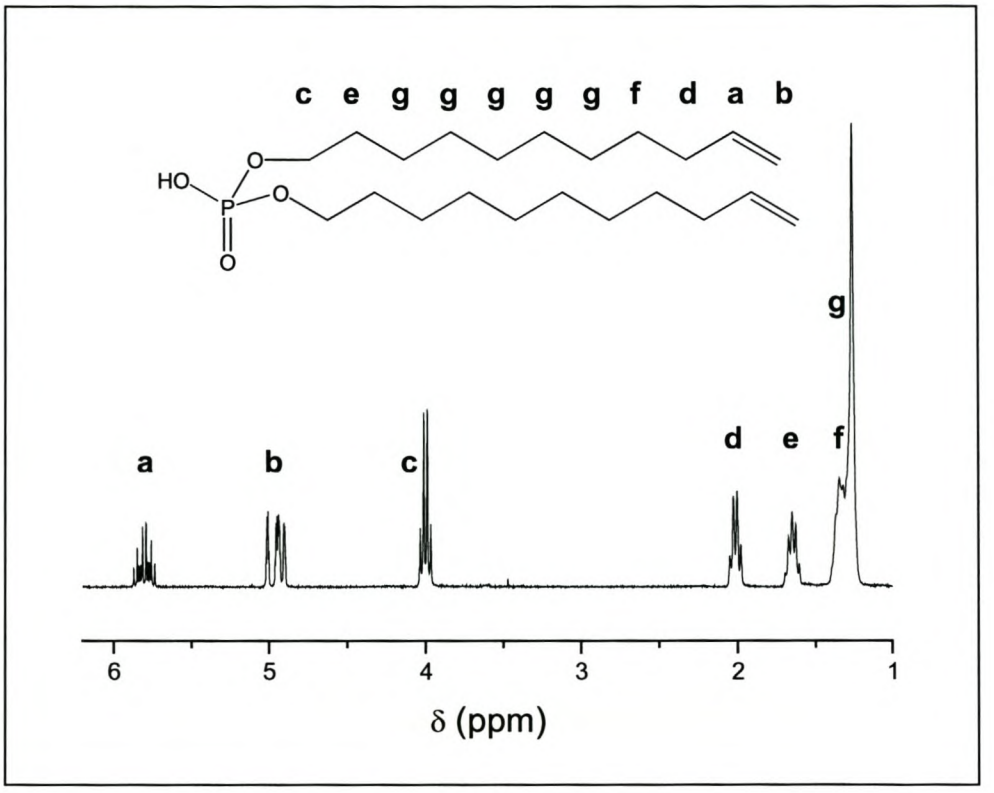

Figure 3.3. *^{1}H-NMR spectrum of ωC11. The peak characteristic of the ester bond, at 4.00 ppm, and those typical for the olefin group, at 4.95 ppm and 5.8 ppm, were present in the spectrum of the surfactant.*

The presence of the ester bond was also confirmed by means of FTIR analysis. The typical stretching vibrations, characteristic of the phosphate ester bond, were observed at 1230 and 1060 cm^{-1}.

3.4.2. Synthesis of polyelectrolyte-surfactant complexes

The purified surfactants were then used for the synthesis of polyelectrolyte-surfactant complexes. The syntheses involved simple mixing of dilute solutions of a charged surfactant and an oppositely charged polyelectrolyte. The following compounds were used as building blocks for the complexation (see scheme 3.3).

Scheme 3.3. Building blocks used for the formation of polyelectrolyte-surfactant complexes.

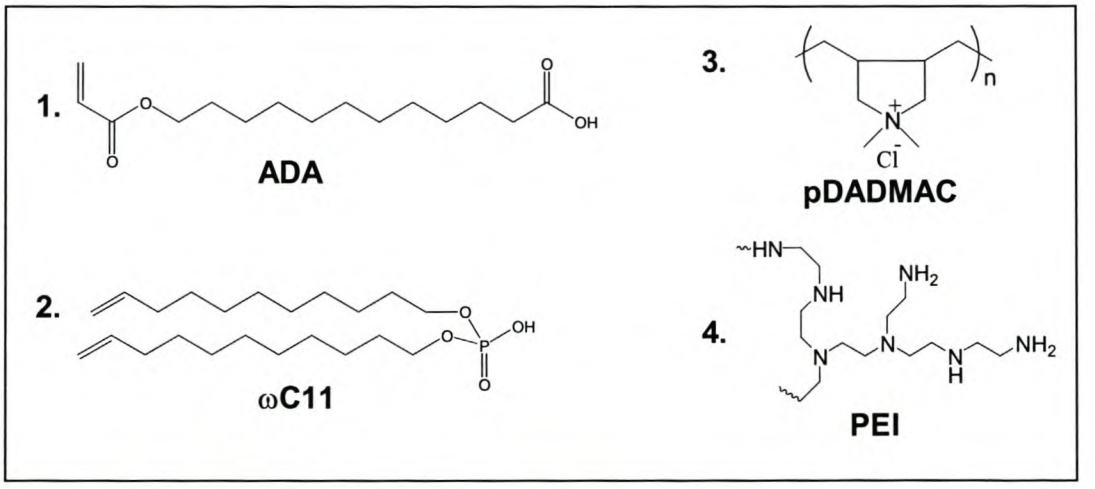

1. 12-acryloyloxydodecanoic acid (ADA), 2. Di(undecenyl)phosphate (ωC11), 3. poly(diallyldimethylammonium chloride) (pDADMAC), 4. Polyethyleneimine (PEI).

High molecular weight pDADMAC was chosen for the polyelectrolyte backbone of the complex due to its good binding properties and high charge density. Its relatively low cost and commercial availability were also advantageous.

Attempts to prepare polyelectrolyte-surfactant complexes, using the sodium salt of the acrylate surfactant and pDADMAC, were unsuccessful. The mixing of equimolar solutions of the polyelectrolyte and the surfactant did not lead to the

formation of complex precipitate. Recently, Li *et al.* observed complexation of pDADMAC and carboxy-terminated surfactants above a well-defined critical pH, corresponding to a critical micelle surface charge density.[21] Thus, in the present work, the pH of the reaction mixture was adjusted between pH 5 and 10 (above pH 10 the ester bond would be expected to be cleaved). However, even above pH 6, where the acid is fully deprotonated, no complex precipitate was formed. Attempts to extract the complex from the water with a suitable organic solvent (2-butanol, chloroform) also proved ineffective. The extraction solution became homogeneous and gelled upon mixing of the organic solvent with the water solution, and it was impossible to separate the organic and the aqueous layers. It could be speculated that complex formation was hindered by steric effects, arising from the tendency of ADA to form "loop-like" structures on polar interfaces.[22] This failure to obtain solid-state complexes of the carboxylic acid surfmer and pDADMAC lead to the search for an alternative polyelectrolyte that would complex with ADA.

Polyethyleneimine (PEI) is a branched water-soluble polymer widely used in the paper industry. It contains primary, secondary and tertiary amine groups, each with a different basicity, distributed along the backbone. At low pH, PEI has the highest known charge density of all polyelectrolytes. It is known to possess a strong tendency to form structured complexes with anionic surfcatants.[23,24] Various lamellar mesophases were observed for the complexes of PEI and n-alkanoic acids with increasing surfactant chain-length.[24] Chen and Hsiao[25] have also shown that the high branching level of commercial PEI does not prevent the ordering of the alkyl tails within PEI – surfactant complexes. Like linear polymer complexes, branched polymer complexes display supramolecular structure.[25]

Complexation between the PEI and carboxylate surfactants proceeds via proton transfer from the surfactant to the amine groups of the PEI, giving rise to

complexes with electrostatic interaction. It is difficult to determine the molar amount of surfactant needed for a stoichiometric PEI / surfactant complex due to the different basicity of the PEI amine groups. The tendency of the different amine groups towards protonation decreases from the primary to the tertiary amino groups rendering the latter unavailable for complexation reactions with the surfactant.[23] Thus, nonstoichiometric PEI / surfactant complexes are formed when a 1:1 molar ratio of surfactant to PEI (with respect to the charges) has been used.[25,26] In order to determine the exact amount of surfactant required for a stoichiometric PEI / surfactant complex, PEI / (undecylenic acid)$_y$ complexes were synthesized, where *y* is the mole fraction of undecylenic acid used for complexation. The undecylenic acid was chosen for the trials, as it is a cheap, commercially available carboxylic acid. Upon decreasing the mole fraction *y* of the undecylenic acid, the intense carboxylic band at a wave number of 1708 cm^{-1} disappeared from the FTIR spectrum of the complex. This spectral change demonstrated the complete proton transfer from the undecylenic acid to PEI (Figure 3.4) and was in agreement with observations made for complexes of PEI and fluorinated surfactants.[27]

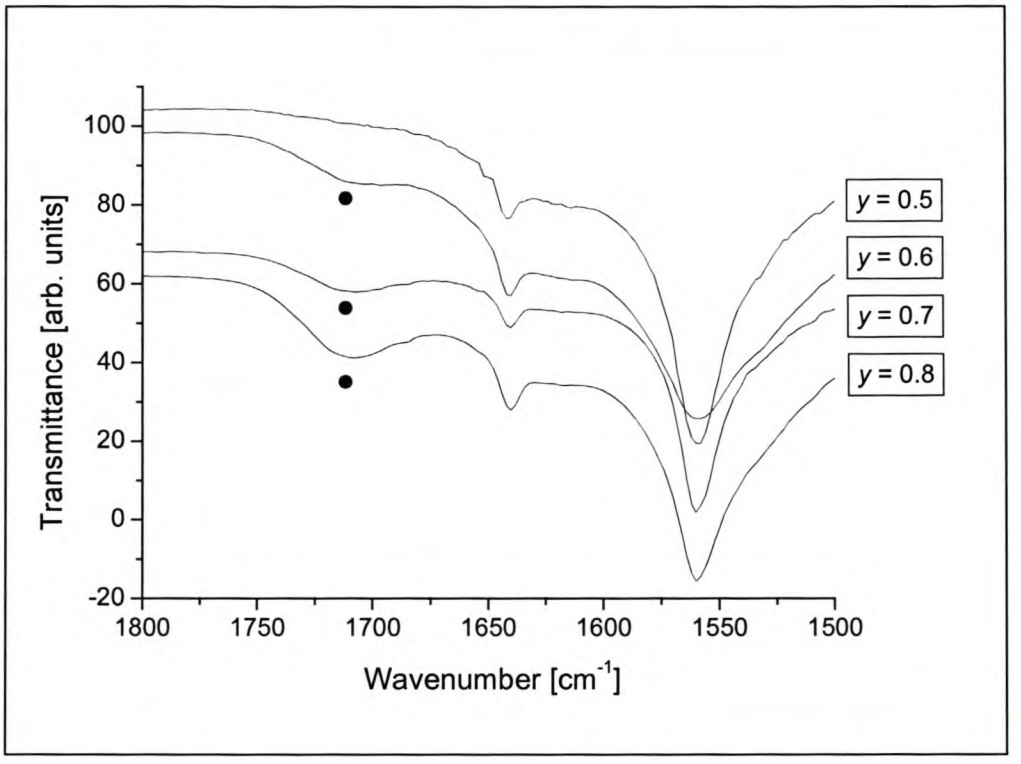

Figure 3.4. *FTIR transmittance bands for PEI / (Undecylenic acid)$_y$ complexes. The formation of the stoichiometric 1:1 complex was seen as the disappearance of the carbonyl-stretching band at 1708 cm^{-1}with the decrease of the molar fraction y of undecylenic acid in the complexes.*

From the IR spectra (Figure 3.4) it could be seen that a 2:1 molar ratio of PEI to surfactant (with respect to the charges) was required for the formation of a stoichiometric PEI/surfactant complex.

The complex of PEI and ADA was prepared using a 2 : 1 molar ratio of the PEI to the surfactant, as determined from our experiment with the undecylenic acid. Unfortunately, upon mixing the two dilute solutions (of the surfactant and the polyelectrolyte in the methanol/water mixture) a precipitate was formed that was not soluble in any of the common organic solvents. This could be attributed to the very reactive nature of the acrylate group, which was most probably in a favourable orientation within the complex for polymerisation, causing immediate

precipitation of the polymerised complex. Because of the insolubility of the resulting product no films could be cast and further structural investigations were abandoned.

3.4.3. Structure of polyelectrolyte-surfactant complexes

Films of the PEI / ωC11 complex were cast from the 4:1 methanol : water mixture and the structure investigated by means of SAXS. Only one broad, low intensity peak was observed at ~ 3.25 nm (Figure 3.5), which was not sufficient to clarify the structure of the complex.

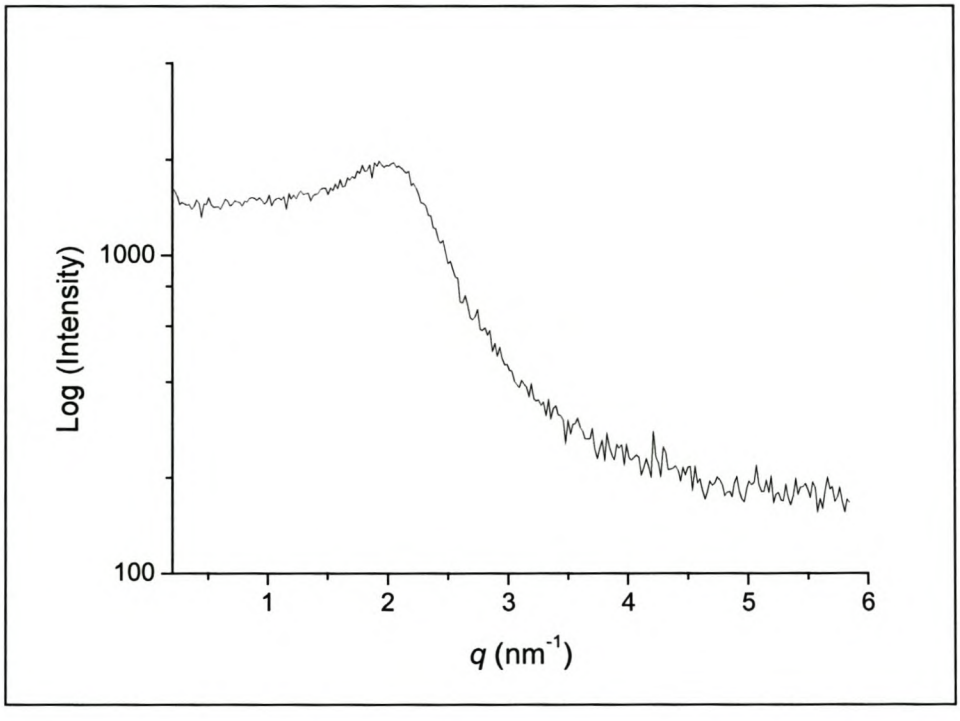

Figure 3.5. *Room temperature SAXS profile of the PEI / ωC11 complex. The broad peak at q = 1.93 indicates the presence of some mesoscopic order in the complex.*

Films prepared from pDADMA / ωC11 were very hygroscopic and deformable. In order to characterize their thermal behaviour, thermogravimetric analysis was performed on the complex. Degradation proceeded in two steps, with the complex losing 60% of its weight at 300 °C, and another 30% at 460 °C. Differential scanning calorimetry (DSC) showed no glass transition in the temperature range between -50 and 200 °C. This might be due to the high ionic character of the materials. Elemental analysis showed that a 1:1 stoichiometric ratio of surfactant to polyelectrolyte was obtained. The experimental values were as follows (%, predicted values in parentheses): C, 63.9 (65.5); H, 11.21 (12.2); N, 2.03 (2.02).

Strongly birefringent domains could be seen with a polarized light microscope (PLM) (without straining / shearing the film mechanically). Unfortunately the observed textures did not allow an unambiguous determination of the liquid-crystalline phases. Small-angle-X-ray scattering (SAXS) diffractograms were therefore recorded. The films of pDADMA / ωC11 showed one scattering peak at 3.02 nm (Figure 3.6).

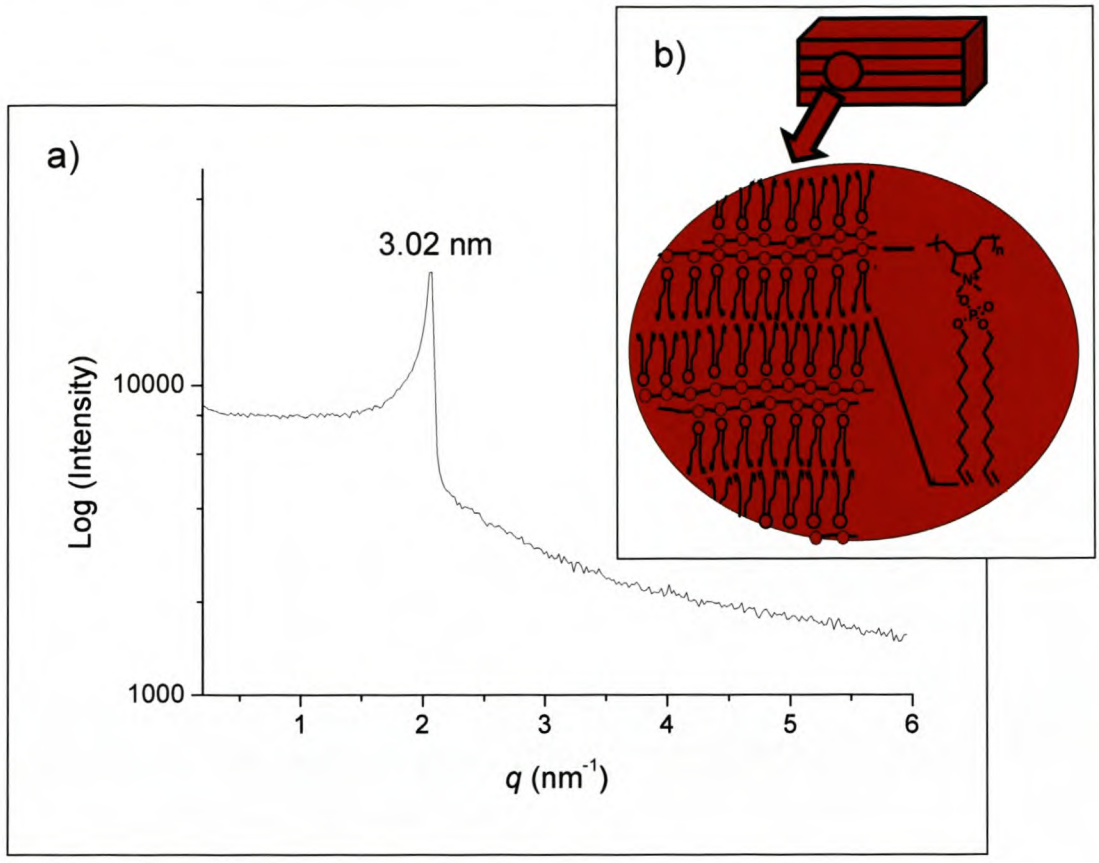

Figure 3.6. *a) SAXS diffractogram of the pDADMA / ωC11 complex (logarithmic representation). The scattering factor is defined as* $q = 4\pi/\lambda \sin\theta$, *where* 2θ *is the scattering angle between incident and scattered light,* $\lambda = 0.154$ *nm. b) Schematic representation of the lamellar structure of the complex.*

The peak could be attributed to a lamellar mesophase in the complex (see Figure 3.6b), as it has been described in literature that not all lamellar polyelectrolyte-surfactant complexes show second order peaks in their SAXS diagrams. The latter has been ascribed to the comparable volume fractions of the polymer and surfactant layers[28] or the correlation in the lamellar stacks being restricted to several adjacent layers of polymers.[29,30] The repeat unit of 3.02 nm derived from the SAXS diffractogram corresponds to a stretched alkyl chain conformation of the surfactant tails within the lamellae.

The first order peak in the SAXS diffractogram of the pDADMA / ωC11 complex was not sufficient to clarify the structure of the complex. In order to reveal higher order peaks WAXS measurements were conducted. The equidistant second, and fourth order peaks identified on the diffractogram (Figure 3.7. a) were characteristic of a lamellar structure.

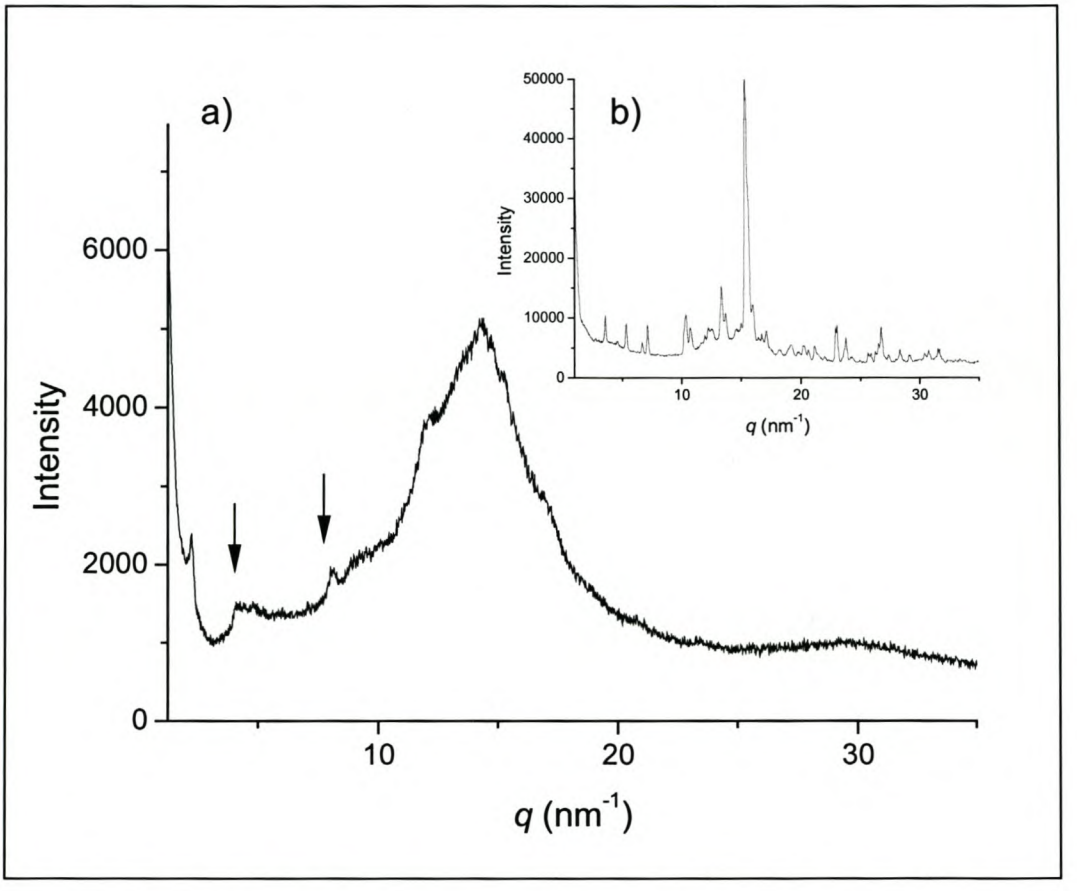

Figure 3.7. *WAXS diffractogram of a) pDADMA / ωC11 and b) the ωC11 surfactant.*

The broad halo in the WAXS diffractogram at q = 14.3 nm^{-1}, which corresponds to a Bragg spacing of 0.44 nm, confirmed the liquid-crystalline arrangement of the surfactant chains inside the complex. The lack of crystalline diffraction on

the diagram provided further proof for the complexation of the surfactant to the polyelectrolyte (pDADMAC), since none of the crystalline peaks characteristic for the pure surfactant (Figure 3.7 b) could be seen.

For further clarification of the structure TEM analysis was performed on thin films of the complex. The contrast between the hydrophilic (pDADMAC) and the hydrophobic parts of the complex (surfactant tails) was enhanced by staining with OsO_4. The staining lead to an increased scattering from the hydrophobic parts of the complex (OsO_4 attacks the olefin groups of the surfactant tails), which appeared dark on the micrograph (Figure 3.8).

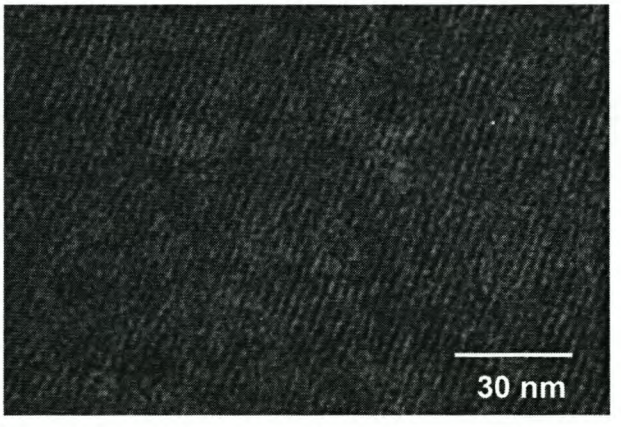

Figure 3.8. *TEM micrograph illustrating the lamellar structure in a pDADMA / ωC11 complex.*

The alternating hydrophilic and hydrophobic layers with a repeat unit of 3.0 nm observed on the TEM micrograph were in very good agreement with the presumptions made from x-ray analyses.

3.5. Conclusions

The complexation of the tail-functionalised, monomeric surfactants, ADA and ωC11, with two different polyelectrolytes was investigated. No complex precipitate was formed during the complexation of the acrylate surfmer ADA and pDADMAC. The most plausible explanation is that steric effects caused by the tendency of the acrylic group to "loop" at polar interfaces hindered complex formation. The relatively high reactivity of the acrylic group proved to be problematic in the synthesis of the PEI / ADA complex. The reaction conditions during complexation favoured the polymerisation of the acrylate tail of the surfactant thus rendering an insoluble, cross-linked and disordered product. The complex of PEI / ωC11 showed order on the mesoscale but the x-ray scattering curve from the SAXS analysis showed only a broad and low intensity signal. On the other hand, the complex of the vinyl surfmer ωC11 and pDADMAC was well structured on the mesoscale, and showed good thermal and mechanical properties. The lamellar mesophase of the complex with a repeat unit of 3.02 nm corresponded to a stretched alkyl chain conformation of the surfactant within the lamellae. The lamellar structure was confirmed using both X-ray analysis and electron microscopy.

3.6. References

1. Freedman, H. H.; Mason, J. P.; Medalia, A. I. *J. Am. Chem. Soc.* **1958**, *23*, 76.
2. Guyot, A.; Tauer, K. *Reactions and synthesis in surfactant systems*; Marcel Dekker, Inc.: NY, **2001**; Vol. 100.
3. Montoya-Goni, A.; Sherrington, D. C.; Schoonbrood, H. A. S.; Asua, J. M. *Polymer* **1999**, *40*, 1359.
4. O'Brien, D. F.; Armitage, B.; Benedicto, A.; Bennett, D. E.; Lamparski, H. G.; Lee, Y.-S.; Srisiri, W.; Sisson, T. M. *Acc. Chem. Res.* **1998**, *31*, 861.
5. McGrath, K. M. *Coll. Polym. Sci.* **1996**, *274*, 399.
6. Cochin, D.; Zana, R.; Candau, F. *Macromolecules* **1993**, *26*, 5765.
7. Tajima, K.; Aida, T. *Chem. Commun.* **2000**, *24*, 2399.
8. Antonietti, M.; Conrad, J.; Thünemann, A. F. *Macromolecules* **1994**, *27*, 6007.
9. Antonietti, M.; Conrad, J. *Angew. Chem. Int. Ed. Engl.* **1994**, *33*, 1869.
10. Faul, C. F. J.; Antonietti, M.; Hentze, H.-P.; Sanderson, R. D. *Langmuir* **2001**, *17*, 2031.
11. Dreja, M.; Lennartz, W. *Macromolecules* **1999**, *32*, 3528.
12. Hamid, S. M.; Sherrington, D. C. *Brit. Pol. J.* **1984**, *16*, 39.
13. Kunitake, T.; Okahata, Y. *Bull. Chem. Soc. Jpn.* **1978**, *51*, 1877.
14. Akimoto, A.; Dorn, K.; Gros, L.; Ringsdorf, H.; Schupp, H. *Angew. Chem. Int. Ed. Engl.* **1981**, *20*, 90.
15. Thünemann, A. F.; General, S. *Langmuir* **2000**, *16*, 9634.
16. Finkelmann, H.; Schafheutle, M. A. *Coll. Polym. Sci.* **1986**, *264*, 786.
17. Haupke, v. K.; Wolf, F. *J. Prakt. Chem.* **1966**, *33 (4)*, 206.
18. Polkovnichenko, I. T.; Chaplanov, P. E.; Merkotun, Z. Y.; Anisimova, O. V. *Neftеprerab. Neftekhim* **1980**, *12*, 32.

19. Paleos, C. M.; Christias, C.; Evangelatos, G. P.; Dais, P. *J. Polym. Sci.: Polym. Chem. Ed.* **1982**, *20*, 2565.
20. Ihara, T.; Yano, S.; Kita, K., *Process for producing phosphoric esters*, US Patent 5565601 5565601, **1996**.
21. Li, Y.; Dubin, P. L. *Macromolecules* **1995**, *28*, 8426.
22. Hamid, S. M.; Sherrington, D. C. *Polymer* **1987**, *28*, 325.
23. Bronich, T. K.; Cherry, T.; Vinogradov, S. V.; Eisenberg, A.; Kabanov, V. A.; Kabanov, A. V. *Langmuir* **1998**, *14*, 6101.
24. Ujiie, S.; Takagi, S.; Sato, M. *High Perform. Polym.* **1998**, *10*, 139.
25. Chen, H.-L.; Hsiao, M.-S. *Macromolecules* **1999**, *32*, 2967.
26. Thünemann, A.; Beyermann, J. *Macromolecules* **2000**, *33*, 6878.
27. Thünemann, A. F.; Kubowicz, S.; Pietsch, U. *Langmuir* **2000**, *16*, 8562.
28. Handlin, D. L. J.; Thomas, E. L. *Macromolecules* **1983**, *16*, 1514.
29. Shilov, V. V.; Tsukruk, V. V.; Bliznyuk, V. N.; Lipatov, Y. S. *Polymer* **1982**, *23*, 484.
30. Shilov, V. V.; Tsukruk, V. V.; Lipatov, Y. S. *J. Polym. Sci.: Polym. Phys. Ed.* **1984**, *22*, 41.

CHAPTER 4

POLYMERISATIONS WITHIN THE ORGANISED PHASES OF DI(UNDECENYL)PHOSPHATE

4.1. Introduction

Surfactant molecules retain their ability to form a variety of ordered mesophases within solid-state, stoichiometric polyelectrolyte-surfactant complexes.[1,2] The facile cooperative process of complex formation results in a range of mesostructures with excellent mechanical and thermal stability. Since template stabilisation is often required for the successful direct templating of organic polymerisation reactions, the excellent properties of polyelectrolyte-surfactant complexes make them potential candidates for use as novel hosts for templating. To date, much effort has gone into clarifying the structure of these highly ordered materials. Results show that they have interesting optical[3,4] and surface-energy lowering properties.[5] However, only a few attempts at using polyelectrolyte-surfactant complexes as templates for directed polymerisations have been described in the literature.[6-8] Attempts to homopolymerise within the complexes of a polyelectrolyte and a head-functionalised surfmer were unsuccessful presumably due to the decreased mobility of the reactive groups within the complex assembly.[7]

Here we would like to present a different approach to direct templating that utilises the mechanically stable, lamellar pDADMA / ωC11 complex (described

in Chapter 3) as template for polymerisation reactions. The tail position of the reactive groups of the ωC11 surfmer employed provides increased mobility of the reactive groups in the complex. Furthermore, stoichiometric amounts of unbound dithiol molecules (1,9-nonanedithiol and 1,6-hexanedithiol) are introduced in the complex in order to improve the possibilities for successful direct templating inside the complex. The thiol-ene polyaddition reaction used offers the advantage of avoiding the volume shrinkage, characteristic of polymerisation reactions, and in this way, improves the chances for preserving the template structure. Other advantages of the reaction are that it proceeds fast,[9] with high yields[10] and is relatively uninhibited by oxygen.[11]

Homopolymerisation reactions of ωC11 inside the complex assembly were also investigated. ^{60}Co γ-irradiation was used to initiate the homopolymerisation within the pDADMA / ωC11 complex, similarly to a reaction performed in vesicles of ωC11.[12] Cross-linking polymerisation reactions were also performed in the inverted hexagonal (H_{II}) phase of the ωC11 surfactant in order to compare the templating stability of the polyelectrolyte-surfactant complex to that of an ordered surfactant mesophase. Divinylbenzene (DVB) was used as a crosslinker in this thermally induced polymerisation. The structure of the resulting polymers was investigated by means of x-ray diffraction and microscopy techniques.

4.2. Materials

The following chemicals were purchased from Aldrich Co. and used as received: 1,9-nonanedithiol (9SH); 1,6-hexanedithiol (6SH) and potassium peroxosulfate (KPS). Water used for the preparation of lyotropic phases was

distilled and deionized in a "Milli-Q" water purification system (Millipore Corp.). Azobis(isobutyronitrile) (AIBN), from Aldrich, was recrystallised from dry ethanol. Divinyl benzene (DVB), from Aldrich, was distilled under reduced pressure to remove inhibitors. The pDADMA / ωC11 complex was synthesized according to a procedure described in Chapter 3, Section 3.3.2.3. Hexane, supplied by SASOL, South Africa, was used as received.

4.3. Experimental procedures

4.3.1. Preparation of the sodium salt of di(undecenyl)phosphate ($\omega C11^{-}Na^{+}$)

The sodium salt of ωC11 was prepared by the treatment of di(undecenyl)phosphate with a stoichiometric amount of NaOH in methanol. Thus 1 g (2.48 mmol) ωC11 was dissolved in 10 ml methanol, and the solution cooled down with ice. To this, 4.49 ml of a 0.0553 M solution of NaOH in methanol was added dropwise. Methanol was evaporated off under vacuum and the residue was dried overnight under vacuum at room temperature. The ^{1}H-NMR spectrum of the product revealed that the signal, characteristic of the phosphoric acid proton, appearing at 9.7 ppm, was absent from the spectrum of the sodium salt.

Yield di(undecenyl)phosphate sodium salt: 94%

^{1}H-NMR (MeOD, 300 MHz): δ/ppm = 1.29m [25H, 2 x –(C$\underline{H}_2$)$_6$-], 1.59p [4H, 2 x (C$\underline{H}_2$-C-O-)], 2.01q [4H, 2 x (C$\underline{H}_2$-C=C)], 3.82q [4H, 2 x (C$\underline{H}_2$-O)], 4.94m [4H, 2 x (=C$\underline{H}_2$)], 5.82m [2H, 2 x (-C$\underline{H}$=CH$_2$)].

4.3.2. Polymerisations in the inverted hexagonal phase (H_{II}) of ωC11Na^+/DVB/water

Lyotropic solutions of ωC11Na^+/water/initiator were prepared by mechanical mixing of 450 mg of the sodium salt of the surfactant, ωC11Na^+, with 50 mg of deionised water and 5 mg initiator. When KPS was used as an initiator, it was first dissolved in water and then added to the surfactant/water mixture. When AIBN was used as an initiator, it was dissolved directly in the surfactant/water mixture at 45 °C. The lyotropic mixtures, containing all reactants, were characterized by polarized light microscopy (PLM) at 60 °C and polymerised for 16 hours at the same temperature. The resulting polymers were washed repeatedly with water at 70 °C to remove any traces of unreacted surfmer. The samples were analysed before and after polymerisation and after template removal by means of PLM, SAXS, TEM and SEM (see results in section 4.4.1).

4.3.3. Polymerisation within the polymerisable polyelectrolyte-surfactant complex of pDADMA / ωC11

4.3.3.1.Polymerisation, using ^{60}Co irradiation

Films of pDADMA / ωC11 were weighed, placed in glass bottles, purged for 10 min with ultra-pure nitrogen and subsequently irradiated, using a γ-ray source and an irradiation dose of 1,66 Mrad. This reaction was similar to a polymerisation reaction within vesicles of the same surfactant, carried out by Paleos et al.[12] An array of fifty ^{60}Co rods of known ages was used as a source. The radiation dosage was measured by dosimeters attached to the samples. The measured dosage was an average of the required irradiation dose.

4.3.3.2. Polyadditon of thiols to terminal olefin groups in the bulk

Equimolar amounts of ωC11 and 1,9-nonanedithiol were mixed with 2 mol% AIBN. The reaction mixture was flushed with argon for 5 min and stirred at 70°C for 24 hours. The resulting polymer was then purified by the extraction of unreacted monomers using a 24-hour soxhlet extraction with hexane. The polymer was then analysed with PLM and SAXS (see results in section 4.4.3).

4.3.3.3. Swelling of pDADMA / ωC11 complex with dithiols

The weighed and dried films of the pDADMA / ωC11 complex were swollen by dipping them into either the 6SH or 9SH dithiol mixed with 2 mol% AIBN. The films were removed from the solution regularly, excess amounts of dithiol and AIBN were removed and the films were weighed. The amount of dithiol incorporated into the films was calculated from the films' weight increase. Swelling continued until a 1:1 molar ratio of thiol groups to double bonds was obtained.

4.3.3.4. Polyaddition of thiols to terminal olefin groups within the lamellar complex of pDADMA / ωC11

Films of pDADMA / ωC11, swollen with the respective dithiols, were weighed, placed in glass bottles and flushed with argon for 2 min. The bottles were sealed and immersed in an oil bath at 70 °C for 24 h. After polymerisation, any unreacted dithiol was removed by an overnight soxhlet extraction of the film with hexane.

4.3.4. Preparation of samples for analyses

4.3.4.1. Samples for polarised light microscopy (PLM)

A Leica DM R optical microscope, connected to a Linkam TP92 heater with THMS 600 heating stage, was used to characterise the lyotropic solutions before and after polymerisation. Thin films of the lyotropic phases were heated between glass slides from 45 °C to 70 °C, to verify that no phase transitions occurred in that temperature range (below 40 °C no lyotropic phase formation was observed).

4.3.4.2. Samples for transmission electron microscopy (TEM)

Samples of pDADMA / ωC11 complex, both before and after the polyaddition reaction, were first stained and embedded prior to analyses, using a procedure described in 3.3.3. Polymers obtained from the polymerisations in lyotropic solutions were characterized directly after purification. No staining or microtoming were required for visualisation.

4.3.4.2. Samples for scanning electron microscopy (SEM)

After removing unreacted surfactant from the lyotropic solutions, the purified polymers were placed on carbon-coated stubs before sputter coating. Samples were characterized using a Zeiss DSM 940 microscope.

4.3.4.4. Samples for small- and wide- angle-X-ray scattering (SAXS and WAXS)

Prior to the analyses all unreacted chemicals were extracted from the polymerised films by means of an overnight soxhlet extraction with hexane and

then dried under vacuum. All polymerised polyelectrolyte-surfactant films were ground fine and the powders analysed in transmission geometry. The same conditions were used for the analysis of purified polymers resulting from the polymerisations in lyotropic solutions. Samples from the polymerisations in the H_{II} phase, before template removal, and those from the swollen polyelectrolyte-surfactant complex were measured under helium atmosphere to avoid water and monomer evaporation, respectively.

4.4. Results and discussion

4.4.1. Polymerisation reactions in the inverted hexagonal phase (H_{II})

The liquid-crystalline behaviour of the surfactant $\omega C11Na^+$ in water was determined by means of the contact preparation method. Thus, crystals of surfactant, pressed in between two glass slides, were placed under cross-polarized light at 45 °C. A few drops of deionised water were dropped on the one side of the slides, and in the concentration gradient created the different liquid-crystalline phases of the surfactant in water were observed (Figure 4.1) (at temperatures lower than 40 °C the surfactant wasn't soluble in water). The phases could be identified owing to the presence of classical birefringent textures.[13]

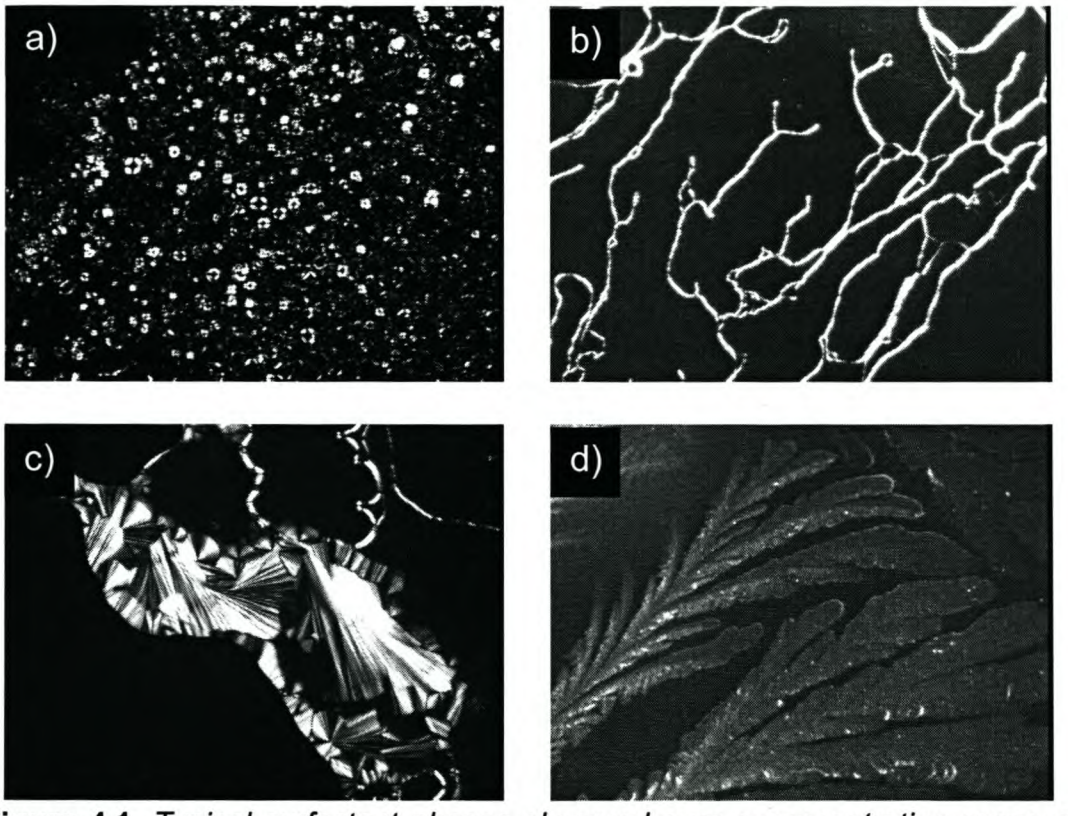

Figure 4.1. *Typical surfactant phases observed over a concentration range of the binary mixture of ωC11Na$^+$ / water. With the increase in the surfactant concentration transitions from a) vesicular to b) lamellar to c) inverted hexagonal to d) crystalline phase were observed.*

Of the three lyotropic, liquid-crystalline phases observed for the binary system ωC11Na$^+$ surfactant / water, the inverted hexagonal phase was chosen for templating due to its high solution viscosity. This high viscosity ensures the slower rearrangement dynamics within the phase, since monomer exchange between assemblies of less viscous liquid-crystalline phases is fast and often prevents direct templating from taking place.

All samples prepared for polymerisation reactions in the H_{II} phase showed the same phase morphology (inverse hexagonal) between 45 °C and 70 °C. Before polymerisation all samples were translucent. Fan textures, characteristic of the

inverse hexagonal phase were observed under polarized light, both before and after polymerisation (Figure 4.2 a and b) when using both KPS and AIBN as initiators for the polymerisation.

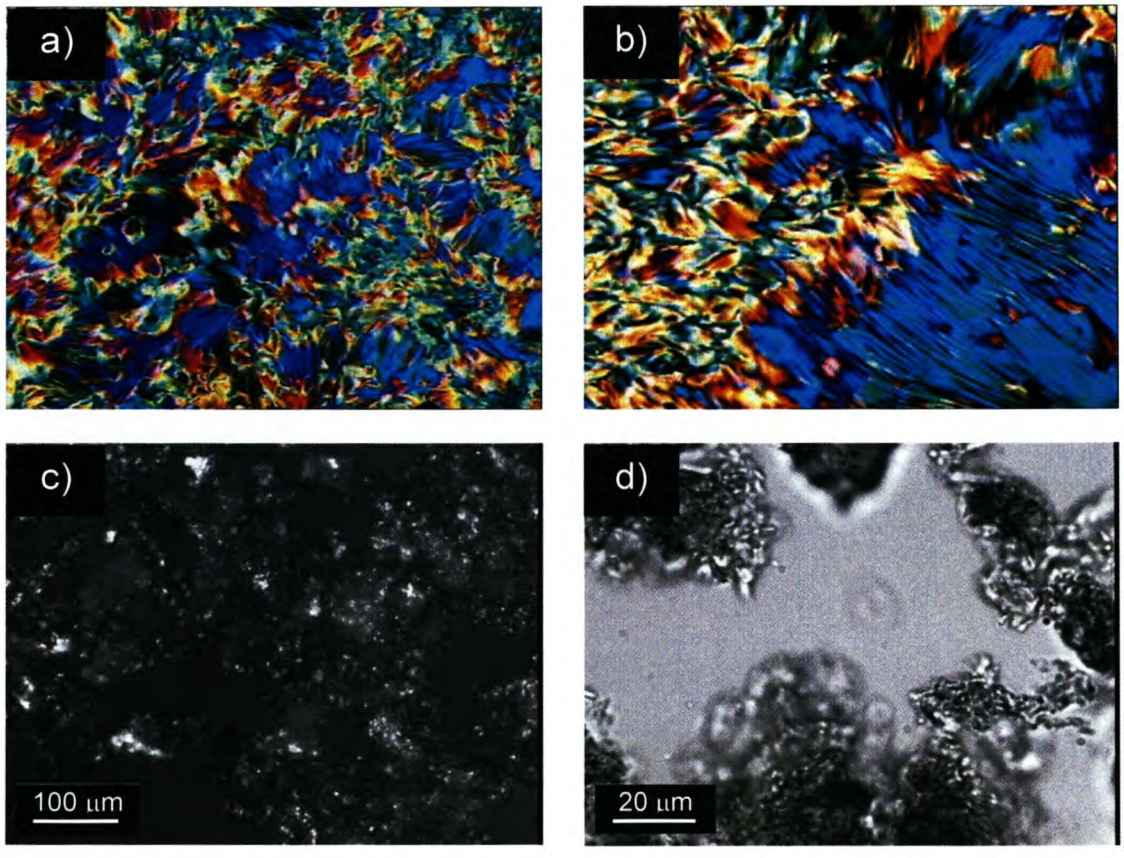

Figure 4.2. *Polarised light micrographs of a sample of ωC11Na$^+$ / H_2O / DVB / AIBN: a) before polymerisation; b) after polymerisation; and c) and d) after template removal by extraction with water at 70 °C.*

After polymerisation, increased turbidity in all of the samples was observed. One reason for this is the higher optical density of the polymer in comparison with the monomer. No macroscopic phase separation was observed, i.e. no significant changes in the fan texture were found after polymerisation.

After the reaction the template (unreacted ωC11Na$^+$ and water) was removed from the polymer matrix by washing with water at 70 °C and centrifugation at 1000 rpm. The structure of the resulting polymer was subsequently investigated by means of PLM, SAXS, SEM, and TEM.

SAXS analysis showed that on removal of the template (unreacted surfactant), the characteristic hexagonal structure of the host was lost and that the polymerised matrix did not have any pronounced long-range order (Figure 4.3b). This showed that, even though no macroscopic phase separation occurred during the reaction, mesoscopic demixing of the polymer phase from the lyotropic phase took place. After polymerisation, the less ordered polymer matrix coexisted with the highly ordered template phase.

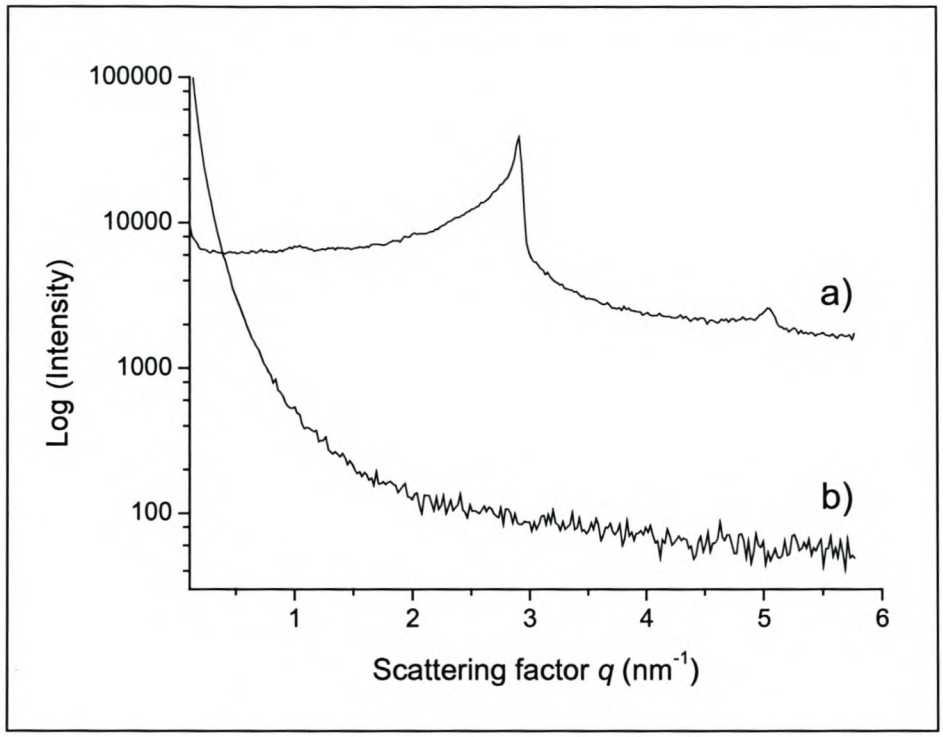

Figure 4.3. *SAXS scattering curves of: a) the binary template ωC11Na$^+$ / H_2O after polymerisation and b) the purified template free polymer. The scattering factor is defined as $q = 4\pi/\lambda \sin\theta$, where 2θ is the scattering angle between incident and scattered light, $\lambda = 0.154$ nm. The peak ratios of 1 : √3, observed after polymerisation, could be attributed to the H_{II} phase.*

The birefringence of the polymer matrix after template removal (Figure 4.2c and d), however, suggested an anisotropic morphology. This was the reason why further investigation of the polymer, using TEM and SEM, was performed. SEM showed that a layer-like morphology, with features on the micrometer scale, was formed (Figure 4.4).

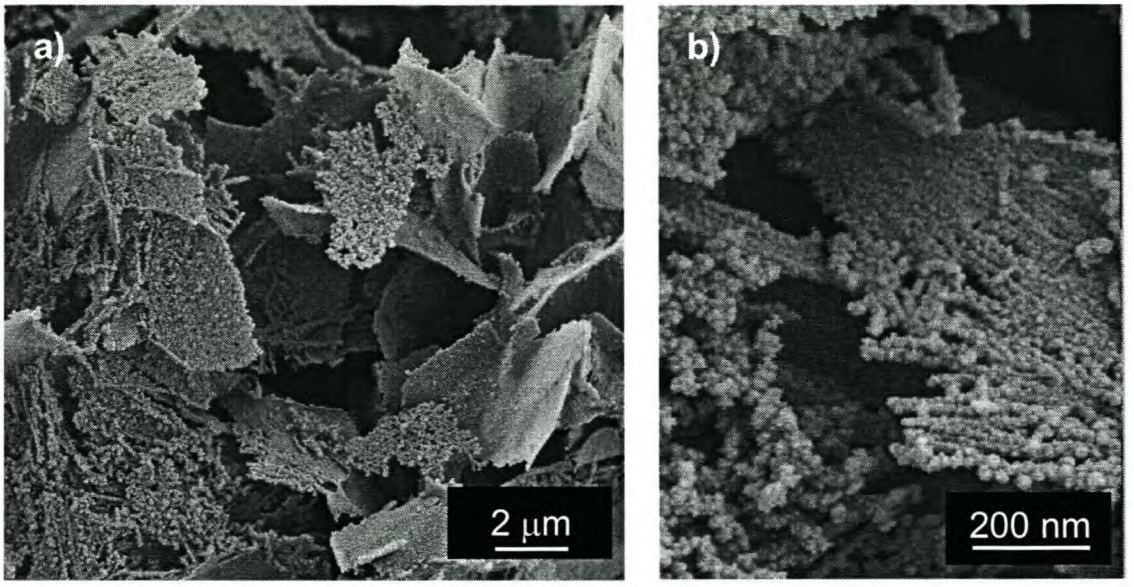

Figure 4.4. *SEM micrographs of the purified polymer matrix, from the polymerisation in the H_{II} phase, after template removal. AIBN was used as an initiator. Micrometer-sized sheet-like structures were observed.*

TEM indicated that there was a hierarchical nanostructure within the layers as each layer consisted of strands of polymer beads with a diameter of about 100 nm (Figure 4.5).

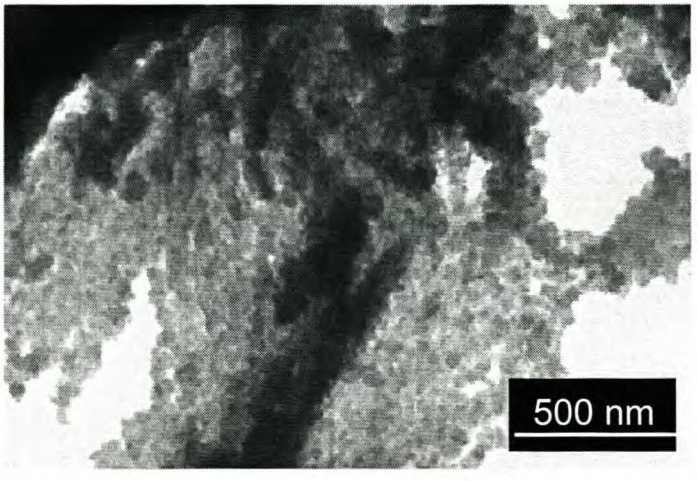

Figure 4.5. *TEM micrograph of the polymer, resulting from the polymerisation of $\omega C11Na^+$ / DVB / AIBN in the H_{II} phase. Chains of polymer beads, ~100 nm each, were observed after template removal.*

Even though the original nanostructure was not retained during the course of the reaction, regular polymer morphologies were obtained. This result hinted at a nucleation and growth mechanism, similar to the one suggested by Hentze *et al.*[14] (Scheme 4.1).

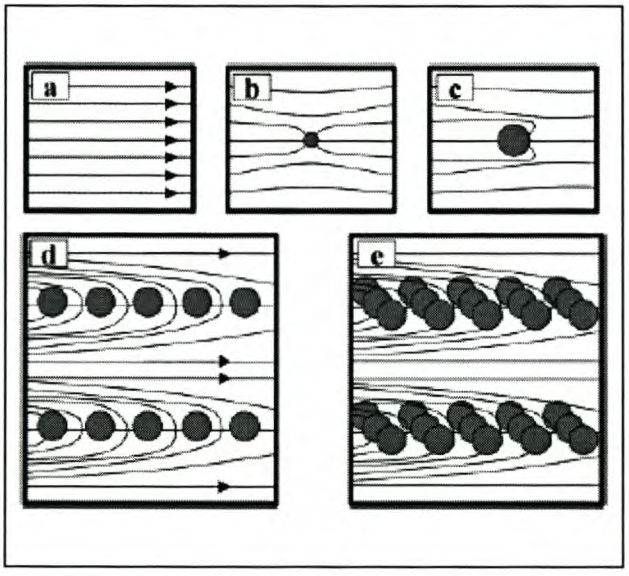

Scheme 4.1. Proposed mechanism of the structure-directed polymerisation: (a) arrows mark the director of the hexagonal phase; (b) in the presence of small polymer particles just slight distortions occur; (c) for bigger particles, normalization of the alignment at the particle surface takes place; (d) cooperative formation of particle chains in two dimensions; and (e) formation of layers of particle chains in three dimensions [ref. 14].

According to this mechanism the template is only the locus of nucleation while structure formation occurs on a larger length scale. Thus, even though the polymer formation is directed by the anisotropic reaction medium, no 1 : 1 templating takes place. The phase distortions observed by Hentze *et al.* during template polymerisations in a three dimensional (3-D) system are analogous to interactions that exist between a liquid-crystalline phase and a second preformed component in the 2-D nematic phase, described earlier by Loudet *et al.*[15]

Even though some ordering was observed in the polymers obtained from the polymerisations in the H_{II} phase, the ordering of the original parental structure could not be preserved. This result was in agreement with previous attempts to

polymerise ordered surfactant phases, which showed that it was not possible to polymerise in such 'soft' organized phases without disrupting the template structure.[16-18] In an attempt to preserve the template structure during organic polymerisation reactions, the ordered polyelectrolyte-surfactant complex of pDADMAC and the polymerisable surfactant ωC11 was applied as template.

Even though the formation and the solid-state structure[19-22] of polyelectrolyte-surfactant complexes have been well studied, to date little is known of reactions performed within the their ordered structure.[7] Polyelectrolyte-surfactant complexes have recently been introduced as a new type of structure-directing host, characterized by high template rigidity but a flexible outside geometry.[8]

As shown in Chapter 3, the complex of pDADMAC and ωC11 was well ordered on the nanoscale, and had a lamellar structure with a repeat unit of 3.02 nm.

4.4.2. Radiation-induced polymerisation in pDADMA / ωC11 complex

Attempts were made to perform a solid state, radiation-induced polymerisation within the pDADMA / ωC11 complex, similar to the reaction performed in vesicles of the same surfactant.[12] However, the analysis of the irradiated complex showed that it was not possible to polymerise the surfactant in the solid complex. No stoichiometric polyelectrolyte-polyelectrolyte complex (symplex) could be obtained, probably due to the decreased mobility of the surfactant within the complex assembly, or a non-appropriate steric arrangement of the double bonds.

The ^{1}H NMR spectra of the complex in chloroform-*d* (Figure 4.6) before and after irradiation were very similar, i.e. the resonances for intact double bonds (indicated by A and B in the figure) were still present in the spectra.

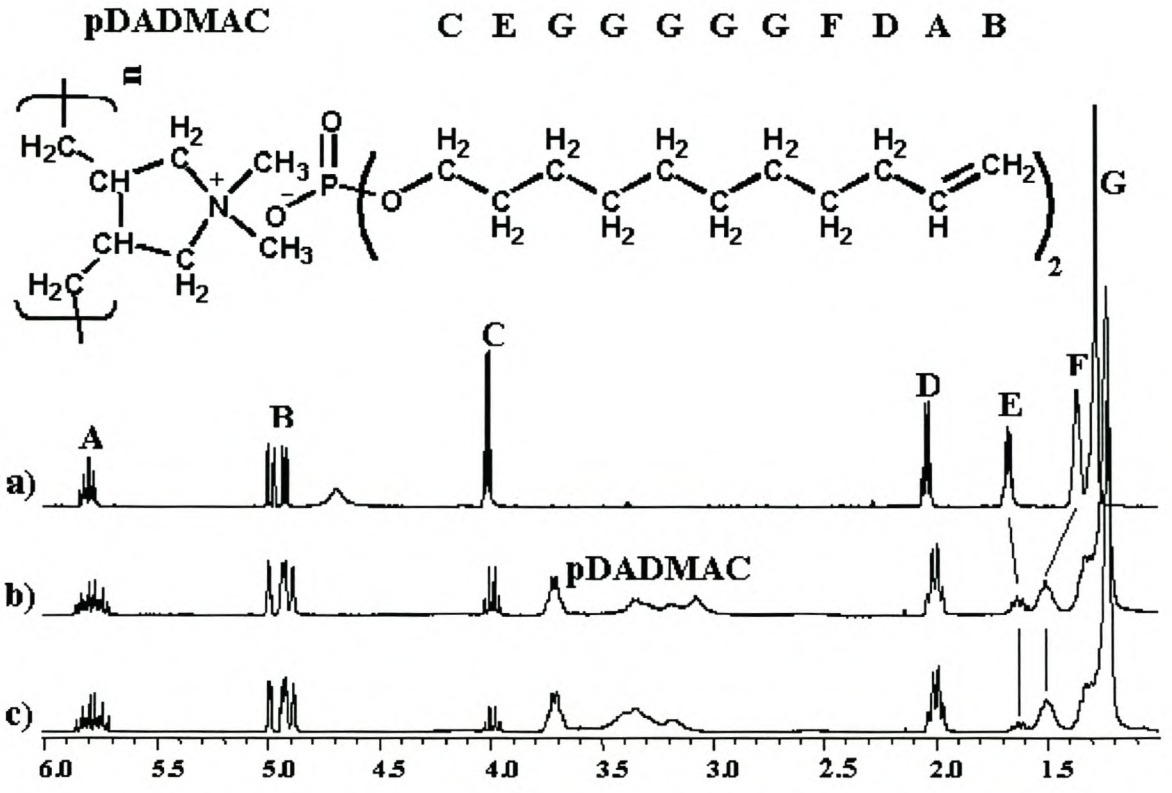

Figure 4.6. *^{1}H-NMR spectra of the a) surfactant ωC11, b) pDADMA / ωC11 complex before and c) after irradiation with a ^{60}Co source.*

4.4.3. Polyaddition of surfactant to 9SH

Based on the above result it was clear that a co-monomer was needed that would react with the surfactant phase by a free radical mechanism. It is known that thiols add to alkenes or alkynes in the presence of radical initiators, via a step-growth mechanism.[23]

The thiol-ene polymerisations are rapid and relatively uninhibited by oxygen.[11,24] The mechanism involves the addition of a thiyl radical to a vinyl functional group, followed by a radical transfer from the resulting carbon radical to a further thiol functional group. The polymerisation kinetics is first order in terms of the thiol functional group concentration, and independent of the ene functional group concentration.[25]

Due to the chemical nature of the reactive group of the surfactant, it should therefore be possible to use dithiols to perform a polyaddition reaction inside the complex. This has the advantage (over conventional free radical polymerisation) that volume shrinkage is largely avoided, and the possibilities for phase disruption minimized.

To ensure that the surfactant reacted with dithiols, equimolar amounts of ωC11 and 9SH were mixed with 2 mol% AIBN and left at 70 °C for 24 h. A white, hard and brittle solid was obtained after the reaction. The characteristic IR vibrations of the terminal double bond of the surfactant, $\nu_{=C-H}$ at 1095 and 3075 cm^{-1}, $\nu_{C=C}$ 1640 cm^{-1}, and $\delta_{=C-H}$ at 900 and 1000 cm^{-1}, could not be detected in the FTIR spectrum of the polymeric material. The characteristic frequency of the S-H bond, ν_{S-H} in the region between 2550 and 2590 cm^{-1}, was also absent from the IR spectrum. This showed that practically all double bonds and thiol groups had reacted. The newly formed polymer was birefringent under polarized light, and

therefore anisotropic in nature. This result was confirmed by SAXS analysis of the polymer (Figure 4.7), which showed that only low order existed. The diffractogram of the polymer showed only broad, low intensity peaks, from which it was impossible to determine the phase.

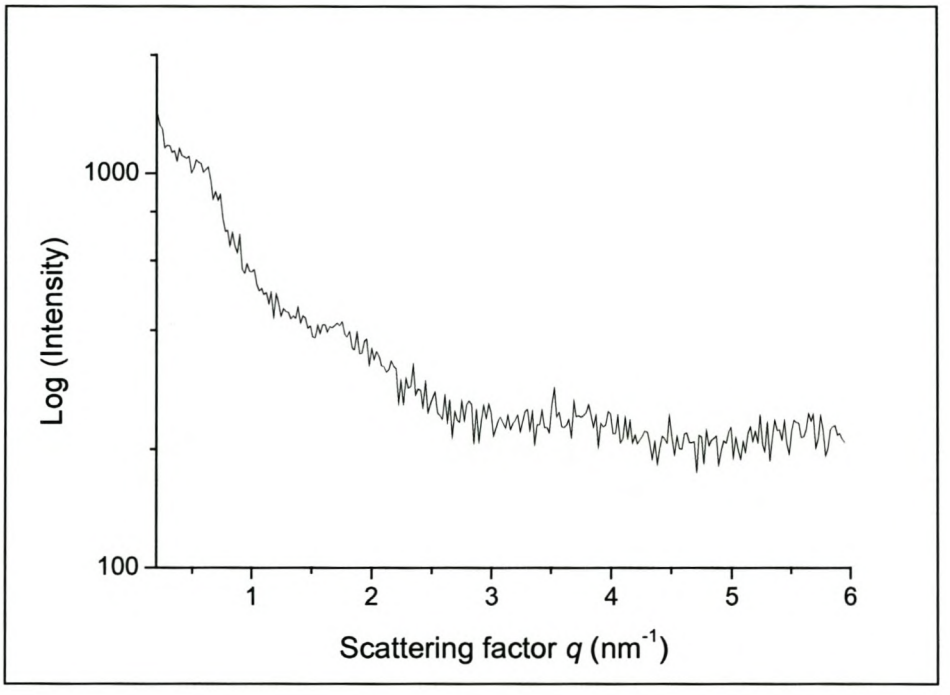

Figure 4.7. *SAXS diffractogram of polymer product from the 24 h bulk polymerisation of 9SH and ωC11, initiated by AIBN at 70 °C.*

4.4.4. Polyaddition within pDADMA / ωC11 complex

4.4.4.1. Swelling of pDADMA / ωC11 with 6SH and 9SH

The pDADMA / ωC11 complex showed linear swelling behaviour during swelling with both thiols. Swelling with 1,6-hexanedithiol however did proceed more rapidly. Films of the pDADMA / ωC11 complex were swollen to a monomer to co-monomer molar ratio of 1:1 (approximately 35 wt% for both thiols). After swelling, SAXS characterization of the complex was performed under helium atmosphere (instead of under vacuum) to ensure no monomer loss through evaporation at reduced pressure. The high order in the complex and the lamellar mesophase were preserved during the swelling experiment, despite the high degree of swelling (Figure 4.8). The main scattering peak was shifted to smaller scattering factors (i.e. larger *d*-spacing), and a slight broadening of the peaks was observed.

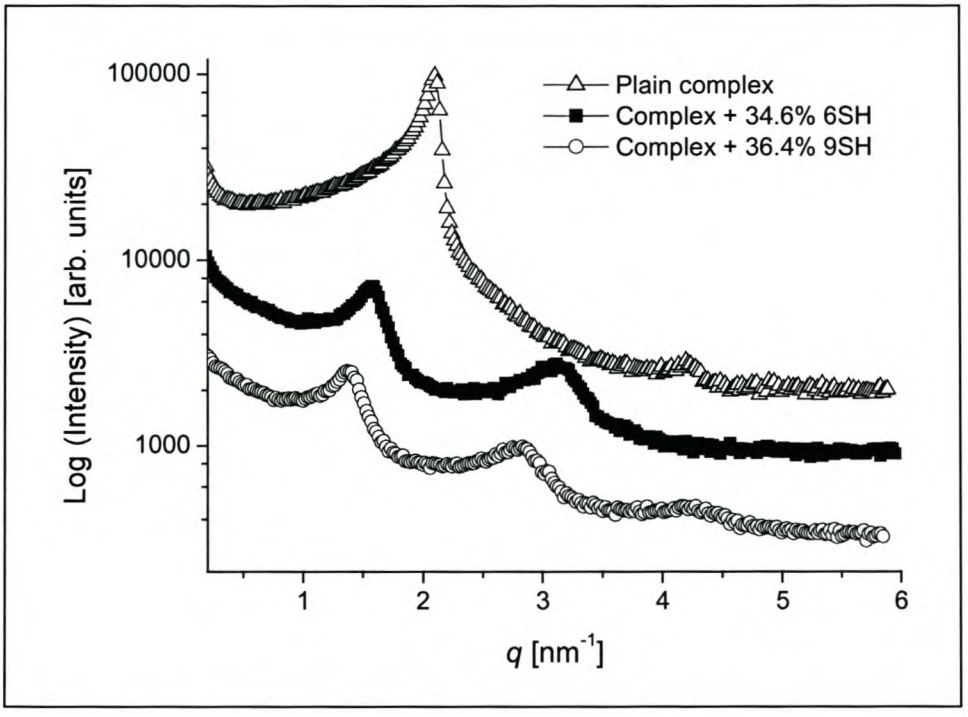

Figure 4.8. *X-ray scattering curves of films of pDADMA / ωC11 swollen with 6SH and 9SH co-monomers. Swelling of films with up to 35 wt % of both monomers proceeded without a phase change.*

In the case of 1,9-nonanedithiol the SAXS profile explicitly showed three diffraction peaks at q = 1.37, 2.84 and 4.28 nm^{-1}. The ratio of 1 : 2 : 3 determined from the location of these peaks indicated a lamellar supramolecular structure. The main scattering peak, at q = 1.37 nm^{-1}, corresponds to a repeat unit of 4.59 nm. The complex swollen with 1,6-hexanedithiol exhibited a main scattering peak at q = 1.57 nm^{-1} (d-spacing = 4.10 nm) and one higher order peak at q = 3.120 nm^{-1}. The peak ratio of 1 : 2 corresponded to a lamellar mesophase. The material properties of the swollen films were similar to those of the original non-swollen complex; they remained flexible and hygroscopic.

4.4.4.2. Polyaddition within the pDADMA / ωC11 complex

After the polyaddition reaction the films were very hard and brittle, and appeared white, compared to the slight yellow colour of the soft non-polymerised complex. It was impossible to dissolve the new material in chloroform (the solvent from which the original films were cast). After a 24 h soxhlet extraction with hexane (a good solvent for the dithiols) the characteristic thiol smell disappeared from the film. The dry weight loss after extraction was negligible, indicating that almost all thiol groups had reacted. SAXS diffractograms after the polymerisation, both before and after soxhlet extraction, confirmed that the high order in the complex was preserved. Only a negligible deviation in the positions of the main scattering peaks was observed in the complex polymerised with both 9SH and 6SH (Figure 4.9a and b).

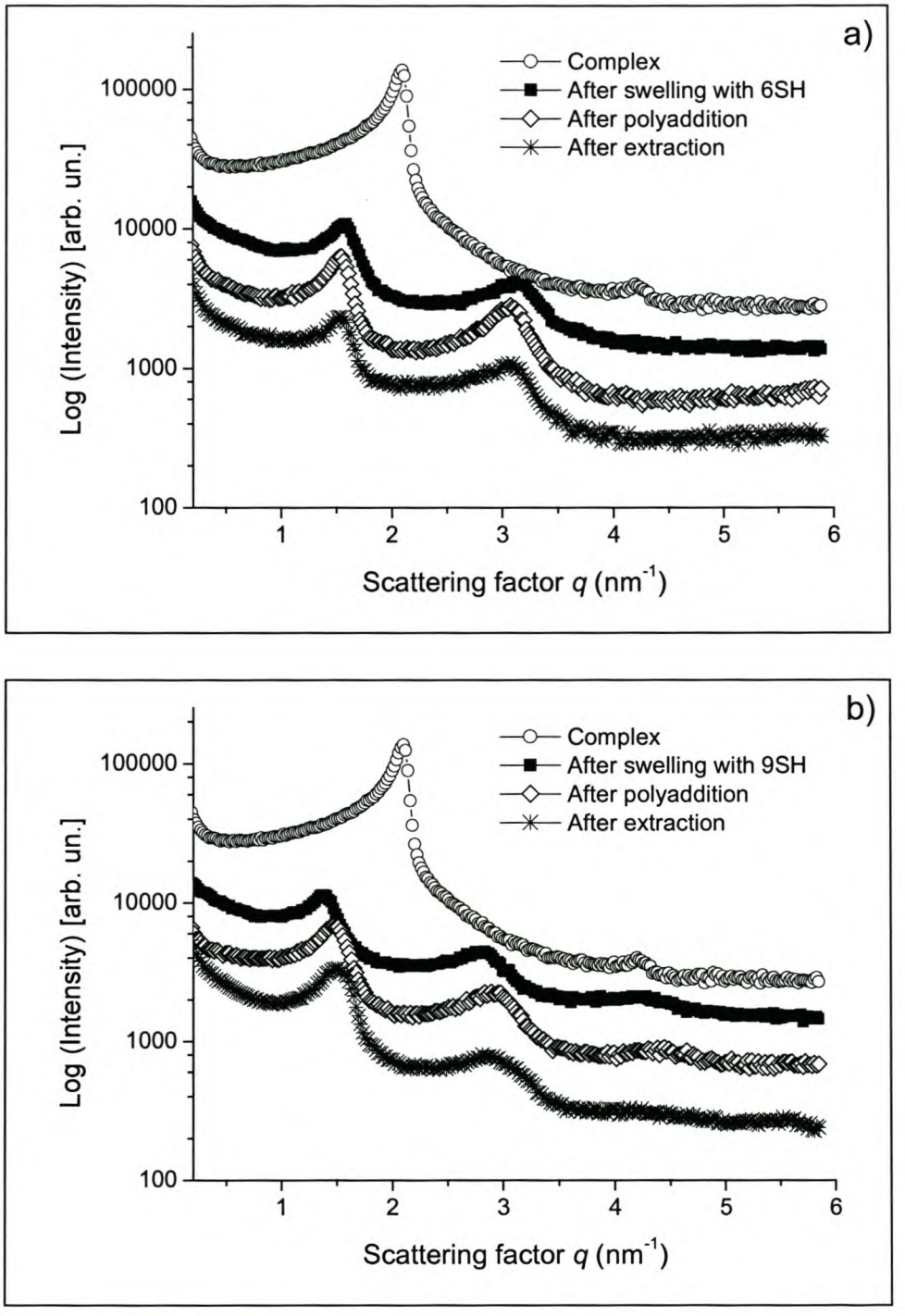

Figure 4.9. *SAXS diffractograms of polyaddition experiments within the pDADMA / ωC11 complex with: a) 1,6-nonanedithiol (6SH) and b) 1,9-nonanedithiol (9SH). SAXS measurements were done before and after swelling with dithiol, and after polyaddition and extraction of unreacted dithiol.*

WAXS analyses after polymerisation with both thiols proved that the complex remained noncrystalline, i.e. the liquid-crystalline arrangement of the alkyl tails was preserved during polymerisation.

Elemental analysis after extraction of the polymerised films confirmed the ratio of surfactant to dithiol molecules in the complex to be 1:1 (Table 4.1).

Table 4.1. Elemental analyses of pDADMA / ωC11 complex after polyadditon of dithiols (6SH and 9SH). Predicted values are calculated assuming complete reaction between the surfactant and the dithiols.

Complex after addition of:	Mass percentages: experimental (predicted values)			
	C%	H%	N%	S%
6SH	58.99 (60.57)	12.72 (10.78)	1.40 (1.58)	10.69 (9.79)
9SH	62.26 (62.03)	13.21 (10.99)	1.49 (1.49)	8.70 (8.17)

DSC analysis of the polymerised materials showed no detectable phase transitions in the temperature range –50 °C to 200 °C. This corresponds to the DSC measurements before polymerisation. TGA however proved the polymerised samples to be more resistant to temperature than the non-polymerised complex. The polymerised samples lost less than 20 wt% in the temperature range 25 to 350 °C, and only decomposed at around 450 °C. This is a significant increase in thermal stability compared to the original, non-polymerised complex, which lost 60 wt% at 300 °C and another 30 wt% at 460 °C.

The characteristic IR frequencies of a terminal double bond and the S-H group (see 4.4.3) could not be detected in the IR spectra of the polymerised samples. This provided further proof that there were no reactive groups left in the complex.

The transmission electron micrographs of the complex before and after the polyaddition reaction provided further proof of the existence of a lamellar phase (Figure 4.10., see next page).

The micrographs obtained were very similar to recently published data on linear elastomer-amphiphile systems.[26] The micrographs showed that continuous copies of the original host structure were formed. The characteristic period increased from approximately 3.0 nm for the non-polymerised complex to 4.1 nm for the 6SH- and 4.3 nm for the 9SH-polymerised complexes. These results were in excellent agreement with SAXS data, where the main scattering vector was observed at repeat units of 4.10 nm and 4.16 nm after the extraction of unreacted dithiol from the complex polymerised with 6SH and 9SH respectively.

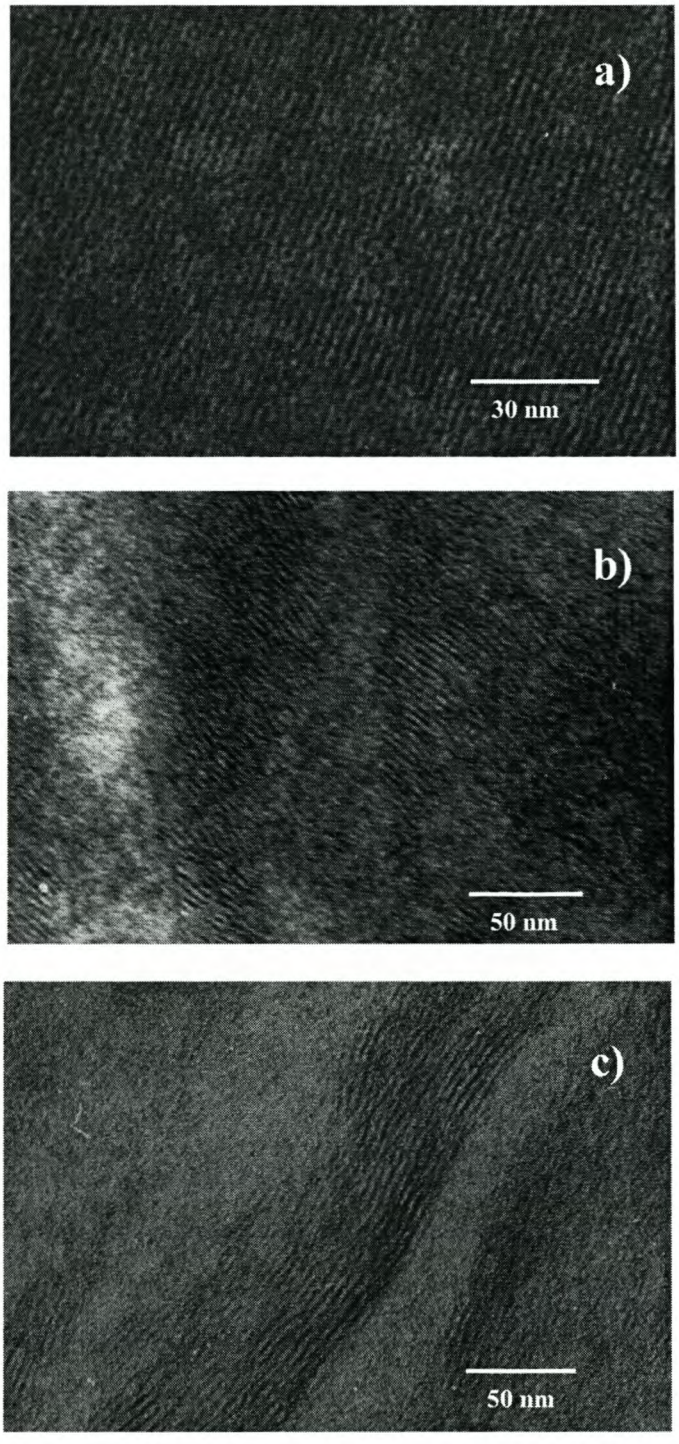

Figure 4.10. *TEM micrographs illustrating the lamellar structure in pDADMA / ωC11 complex a) before and after the polyaddition of b) 6SH and c) 9SH.*

4.5. Conclusions

The decreased surfmer mobility within polyelectrolyte-surfactant complexes makes the latter stable templates for organic polymerisation reactions. While only indirect templating was observed when polymerising in the H_{II} phase of the $\omega C11Na^+$ / H_2O / DVB / AIBN(KPS) system (sheet-like chains of polymer beads, ~ 100 nm in diameter, were produced), a 1:1 copy of the template was produced during polyadditions in the lamellar pDADMA / ωC11 complex. These results were confirmed by both SAXS and TEM.

The decreased mobility of the surfactant chains within the solid complex assembly prevented radiation-induced homopolymerisation from taking place. Monomer degradation rather than polymerisation was the preferred reaction pathway. Polymerisation and 1:1 templating was achieved only on incorporation of a comonomer inside the complex and following a polyaddition reaction route.

The pDADMA / ωC11 complex was stable to swelling with ~35 wt% of comonomer (thiol) without signs of phase disruption. No phase disruption or disordering occurred during polyaddition and the extraction of the polymer films. Polyaddition proceeded until all reactive groups were consumed (as proved by FTIR analyses). Furthermore, the resulting lamellar polymer symplex showed improved thermal and mechanical properties.

4.6. References

1. Macknight, W. J.; Ponomarenko, E. A.; Tirrel, D. A. *Acc. Chem. Res.* **1998**, *31*, 781.
2. Ober, C. K.; Wegner, G. *Adv. Mater.* **1997**, *9*, 17.
3. Thünemann, A. *Adv. Mater.* **1999**, *11*, 127.
4. Thünemann, A. F.; Ruppelt, D. *Langmuir* **2001**, *17*, 5098.
5. Thünemann, A. F. *Prog. Polym. Sci.* **2002**, *27*, 1473.
6. Antonietti, M.; Kublickas, R.; Nuyken, O.; Voit, B. *Macromol. Rapid Commun.* **1997**, *18*, 287.
7. Dreja, M.; Lennartz, W. *Macromolecules* **1999**, *32*, 3528.
8. Faul, C. F. J.; Antonietti, M.; Hentze, H.-P.; Sanderson, R. D. *Langmuir* **2001**, *17*, 2031.
9. Griesbaum, K. *Angew. Chem. Int. Ed. Engl.* **1970**, *9*, 273.
10. Marvel, C. S.; Chambers, R. R. *J. Am. Chem. Soc.* **1948**, *70*, 993.
11. Cramer, N. B.; Scott, J. P.; Bowman, C. N. *Macromolecules* **2002**, *35*, 5361.
12. Paleos, C. M.; Christias, C.; Evangelatos, G. P.; Dais, P. *J. Polym. Sci.: Polym. Chem. Ed.* **1982**, *20*, 2565.
13. Rosevear, F. B. *J. Am. Oil Chem. Soc.* **1954**, *31*, 628.
14. Hentze, H.-P.; Kaler, E. W. *Chem. Mater.* **2002**.
15. Loudet, J.-C.; Barois, P.; Poulin, P. *Nature* **2000**, *407*, 611.
16. Pacios, I. E.; Renamayor, C. S.; Horta, A.; Lindman, B.; Thuresson, K. *Macromolecules* **2002**, *35*, 7553.
17. Holtzscherer, C.; Wittmann, J. C.; Guillon, D.; Candau, F. *Polymer* **1990**, *31*, 1978.
18. Antonietti, M.; Goltner, C.; Hentze, H.-P. *Langmuir* **1998**, *14*, 2670.
19. Antonietti, M.; Conrad, J.; Thünemann, A. F. *Macromolecules* **1994**, *27*, 6007.

20. Antonietti, M.; Conrad, J. *Angew. Chem. Int. Ed. Engl.* **1994**, *33*, 1869.

21. Yeh, F.; Sokolov, E. L.; Khokhlov, A. R.; Chu, B. *J. Am. Chem. Soc.* **1996**, *118*, 6615.

22. Zhou, S.; Chu, B. *Adv. Mater.* **2000**, *12*, 545.

23. Stacey, F. W.; Harris, J. F. J. *Formation of carbon-hetero atom bonds by free radical chain additions to carbon-carbon multiple bonds*; John Wiley & Sons, Inc. NY, **1963**; Vol. 13.

24. Kharasch, M. S.; Nudenberg, W.; Mantell, G. J. *J. Org. Chem.* **1951**, *16*, 524.

25. Cramer, N. B.; Davies, T.; O'Brien, A. K.; Bowman, C. N. *Macromolecules* **2003**.

26. Luyten, M. C.; Alberda van Ekenstein, G. O. R.; Wildeman, J.; ten Brinke, G.; Ruokolainen, J.; Ikkala, O.; Torkkeli, M.; Serimaa, R. *Macromolecules* **1998**, *31*, 9160.

CHAPTER 5

POLYMERISATION OF THE ORGANISED PHASES OF POLYELECTROLYTE – SURFACTANT COMPLEXES

5.1. Introduction

Polymerisations in organised media, the subject of intense research in recent years,[1] aim at turning the fragile, assembled template structures into mechanically and chemically durable materials.[2] This endeavour is complicated because of the influence of the growing polymer chain on the ordered template, causing disruption and phase separation to occur during the reaction. Recent investigations have subsequently focused on templates with increased stability and slow exchange dynamics, which should provide stable templates for successful directed polymerisations.[3,4]

Polyelectrolyte-surfactant complexes have only recently been introduced as a new type of mesoscopically ordered polymer structure-directing host.[5,6] Despite their potential (robustness and structural diversity), direct templating of their ordered phases have not yet been reported in the literature.

Recent work carried out by Faul *et al.* concentrated on the structure-directed polymerisation of some vinyl monomers in polyallyldimethylammonium-dodecylsulfate (PDADMA/DS) complexes.[5] Polymer nanoparticles (instead of extended replicas of the structure-directing phase) with interesting anisotropic

shapes were obtained. Further investigations into reactions within these promising organised systems led to the synthesis of the reactive surfactant di(undecenyl)phosphate (ωC11). This surfactant monomer or surfmer, originally synthesized as a model synthetic lipid membrane component,[7,8] was used to prepare complexes with polyallyldimethylammonium chloride (pDADMAC). A radical addition reaction of dithiols to these ωC11 surfmers, organised within the polyelectrolyte-surfactant complex, produced systems where the hydrophobic subphase of the complex was polymerised.[9] Making use of this addition strategy, the original structure of the polyelectrolyte-surfactant complex was preserved (as proved by SAXS and TEM analyses) and high-performance polymer films produced. Since the quantity of vinyl groups (fixed within the complex due to charge coupling) and thiol groups have to be carefully balanced, the stoichiometry and the resulting film composition is fixed and not subject to broader variation.

The topic of the present chapter is to extend previous trials (described in Chapter 4) carried at polymerisation reactions within the organised pDADMA/ωC11, by performing a ternary copolyaddition of an unsaturated surfmer, a α-ω-diene, and a dithiol. The use of a ternary copolyaddition provides an opportunity to vary the composition within the polyelectrolyte-surfmer complex, a parameter that was not subject to variation in the original binary system. Using this approach it was possible to investigate how polyelectrolyte-surfactant complexes can be swollen, and polymerised, under preservation of their nanostructure, i.e. to what degree (otherwise unstructured) material can be organized by the template while it is only bound via a few linkages to the matrix.

Weight uptake and polarized light microscopy (PLM) were used to determine the swelling behaviour of the organized films with monomer and cross-linking agent. The films after polymerisations, i.e. the hybrids between polymer and

complexes, were examined by total weight uptake, wide angle X-ray scattering (WAXS), SAXS, IR and TEM (after the extraction of reactive compounds not included in the polymerised complex).

5.2. Materials

The following chemicals were purchased from Aldrich Co. and used as received: 1,9-nonanedithiol (9SH); 1,6-hexanedithiol (6SH); 1,9-decadiene (1,9-D); hexane and high molecular mass polydiallyldimethylammonium chloride (pDADMAC, M_w 375 000 – 500 000). Azobis(isobutyronitrile) (AIBN) was recrystallised from dry ethanol. The pDADMA/ωC11 complex was synthesized as described in Section 3.3.2.3.

5.3. Experimental procedures

5.3.1. Polymerisations in solution

Equimolar $CDCl_3$ solutions of: 1.) 9SH and 1,9-D; 2.) 6SH and 1,9-D; 3.) 9SH and ωC11; 4.) 6SH and ωC11 were prepared. The respective solutions were mixed in NMR tubes, flushed with N_2, sealed and placed in a 600 MHz Varian Unity Inova spectrometer at 50 °C. Standard pulse sequences were used, and for each datum only one acquisition (FID), nt = 1, was used to ensure that the measurement corresponded to instantaneous composition/conversion and not to an average. The sample temperature was maintained at 50 °C using the heater controller of the NMR equipment. A D_2O solution of N,N-

dimethylaminopyridine (DMAP, 10 mg) in a thin-wall capillary tube, introduced in the NMR tube, was used as a reference. The decrease in intensity of the signals characteristic of the reactive olefin groups of either the surfactant (ωC11) or the diene (at 5.08 and 5.88 ppm), relative to the DMAP reference signal, was followed during the course of the reactions. 2 mol% AIBN was used as initiator in all cases.

5.3.2. Polymerisation inside pDADMA / ωC11 complex

5.3.2.1. Swelling of complex with diene and thiol (6SH / 9SH) solutions

Dried sections of the pDADMA/ωC11 complex were first dipped into the liquid 1,9-D until the desired weight uptake was reached. Samples were then transferred to pure 6SH and 9SH respectively, in order to swell and achieve 1:1 stoichiometry of thiol groups to the total amount of vinyl groups (i.e. surfmer and 1,9-D). 2 mol% AIBN, with respect to the thiol, was used as an initiator. The films were removed from the swelling solutions and weighed regularly. Residual thiol solutions were analysed to detect traces of diene (that could have diffused back from the solid complex film and into the thiol swelling solution) using NMR spectroscopy.

For the polymerisations with 9SH and 1,9-D, films were initially swollen with 8, 16, and 24 wt% of the diene, followed by a swelling with 9SH until the correct stoichiometry was reached. The total weight uptake, after the swelling with 9SH, thus increased to 50, 72, and 94 wt% respectively. Throughout the discussion that follows, the weight percentages given indicate the total of both thiol and diene incorporated into the complex. For the polymerisations with 6SH, films were swollen with diene only to 4, 10, and 23 wt% respectively, translating to a total (with both 6SH and 1,9-D) of 39, 50, and 78 wt%.

Approximately 35 wt% of thiol is the minimum required to react with the vinyl groups of the ωC11 surfmer bound within the complex. Performing ternary polymerisations within complexes containing less than 35 wt% comonomers would therefore render residual reactive surfmer/diene groups. The range of the experiments was extended to higher comonomer content, with the specific aim of reaching the limit of swelling where the parental lamellar order no longer exists, i.e. where disorder is found. This was done to determine the maximum amount of unstructured material that could be organised within the lamellar polyelectrolyte-surfactant complex before the phase disruption of the host.

5.3.2.2. Polyaddition.

After swelling, the films were weighed, placed in glass bottles and flushed with nitrogen for 2 min. The bottles were sealed and immersed in an oil bath at 70 °C for 24 h. The nitrogen blanket serves to ensure rapid polymerisation, since the reaction proceeds more slowly in the presence of oxygen.[10,11] After reaction, samples were weighed, and traces of unreacted chemicals were removed by an overnight soxhlet extraction of the films with hexane. Insignificant or no dry weight changes were observed after extraction of the polymerised samples.

5.3.3. Preparation of samples for analysis

Prior to analysis all samples were dried overnight under 20 mbar vacuum. Dried pieces of film were then analysed using FTIR, DSC and TGA. Samples for TEM, SAXS and WAXS were prepared using procedures described in Section 3.3.3.

5.4. Results and Discussion

5.4.1. Thiol-ene addition in solution

Solution polymerisations were performed between the different reagents (ωC11 and 6SH or 9SH, as well as 1,9-D with 6SH or 9SH) to ensure that the reactions proceed until completion. NMR results from the proton spectra of these solution polymerisation showed that polymerisation reactions proceeded smoothly until all reactive groups were consumed, but reaction times differed significantly for the different systems (Figure 5.1).

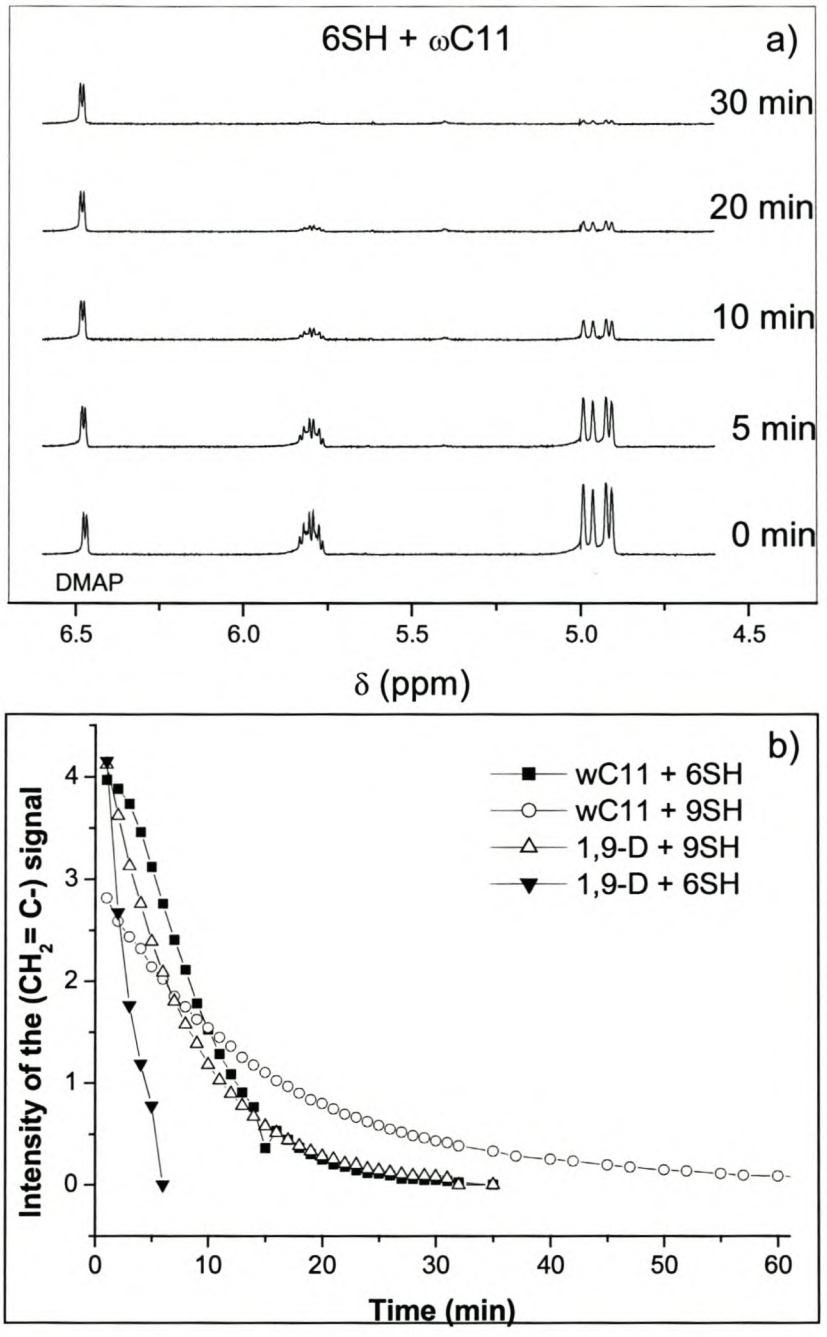

Figure 5.1. *a) Details of the vinyl region of some representative ^{1}H-NMR spectra from the copolymerisation reaction of 6SH and ωC11. The characteristic vinyl group resonances at 5.0 and 5.8 ppm disappear, indicating that all reaction groups are consumed during the reaction. b) An overview of the solution polymerisations of 6SH/9SH with either diene or surfactant ωC11. The intensity of the CH_2=CH- signal (at 5.0 ppm) was monitored with reaction time.*

From Figure 5.1b it can be seen that reaction times vary between 5 and 30 minutes for the different systems. 6SH reacted with the ωC11 surfactant and with the diene in the matter of a few minutes, while reaction times for the 9SH thiol were 4-5 times longer. The addition of the diene to both thiols resulted in a marked increase of the speed of reaction (in comparison with the addition of ωC11 only), fitting well with our simple expectations based on the higher flexibility and lower steric constraints of this unbound compound. Under these chosen conditions, the reactions were almost fully completed in all cases after 60 minutes, i.e. in the correct stoichiometric ratios.

5.4.2. Ternary polyaddition within the lamellar, solid-state pDADMA/ωC11 complex

5.4.2.1. pDADMA/ωC11 complex swollen with thiol and diene

The parental pDADMA/ωC11 complexes were easily swollen with both diene and thiol solutions (see 5.3.2.1). The initial swelling of the films with 1,9-D proceeded significantly faster than the following swelling with 6SH or 9SH. The rate of swelling with thiols decreased slowly with an increase in the amount of diene incorporated into the complex. A marked decrease in the 9SH swelling rate was observed in the case of the complex swollen with 24 wt% of 1,9-D. This corresponded to a total weight uptake of 94 wt% (of 9SH and 1,9-D), and indicated a possible phase disruption or transition occurring within the complex (see Figure 5.2. a).

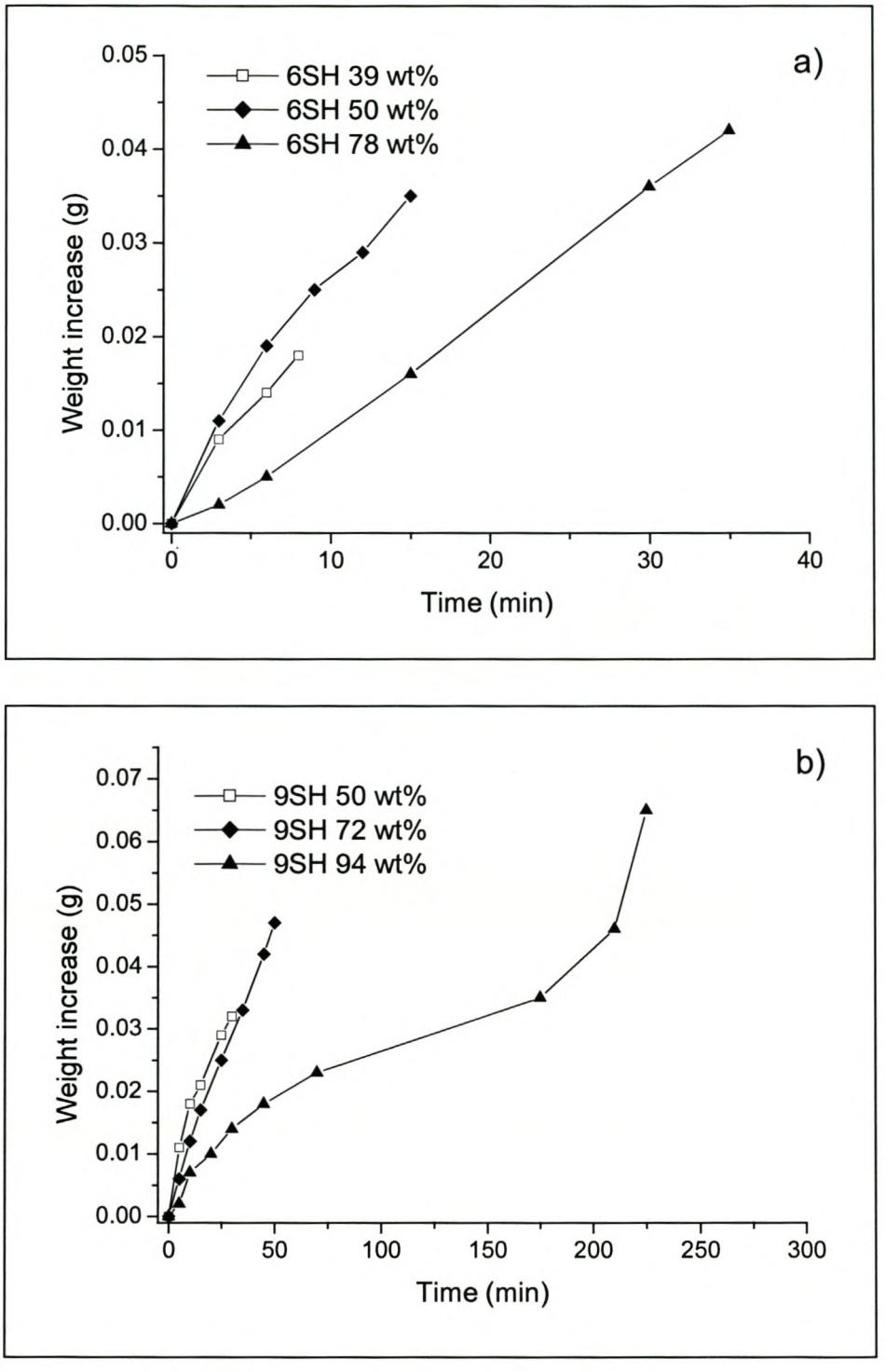

Figure 5.2. *Weight increase during swelling of PDADMA/ωC11 complex with a) 9SH up to 50, 72, and 94 wt% and b) 6SH up to 39, 50, and 78 wt%. The complex films were initially swollen with various weight percentages of 1,9-D.*

Swelling took place with preservation of the clear appearance of the films, indicating the absence of macroscopic demixing. Typical textures of polyelectrolyte-surfactant complexes were observed using polarization microscopy in all films, including the ones swollen with 94 wt% of 9SH and 1,9-D. These results indicated the absence of macroscopic demixing and the maintenance of the organized phases.

After swelling, the residual thiol solutions were analysed by ^{1}H-NMR in order to ascertain whether diene diffused from the film into the thiol swelling solutions. The characteristic resonances of the vinyl group of 1,9-D at 5.08 and 5.88 ppm were absent from the spectra of the thiol, confirming that no back diffusion had taken place.

5.4.2.2. pDADMA/ωC11 complex polymerised with thiol and diene

After polymerisation, all samples, except the one swollen until 94 wt%, appeared opaque, and very hard. The film swollen to 94 wt% remained transparent, even after polymerisation. No significant weight change was observed after the hexane extraction of the samples polymerised with thiol and diene, i.e., all monomers were at least partially reacted and bound to the matrix.

FTIR measurements of ground samples of the polymerised complex films showed that there were some residual double bonds left in the complex. Good miscibility of the components, together with the fast diffusion (and no back diffusion) of diene into the complex, indicated that the reagents for polymerisation were evenly distributed throughout the complex. This result suggests that due to the topological constraints of the solid-state system, full 1:1 conversion could not be reached in the bulk of the complex and that isolated reactive sites are kept apart by the already condensed network.

The PDADMA/ωC11 complex, swollen with the comonomers, presents different possibilities for covalent bond formation. These are presented in Scheme 5.1 below.

Scheme 5.1. Schematic representation of some of the possible cross-layer and other covalent linkages formed during polyaddition within the pDADMA / ωC11 complex. Cross-layer linkages are suggested due to the insolubility of the crosslinked complex.

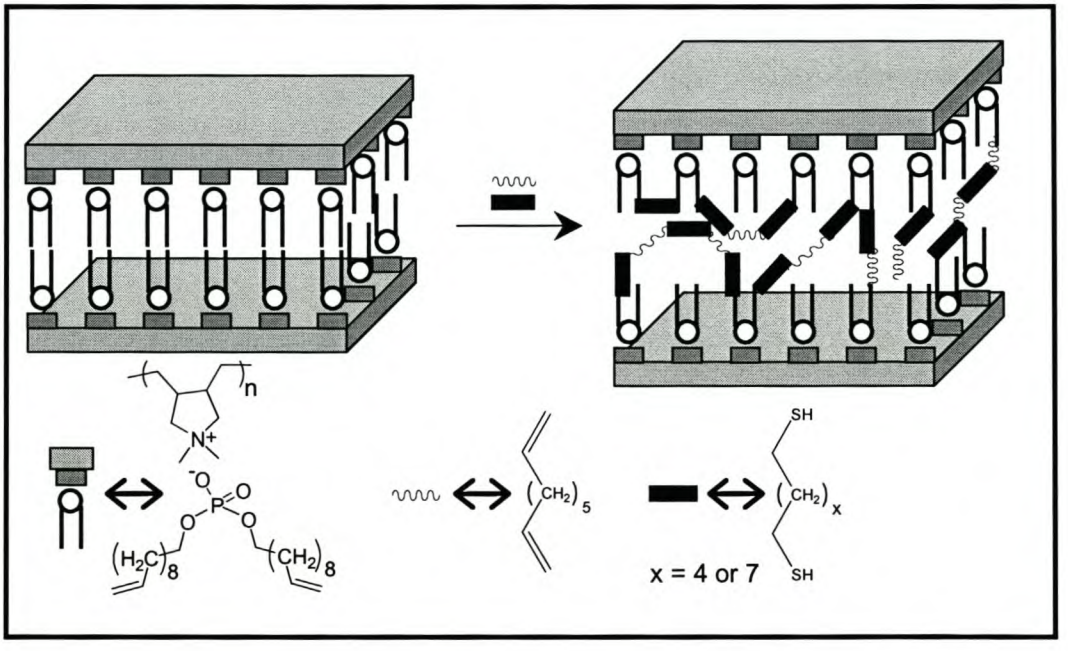

The radical thiol addition, which was chosen as the basis of our polymerisations in the organised pDADMA / ωC11 complex, has been well described in the literature; it is generally considered to proceed via a multistep chain mechanism.[12,13] Due to the oleophilic nature of both the comonomers and the initiator, the locus of the polymerisation should be situated within the hydrophobic parts of the layered complex, occupied by the alkyl tail of the ωC11 surfactant.

Thermal gravimetric analyses showed that samples polymerised with 1,9-D and thiol, 6SH/9SH, started degrading between 381 °C and 397 °C. This is close to 100 °C increase in the thermal stability of the sample compared to pDADMAC / ωC11, and another 20 °C increase in comparison with the samples polymerised with thiols only (see Table 5.1). The onset of degradation (T_{onset1}) was determined by extrapolating the tangents of the weight loss curve. The temperature of the second degradation step (T_{max2}) was determined as the minimum of the first derivative of the weight loss curve.

Table 5.1. A summary of the results from thermal gravimetric analyses of films of pDADMAC / ωC11, before and after the polyaddition of different amounts of comonomers (6SH/9SH, 1,9-D).

Sample (% comonomer)	Degradation (°C)		Sample (% comonomer)	Degradation (°C)	
	T_{onset1}	T_{max2}		T_{onset1}	T_{max2}
pDADMAC	326	477	PDADMAC	326	477
Plain complex (0 %)	302	464	Plain complex (0 %)	302	464
6SH (35 %)	363	451	9SH (36 %)	366	458
6SH+1,9-D (39 %)	381	480	9SH+1,9-D (50 %)	391	479
6SH+1,9-D (50 %)	398	491	9SH+1,9-D (72 %)	389	481
6SH+1,9-D (78 %)	381	479	9SH+1,9-D (94 %)	381	480

The increase in thermal stability after polymerisation corresponded well with our expectations that the polymerised samples would be thermally more stable than the unpolymerised pDADMAC / ωC11 complex. The incorporation of diene led to an increase in the onset of degradation. Furthermore with the increasing amounts of diene, the onset of degradation shifted to higher temperatures. The

reason for the decrease of the degradation temperature, at very high comonomer content (> 72 wt%), could be attributed to a possible phase disruption and demixing taking place.

The degradation proceeded in two steps with the second step losing its definition in the polymerised samples compared to the plain complex before polymerisation (Figure 5.3).

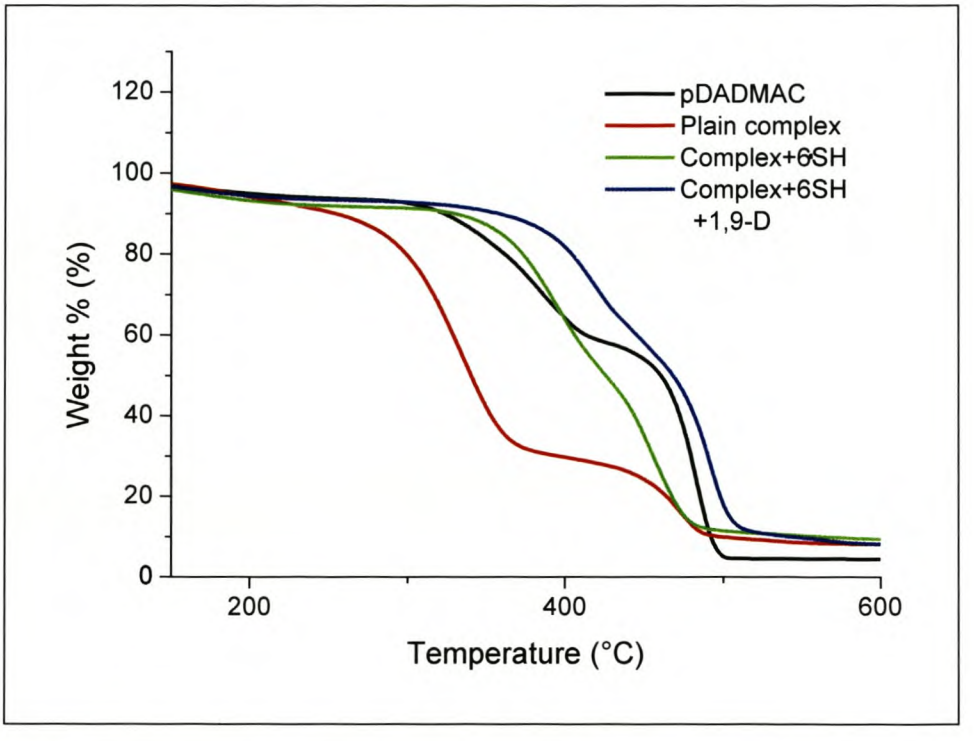

Figure 5.3. *TGA curves of films of pDADMAC / ωC11 before and after the polyaddition of thiols, and mixtures of thiol and diene.*

The first step was associated mainly with the degradation of bound surfactant, and the second with that of the pDADMAC. Since the polymerisation reactions performed inside the complex involved the crosslinking of the surfactant phase, and formation of a stable polyelectrolyte-polyelectrolyte complex (simplex), the

shift of T_{onset1} to higher temperatures and its overlapping with the second peak (characteristic for the degradation of the polyelectrolyte) was in good agreement with the experiment. This assumption was also confirmed by the fact that the position of the second degradation peak remained relatively constant before and after polymerisation.

5.4.3. Structure of the polymerised complexes

Order on the atomic length-scale was determined by WAXS. Broad reflections at $q \approx 14.4$ nm^{-1} (Bragg spacing of 0.43 nm) and 26.8 nm^{-1} (0.22 nm) were found (Figure 5.4), indicating the liquid-like amorphous arrangement of both the ionic and the hydrophobic alkyl phases. The observed Bragg spacing of 0.43 nm is close to the known value of a densely packed alkane layer.[14]

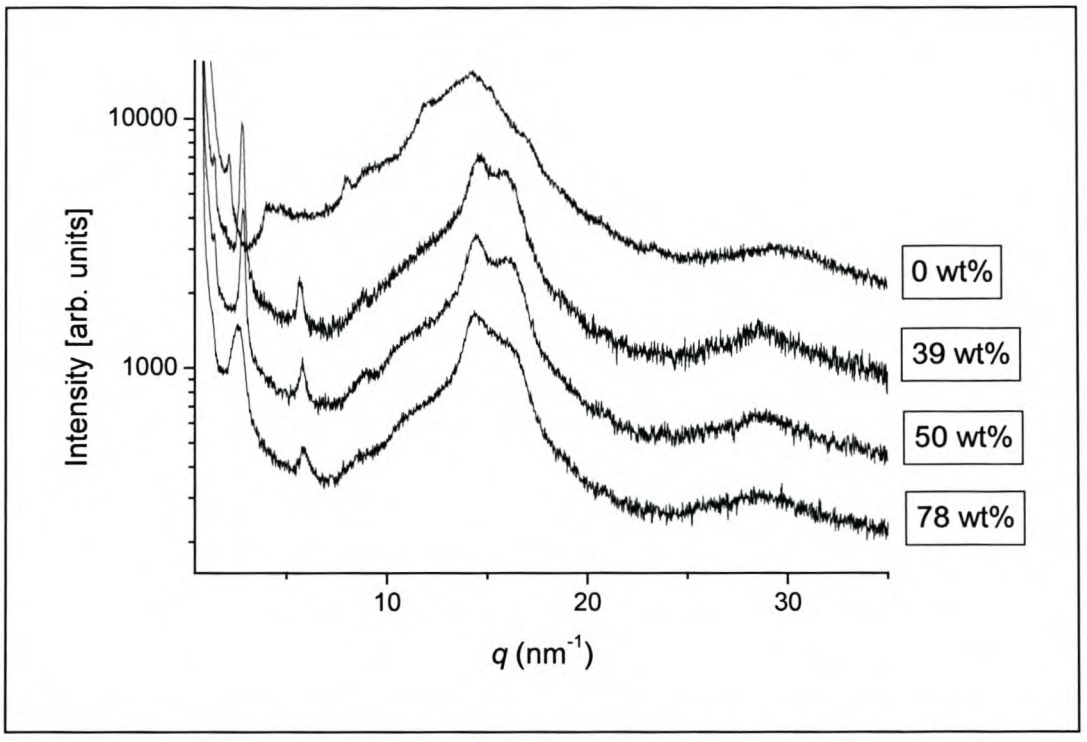

Figure 5.4. *WAXS diffractograms of films of pDADMA / ωC11 after polymerisation with 6SH and 1,9-D. The quantities of comonomers (6SH and 1,9-D) was varied in the different films. The 0% curve corresponds to the plain complex before polymerisation.*

This was true for both the original polyelectrolyte-surfactant complex as well as for the polymerised samples, i.e. no detectable change due to polymerisation had taken place on the atomic scale. Interesting to note were the reflections appearing in the small angle region, already indicate highly ordered materials. Broadening of these peaks with increasing copolymer content is also worth mentioning.

In order to follow the changes in the mesoscopic arrangement of the material, already hinted at in the WAXS measurements, SAXS analyses of all polymerised samples were performed after a 24 h extraction with hexane (a good solvent for all of the non-reacted components: 6SH, 9SH, 1,9-D). Diffractograms are shown in Figure 5.5.

It is seen that the primary complex is ordered, but just one peak is visible in the scattering diagram. This is to be expected when, for instance, the material consists of two consecutive layers/phases of equal thickness, causing drastic lowering in intensity of the second-order peak. For all swollen and polymerised samples, the scattering peaks are broadened, but up to three equidistant orders of reflection are observed. From these data it is clear that only one of the two phases was swollen, causing the higher order peaks to increase in intensity.

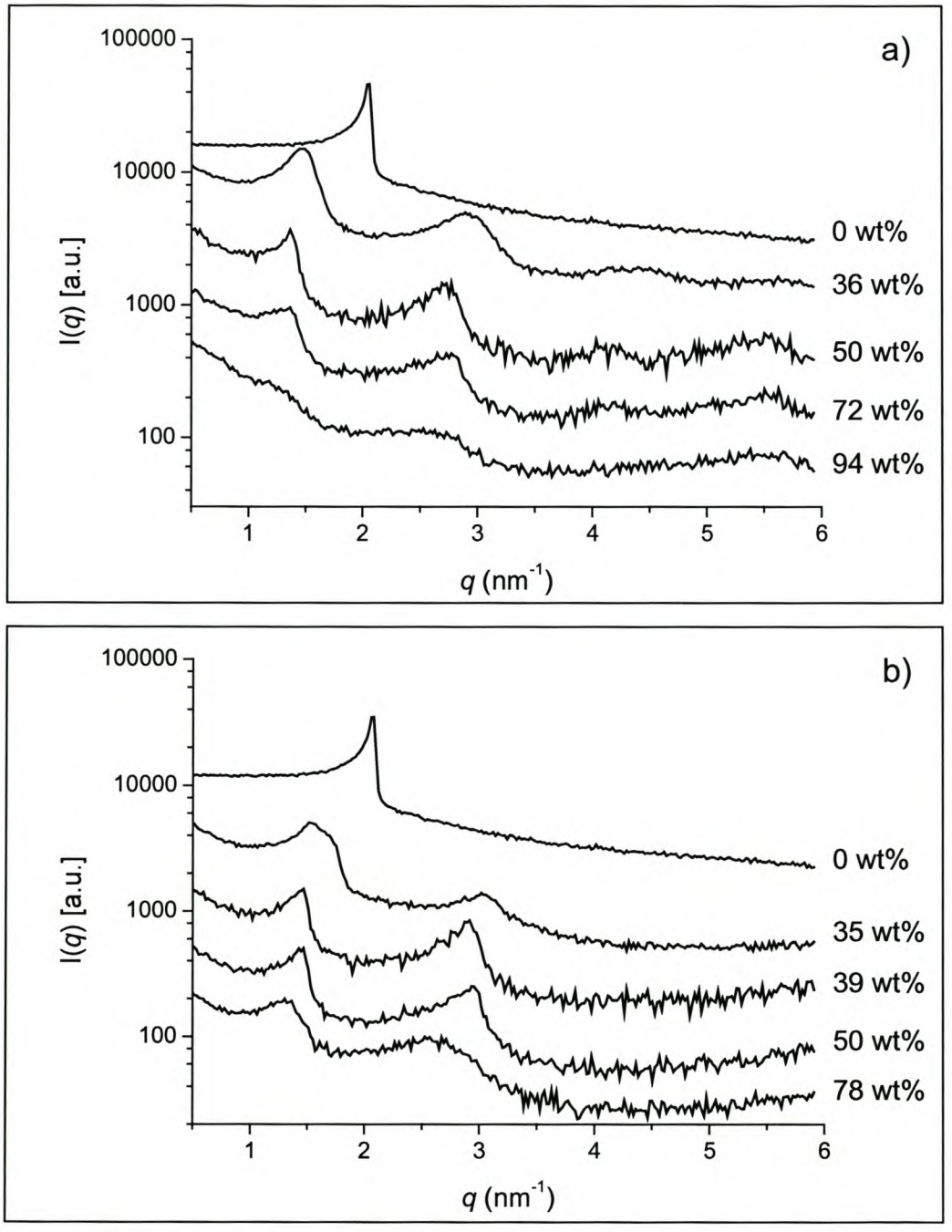

Figure 5.5. *X-ray scattering curves of pDADMA / ωC11 complex after the polyaddition of a) 36 wt% 9SH and 50, 72, and 94 wt% 9SH and 1,9-D; and b) 35 wt% 6SH and 39, 50, 78 wt% 6SH 1,9-D. Equidistant reflections consistent with a lamellar structure were present in all diagrams. The 0 wt% curve corresponds to the plain complex.*

The results showed that the lamellar structure, characteristic of the non-swollen pDADMA / ωC11 complex, was preserved up to a total monomer uptake of ~80 wt%. Above 90 wt% monomer, however, a limit of swelling is reached, where disorder was found. The *d*-spacing of the lamellae, as indicated by the shift of the peaks towards smaller angles, increased due to swelling with the monomer (See Table 5.2 for a summary of the results). This is in good agreement with the expected linear swelling behaviour of lamellar mesophases.

Table 5.2. Shift of the position of the main scattering peak in the SAXS diffractograms of films of pDADMA / ωC11 with an increase in the amount of incorporated monomer.

Sample (% swelling)	*d* – spacing [nm]	Sample (% swelling)	*d* – spacing [nm]
Plain complex (0 wt%)	**3.02**	Plain complex (0 wt%)	**3.02**
6SH (35 wt%)	**4.16**	9SH (36 wt%)	**4.34**
6SH + 1,9-D (39 wt%)	**4.28**	9SH + 1,9-D (50 wt%)	**4.59**
6SH + 1,9-D (50 wt%)	**4.40**	9SH + 1,9-D (72 wt%)	**4.59**
6SH + 1,9-D (77 wt%)	**4.81**	9SH + 1,9-D (94 wt%)	**Total disruption**

It is interesting to note that the 9SH + 1,9-D (72 wt%) sample shows no increase in *d*-spacing, as expected. This is attributed to the onset of phase disruption and start of the demixing of the 'excess' copolymer phase.

The observed preservation of order of the polymerised complexes was confirmed by transmission electron microscopy. TEM micrographs taken of the complex after the polyaddition of the diene, and both 6SH and 9SH, depict the

presence of a lamellar phase (Figure 5.6), as alternating dark (hydrophobic) and light (hydrophilic) layers.

Compared to the original phase (d = 3.02 nm), the interlayer distance was indeed significantly expanded for both the 6SH and the 9SH copolyaddition systems. The lamellar structure was preserved up to ~ 80 wt% of 6SH and 1,9-D included in the complex (Figure 5.6a,b,c) while in the case of complex swollen with 9SH and 1,9-D the onset of phase disruption was observed at lower guest co-monomer content of ~ 70 wt% (Figure 5.6e,f).

The above results were in good agreement with SAXS measurements furthermore the interlayer distances determined from the TEM micrographs corresponded well with the ones from SAXS diffractograms.

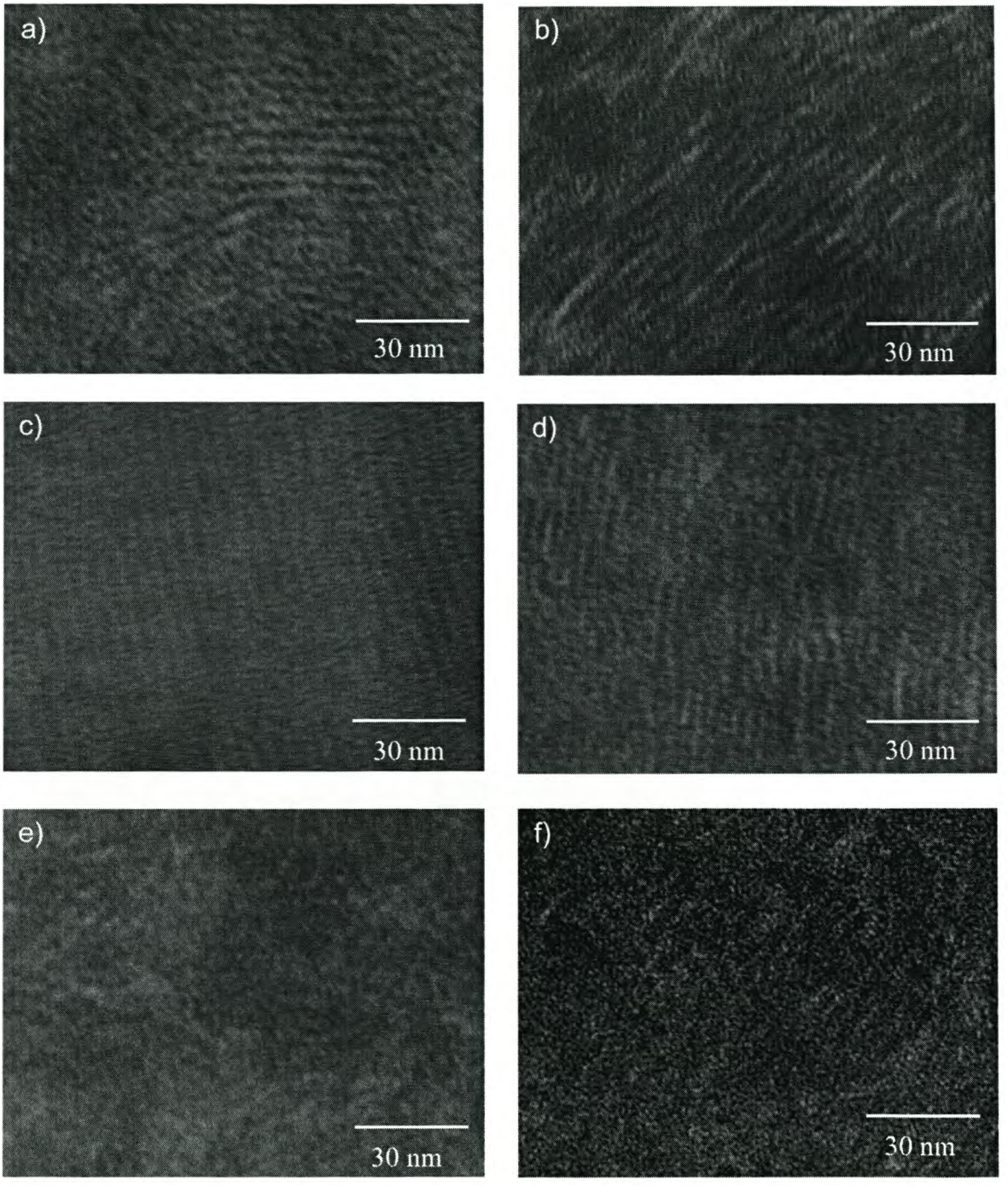

Figure 5.6. *TEM micrographs illustrating the lamellar structure in the pDADMA / ωC11 complex polymerised with a) 39 wt%, b) 54 wt%, c) 78 wt% of 6SH and 1,9-D, and d) 50 wt%, e) 72 wt%, f) 94 wt% of 9SH and 1,9-D.*

5.5. Conclusions

The ternary copolyaddition of a dithiol, diene and a surfmer into the organized phases of a polyelectrolyte-surfactant complex leads to the formation of highly ordered, crosslinked materials. The use of a ternary copolyaddition provides a possibility to vary the composition of such novel composite materials, enabling the effect of increasing the amount of guest polymer on the structure of the host polyelectrolyte-surfactant complex to be investigated. The successful preservation of organized self-assembly structures with increasing guest content was proven by SAXS and TEM analyses. These show an increased *d*-spacing of the host structure. Onset of phase disruption was only observed with 72 wt% copolymer included within the host.

Swelling under structural preservation gives the possibility to adjust the material properties of those highly anisotropic networks, and the residual reactive groups enable further post modification. The behaviour and potential applications of the present class of polymer mesostructures has to be seen in strict analogy with polymerised smectic liquid-crystalline networks, where unusual tensorial mechanical properties,[15] piezo-[16] and pyroelectricity[17] have been examined. Thus, the incorporation of functional groups within polyelectrolyte-surfactant complexes may also lead to further development of smart functional materials.

5.6. References

1. Paleos, C. M. *Polymerization Reactions in Organized Media*; Gordon and Breach Science Publishers, Philadelphia, **1994**.
2. Hentze, H.-P.; Kaler, E. W. *Curr. Op. Coll. Interf. Sci.* **2003**, *8*, 164.
3. Lee, Y.-S.; Yang, J.-Z.; Sisson, T. M.; Frankel, D. A.; Gleeson, J. T.; Aksay, E.; Keller, S. L.; Gruner, S. M.; O'Brien, D. F. *J. Am. Chem. Soc.* **1995**, *117*, 5573.
4. Hentze, H.-P.; Krämer, E.; Berton, B.; Förster, S.; Antonietti, M. *Macromolecules* **1999**, *32*, 5803.
5. Faul, C. F. J.; Antonietti, M.; Hentze, H.-P.; Sanderson, R. D. *Langmuir* **2001**, *17*, 2031.
6. Dreja, M.; Lennartz, W. *Macromolecules* **1999**, *32*, 3528.
7. Kunitake, T.; Okahata, Y. *Bull. Chem. Soc. Jpn.* **1978**, *51*, 1877.
8. Akimoto, A.; Dorn, K.; Gros, L.; Ringsdorf, H.; Schupp, H. *Angew. Chem. Int. Ed. Engl.* **1981**, *20*, 90.
9. Ganeva, D.; Faul, C. F. J.; Gotz, C.; Sanderson, R. D. *Macromolecules* **2003**, *36*, 2862.
10. Kharasch, M. S.; Nudenberg, W.; Mantell, G. J. *J. Org. Chem.* **1951**, *16*, 524.
11. Cramer, N. B.; Scott, J. P.; Bowman, C. N. *Macromolecules* **2002**, *35*, 5361.
12. Stacey, F. W.; Harris, J. F. J. *Formation of carbon-hetero atom bonds by free radical chain additions to carbon-carbon multiple bonds*; John Wiley & Sons, Inc., NY, **1963**; Vol. 13.
13. Cramer, N. B.; Davies, T.; O'Brien, A. K.; Bowman, C. N. *Macromolecules* **2003**.
14. Antonietti, M.; Conrad, J.; Thünemann, A. F. *Macromolecules* **1994**, *27*, 6007.
15. Assfalg, N.; Finkelmann, H. *Macromol. Chem. Phys.* **2001**, *202*, 794.

16. Meier, W.; Finkelmann, H. *Macromolecules* **1993**, *26*, 1811.

17. Leister, N.; Lehmann, W.; Weber, U.; Geschke, D.; Kremer, F.; Stein, P.; Finkelmann, H. *Liq. Cryst.* **2000**, *27*, 289.

CHAPTER 6

CONCLUSIONS AND RECOMENDATIONS

6.1. Conclusions

The general objective of this research was to develop a novel approach to direct templating, where the organised phases of polyelectrolyte-surfactant complexes are used as hosts for organic polymerisation reactions.

The polyelectrolyte-surfmer complex of the tail-functionalised di(undecenyl)phosphate (ωC11) and pDADMAC was identified as a host for organic polymerisation reactions. The lamellar complex with a repeat unit of 3.02 nm showed higher stability (than the one found in the case of ωC11 alone) when used as a template, owing to the presence of the polyelectrolyte backbone.

The mobility of the surfactant tails within the complex proved to be insufficient for radiation-induced homopolymerisation reactions to take place. Monomer degradation rather than polymerisation was observed in the ^{1}H NMR spectra of the complex recorded before irradiation. Polymerisation and 1:1 templating was achieved only on the incorporation of an unbound flexible co-monomer inside the complex and following a polyaddition reaction. The latter has the advantage (over conventional free radical polymerisation) that volume shrinkage is largely avoided, and the possibilities for phase disruption are minimized.

The pDADMA / ωC11 complex was able to withstand swelling with ~35 wt % of thiol co-monomer (constituting a 1:1 ratio of thiol to vinyl groups) without signs of phase disruption. No phase disruption or disordering occurred during the polyaddition reaction or during the extraction of any unreacted monomer from the polymer films. Polyaddition proceeded until all reactive groups were consumed (as proved by FTIR analyses). Furthermore, the resulting lamellar polymer symplex, a cured copy of the template, showed improved thermal and mechanical properties.

This is the first case of successful polyaddition within the organised phases of polyelectrolyte-surfactant complexes to be reported.

The addition of a second co-monomer (a diene) to the reaction system provided a possibility by which to vary the composition of the novel composite materials obtained through the ternary thiol-ene polyaddition within the complex. it therefore allowed for the investigation of the effect of increasing the amount of guest polymer on the structure of the host polyelectrolyte-surfactant complex. The successful preservation of organised self-assembly structures with increasing guest content was proven by SAXS and TEM analyses. The increased *d*-spacing of the host structure with the increase in guest polymer content gave the possibility to tune the material properties of those highly anisotropic networks. Onset of phase disruption was only observed with 72 wt% copolymer included within the host. This unusually high degree of swelling under preservation of nanoscale order could be attributed to the flexible, linear structure of the co-monomers used, since the addition of rigid co-monomers was reported to cause phase disruption at only ~ 17 wt% of swelling of the host polyelectrolyte-surfactant complex.[1] The high loading capability of the pDADMA / ωC11 allowed for a large amount of otherwise unstructured material to be organised within the template.

In summary, it can be said that the objective of the research was achieved. The major advantages of using this new route to molecular templating are the simplicity of the building blocks and the synthetic procedures used together with the robustness of the template to flexible co-monomers, allowing the organisation of large amount (~ 70 wt%) of unstructured materials. The results described in the dissertation have been presented in two publications:

1. Directed Reactions within Confined Reaction Environments: Polyadditions in Polyelectrolyte-Surfactant Complexes. Desislava Ganeva, Charl F. J. Faul, Christian Götz and Ronald Sanderson, *Macromolecules*, ***36***, 2862-2866, **2003**
2. Polymerisation of the Organised Phases of Polyelectrolyte-Surfactant Complexes. Desislava Ganeva, Markus Antonietti, Charl F. J. Faul and Ronald Sanderson, *Langmuir*, ***19***, 6561-6565, **2003**

A poster was presented at the 2002 POLY Biennial conference for polymeric nanomaterials held in California, USA, in November 2002.

6.2. Recommendations for future research

Future work should focus on (i) gaining a better understanding of the changes that occur during polymerisation within the ordered template and (ii) looking at possible materials applications. This can be done in the following way:

- Theoretical interpretation of the available SAXS data allows the determination of the individual thickness of the hydrophilic and the hydrophobic layers. By following the changes in the layers thickness in the initial complex, during swelling and during polyaddition one should obtain an idea about changes occurring in the system during the reaction.
- Studying the influence of various host morphologies on the successful application of the technique.
- Studying the influence of the type of surfactant and comonomer on the loading capabilities of the template.
- Employing polyelectrolytes and / or surfmers with some 'useful' functionality (e.g. conductive polyelectrolyte) in the complex.

6.3. References

1. Faul, C. F. J.; Antonietti, M.; Hentze, H.-P.; Sanderson, R. D. *Langmuir* **2001**, *17*, 2031.

APPENDIX 1

COMPLEXES OF PDADMAC WITH DI(*N*-ALKYL)PHOSPHATE SURFACTANTS

A1.1. Introduction

A homologous series of saturated di(*n*-alkyl)phosphates was synthesised and complexed with pDADMAC in order to investigate the effect of increasing surfactant chain length on the structure of the polyelectrolyte-surfactant complexes. The length (*n)* of the hydrocarbon tail was varied from 9 to 16 carbon atoms (*n* = 9, 12, 16). The structure of the complexes was investigated using SAXS analyses.

A1.2. Materials

The following chemicals were purchased from Aldrich Co. and used as received: 1-nonanol, 1-dodecanol, 1-hexadecanol, phosphorous oxychloride, sodium tetraborate decahydrate, sodium hydroxide, high molecular mass polydiallyldimethylammonium chloride (pDADMAC, M_w 375 000 – 500 000). Water used for the synthesis of the complexes was distilled and deionised in a "Milli-Q" water purification system (Millipore Corp.). Dry benzene (refluxed over calcium chloride, distilled and stored over molecular sieve, 4Å) was used as

solvent for the preparation of di(*n*-alkyl)phosphates. Other solvents used for the syntheses: chloroform, dichloromethane, ethylacetate, methanol, acetone, hydrochloric acid (37%), were purchased from Acros Organics.

A1.3. Experimental procedures

A1.3.1. Synthesis of di(*n*-alkyl)phosphates and their complexes with pDADMAC

Di(*n*-alkyl)phosphates were prepared by refluxing phosphorous oxychloride and three equivalents of the respective alcohols in dry benzene for 24 h. The solvent and the excess alcohol were removed under 20 mbar vacuum and the residue recrystallised twice or more: di(nonyl)phosphate (C9), m_p 35.7 °C, (white crystals from ethylacetate), di(dodecyl)phosphate (C12), m_p 61 °C, (white crystals from 4:1 mixture of acetone:methanol), di(hexadecyl)phosphate (C16), m_p 74 °C (white crystals from benzene). The purity of the compounds was confirmed by elemental analysis (Table A1.1) and spectroscopy. IR ($\nu_{P=O}$ 1231 cm^{-1}, ν_{P-O-R} 1091 cm^{-1}) and ^{1}H-NMR [($CDCl_3$, 300 MHz): 1.64p [3.8H, 2 x ($C\underline{H}_2$-C-O-)], 3.96q [4H, 2 x ($C\underline{H}_2$-O)] data of the synthesised diesters corresponded to the expected surfmer structures. The pDADMA / di(*n*-alkyl)phosphate complexes were synthesised using a procedure described in Section 3.3.2.3.

Table A1.1. Elemental analysis data obtained for the homologous series of saturated di(*n*-alkyl)phosphates.

Compound	Mass percentage	
	C %	H %
Di(nonyl) phosphate	Calc. 61.68	Calc. 11.20
$C_{18}H_{39}O_4P$	Found 61.65	Found 10.97
Di(dodecyl) phosphate	Calc. 66.32	Calc. 11.82
$C_{24}H_{51}O_4P$	Found 66.11	Found 12.69
Di(hexadecyl) phosphate	Calc. 70.28	Calc. 12.34
$C_{32}H_{67}O_4P$	Found 70.60	Found 13.20

A1.4. Results and discussion

Di(*n*-alkyl)phosphates were synthesised with high purity (> 90%) and yields (~ 60%). Their complexes with pDADMAC formed optically clear films when cast from chloroform. The pDADMA / C9 complex was a flexible film in the solid state while the complexes of pDADMAC and homologues with longer alkyl tails were hard and brittle. Since it was shown (Chapter 3) that the pDADMA / ωC11 complex forms a highly ordered, lamellar mesomorphous structure, it was expected that the complexes di(*n*-alkyl)phosphates and pDADMAC will show similar mesoscale ordering. SAXS analyses showed characteristic scattering curves for all pDADMA / di(n-alkyl)phosphate complexes (Figure A1.1).

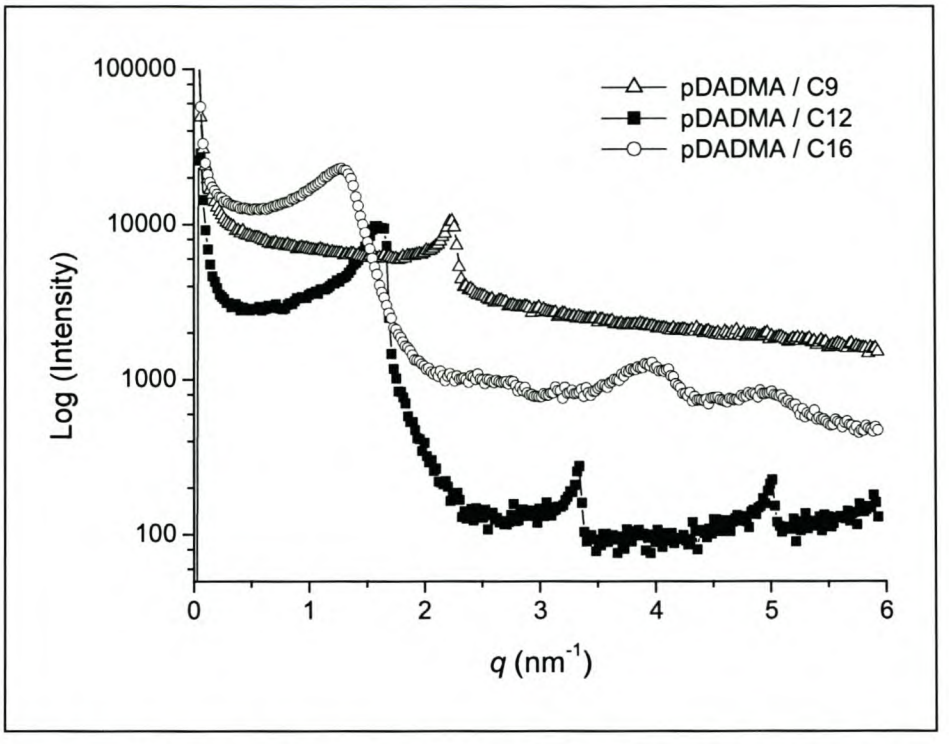

Figure A1.1. *SAXS diffractograms of the complexes of pDADMAC and homologous di(n-alkyl)phosphates.*

The pDADMA / C9 complex was ordered, but just a single reflection was found in the scattering diagram at q = 2.24 nm^{-1}. This corresponded to a Bragg spacing of 2.8 nm. By contrast, three and four equidistant reflections were observed for the complexes of the longer chain surfmers, C12 and C16. The ratio of the reflex positions, determined to be 1.0 : 2.1 : 3.1 for pDADMA / C12 and 1.0 : 1.9 : 3.0 : 3.8 for pDADMA / C16, was characteristic of a lamellar mesomorphous structure. The increasing number of reflections in the SAXS diagrams indicated an increase of ordering in the complexes with an increase in the surfmer chain length. Furthermore, the long period of the lamellae increased from 2.8 nm to 4.87 nm with the increase in the length of the surfmers tails. The increase in the long period with surfactant chain length did not follow the simple linear dependence characteristic of lamellar systems

(Figure A1.2), which suggested that a change in morphology occurs with increasing surfactant chain length.

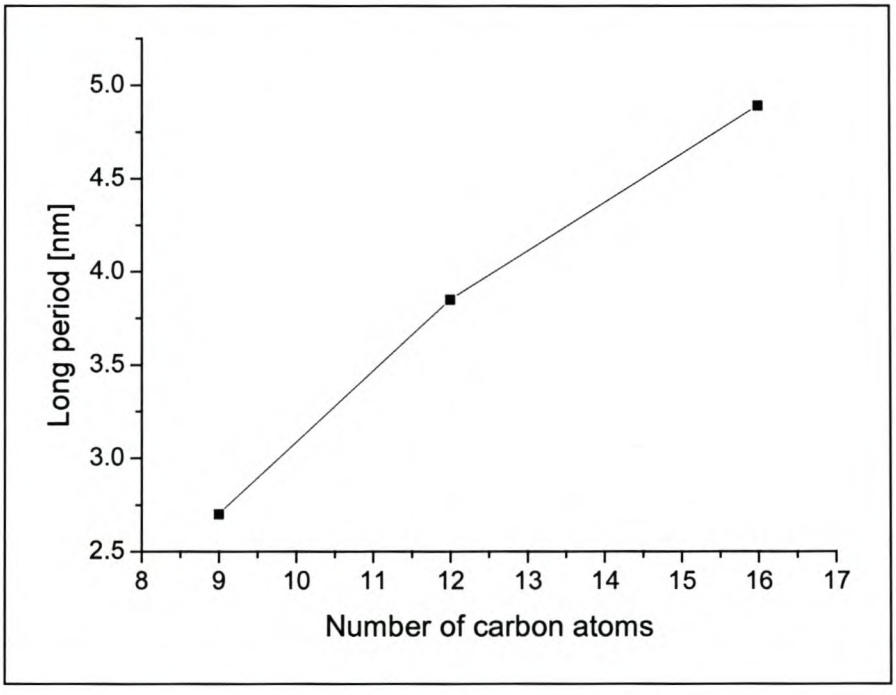

Figure A1.2. *Long period of the different pDADMA / di(n-alkyl)phosphate complexes plotted against length of the alkyl tails (number of carbon atoms).*

The observed deviation from linearity of the long period to surfmer chain length dependence has previously been attributed to the appearance of undulations or perforations of the lamellar phase.[1,2] In the latter case additional scattering peaks are expected to appear. Such additional peaks could be found in the SAXS diffractogram of the pDADMA / C16 complex at scattering factor q = 3.14 and 4.52 nm^{-1} (Figure A1.1). The 1 : 1.4 ratio of the scattering peaks could possibly be attributed to a cubic arrangement of the perforations. High resolution SAXS, TEM analysis or even solid-state NMR analysis could be employed for further structure elucidation of the complexes. This, however, falls outside the scope of this investigation.

A1.5. References

1. Antonietti, M.; Conrad, J.; Thünemann, A. F. *Macromolecules*, **1994**, *27*, 6007.
2. Thünemann, A. F. *Langmuir*, **2000**, *16*, 824.